DESIGN, PERFORMANCE, AND ANALYSIS OF A MULTI-LEVEL AIR PERMEABILITY TEST

by

Orrick R. Haney

Thesis submitted to the faculty of the
Virginia Polytechnic Institute and State University
in partial fulfillment of the requirements for the degree of

MASTER OF SCIENCE

in

Civil Engineering

APPROVED:

Mark A. Widdowson
M.A. Widdowson, Chairman

George F. Filz
G.G. Filz

Panayiotis Diplas
P. Diplas

February, 1994

Blacksburg, VA

C.2

Design, Performance, and Analysis of a Multi-Level Air Permeability Test

by

Orrick R. Haney

Committee Chairman: Dr. Mark A. Widdowson

Civil Engineering

(ABSTRACT)

The design, performance, and analysis of a soil vapor extraction system to identify zones most conductive to air transport and quantify k_{air} in sequential soil layers is presented. A multi-level extraction well, with alternating solid and screened sections, was utilized to characterize multi-layered media. The field site, located in the Carolina Slate Belt within the physiographic region known as the Piedmont, is comprised of alternating layers of different soil types of varying k_{air}, including thin bands of clay, silt, and sand.

The pneumatic test consisted of one multi-level extraction well and four multi-level pressure monitoring wells. Screen locations were based on previous site characterization. Vapors were extracted at one screen while pressure, temperature, and volumetric flow rate were monitored using a computer data acquisition system. Data was analyzed

by both steady-state and transient solution techniques using pressure drawdown versus time data collected at various locations.

Results from vapor extraction tests indicate that the multi-level approach is advantageous when dealing with heterogenous media, since the most permeable layer was identified. Transient and steady-state solutions indicate that a k_{air}= 2.0 X 10^{-7} cm^2 is representative of the located permeable layer within the subsurface. Vacuum system, formation, and extraction well characteristics are evaluated to determine pressure as a function of volumetric flow rate.

ACKNOWLEDGEMENTS

I would like to thank my advisor, Dr. Widdowson, for the countless hours of devotion to my professional development. He provided direction in the beginning of my studies by means of sharing knowledge, setting high standards, providing direction, and most of all giving advise. His demonstration of patience, optimism, and trust in my abilities was important in the beginning of the research. Throughout the research these characteristics were crucial in providing motivation, while at the same time leading to an understanding that a strong effort and thorough understanding of a subject produces quality results.

A special thanks goes to Dr. Diplas and Dr. Filz for serving on my committee. Both of them have given me expert advise during my research and knowledge in areas of geoenvironmental and hydraulic engineering, subjects of great interest to me.

A thanks also goes to Krista Evans for giving me encouragement during hard times. Your advise allowed to me to concentrate on goals already met, while creating a strong will to continue excelling in my studies. Finally, a very special thanks goes to my loving parents for always believing in my abilities and leading me to understand that any goal is possible if the right attitude is present.

TABLE OF CONTENTS

LIST OF FIGURES

LIST OF TABLES

CHAPTER 1

INTRODUCTION

1.1 BACKGROUND

The growing number of sites contaminated with volatile organic compounds (VOCs) has sparked the need for techniques to remove these compounds from soil and groundwater. Soil vapor extraction (SVE) is a remediation technique that has gained attention for application to VOC-contaminated sites. SVE, often referred to as soil venting, serves as means of removal of VOCs in the unsaturated zone. A blower or vacuum pump, connected to an extraction well screened in the unsaturated zone, promotes VOC extraction by means of vaporization and removal of VOCs in the vapor-phase. Vapors extracted from the vadose zone are treated according to state and federal regulations or discharged into the atmosphere. SVE is a preferred method of remediation since it is cost effective and works well with other technologies such as bioremediation and pump and treat schemes (Johnson et al., 1990a; Hinchee et al., 1991; Krishnayya, et al., 1988).

Factors influencing the applicability of SVE at a site are soil permeability, moisture content, vacuum pressure, air flow rate, temperature, and boundary conditions (Krishnayya et al., 1988). Field tests to determine design parameters usually employ a single screen extraction well over an area

where the contaminants are concentrated. The basic components of a SVE pilot system are a blower, an extraction well, surface seal, surface treatment devices for vapor and liquids, and pressure monitoring wells. Results from pilot tests serve as a guide in determining well spacing, well depth, volumetric flow rate (Q_{air}), and pressure at the extraction well (P_w).

The single most important parameter attained from pilot tests is soil air-phase permeability (k_{air}), an indicator of the ability of the media to permit passage of vapors through non-wetted pore space. Air permeability is a function of intrinsic permeability (k) and moisture content, in which k_{air} approaches k in dry soils and approaches zero for 100% saturation (Bear, 1979). Although use of soil venting in highly permeable soils such as sand and gravel has proven to be very effective, application of SVE in silt and clay is questionable due to their relatively low permeabilities (Gibson et al., 1993). However, cases have been cited where fractures in clay media permit the passage of air sufficient for the implementation of a SVE system (e.g., Gibson et al., 1993; Abdul et al., 1990).

Because air permeability is an essential parameter in SVE design, characterization of k_{air} distribution in the subsurface is vitally important. The successful design and overall performance of a SVE system is dependent on the accuracy of

the quantification of soil air-phase permeability. This is especially true for sites where the subsurface is highly heterogenous. Previous designs have mostly focused in areas of high permeability and homogenous media. Ordinary single screen venting wells may not be effective in the quantification of air permeability in regions that are heterogenous or have fractured soil media. An ideal situation would permit the identification of the subsurface in terms of layers most permeable to soil venting and subsequent design of a full-scale system to focus on the layers of the vadose zone where the passage of vapors are most significant.

1.2 OBJECTIVE

The objective of this thesis is to present the design, performance, and analysis of a multi-level SVE test to determine permeable zones within sequential soil layers. A multi-level extraction well was designed as a means to identify the zones most conductive to the passage of air and to quantify k_{air} in these zones. Pneumatic tests were conducted at a leaky underground storage tank site in South Carolina within the Piedmont physiographic region known as the Carolina slate belt (Johnson, 1972). The multi-level approach was important at this site due to thin, alternating bands of sand, clay, and silt in the subsurface. Likewise, this "novel" approach is designed for use in other geological

environments.

1.3 APPROACH

The pneumatic test design consisted of one multi-level extraction well and four multi-level pressure monitoring wells. Screen locations were based on previous site characterization data. Soil gas was extracted at one screen while soil gas pressure was monitored at various locations over time. A fully-automated data collection system included a datalogger programmed to collect data at specific time intervals.

A series of tests were conducted to achieve research objectives. The first test aimed at determining a blower size needed to accomplish favorable vapor extraction rates. The remainder of the tests focused on obtaining data to quantify the air permeability of the layers in the zone of contamination. A number of techniques were used to analyze the data from the tests. Both steady-state and transient solutions were employed using pressure drawdown versus time data collected on various occasions as well as steady-state pressure data. Both steady-state solutions by Johnson et al. (1990b) and Baehr and Hult (1991) were used as methods of analysis. Transient solutions used were Cooper-Jacob (1946) for confined radial flow and Hantush (1956) for leaky aquifer radial flow, as modified for the air-phase by Johnson et al.

(1990) and Massmann (1989), respectively.

Chapter 2 surveys the literature for SVE field tests for determining k_{air}, solution techniques, and methods of analysis for field tests. Next, the field site will be described in terms of the source of contamination, and conditions unique to this particular region and site. The experimental apparatus and procedure will be discussed in Chapter 4 including a description of the test design (wells, vacuum systems, and data acquisition systems). Chapter 5 contains pneumatic test performance data and results. Chapters 6 and 7 include analyses of the data and a discussion of the results. The conclusion will present the major findings (with emphasis on air permeability) and will discuss how this research compliments and adds new insights to field techniques for determining k_{air}.

CHAPTER 2

BACKGROUND

Since SVE is a relatively new technology, few investigations have been published on field tests and methodologies for data analysis. Pneumatic pilot tests are necessary to adequately determine design components for a full-scale soil venting system. Important parameters determined from a pneumatic test are the vapor extraction rate (Q), radius of influence (R), and the air permeability (k_{air}). Design considerations for pneumatic pilot tests are well spacing, well depth, screen location(s), and blower capacity. Similar to groundwater pumping tests, pneumatic test design is variable from site to site, depending on geology and soil properties. Likewise, pressure drawdown data is analyzed and k_{air} is calculated from data analysis techniques. The following sections will focus on describing current field methods, solution techniques, and options for analysis of data.

2.1 FIELD TESTS FOR DETERMINING AIR PERMEABILITY

A variety of field studies cited in the literature are helpful in terms of the design of pneumatic pilot tests. These tests are useful for determining general guidelines; however, most of these tests have focused on highly permeable

and homogenous media and have not considered multi-layered media. This section will focus on examining specific tests conducted to quantify the air permeability in different geological conditions.

2.1.1 USGS BEMIDJI SITE

Field tests were conducted in August 1987 (Baehr and Hult, 1988) at Bemidji, Minnesota in conjunction with a U.S. Geological Survey study of an oil spill-contaminated aquifer. Two 60-cm (1.97-ft) screened extraction wells were installed in the middle of the 840-cm (27.56-ft) thick vadose zone. Because the strata under investigation contained a confining bed in the middle of the vadose zone, wells were placed above and below this zone of low permeability. The confining unit consisted of a silt and fine-grained sand unit separating an upper stratum of medium-grained, moderately well sorted sand and a lower stratum unit of medium-grained, moderately well-sorted sand. Pneumatic tests consisted of either injecting or extracting air through the venting well and measuring the response at adjacent probes. A flow meter, thermistor, and pressure transducer at the extraction well were used to determine the mass flow. Probes were installed adjacent to the extraction well to measure pressure at various radial and vertical distances. Recorded pressures from probes indicated that heterogeneity was present (Baehr and Hult, 1991).

Initially, a single-screen extraction well was chosen to quantify the air-phase permeability of the vadose zone at the Bemidji site (Baehr and Hult, 1988). However, the existence of a silt and fine-grained sand lens above the well screen was unknown. During tests only pressure probes below the lens relayed measurable responses. Therefore, a second well was installed above the confining lens creating two zones of monitoring. For practical purposes heterogeneity was treated as an apparent anisotropy, i.e., set $\partial k/\partial z = 0$. However, the results from the lower zone showed that the k_r/k_z (ratio of radial to vertical air permeability) varied as a function of the extraction rate. Thus, the assumption of homogeneity within the lower zones was not completely valid (Baehr and Hult, 1991).

Data from pneumatic tests was input into an algorithm developed to determine the air permeabilities as a function of mass and volumetric flow through a least squares analysis (Joss and Baehr, 1993). Results from the least squares analyses generated air permeabilities for the confining silt lens within an order of magnitude of 10^{-9} cm^2. Air permeabilities for the upper region were within an order of magnitude of 10^{-6} cm^2 while the lower stratum permeabilities were within an order of magnitude of 10^{-7} cm^2 . The difference in permeabilities of the two zones was in accordance with site geology.

2.1.2 MASSMANN STUDY: PACIFIC NORTHWEST GLACIAL DEPOSITS

A similar pilot test was conducted at a landfill in Kent, Washington (Massmann, 1989). This site consisted of three distinct layers of porous media: a layer of sand and gravel in the intermediate region, an upper region consisting of glacial till, and a bottom region containing clay and clayey-silt. The design of the extraction well included a screened interval that started at the lower portion of the glacial till and extended down into the sand and gravel region.

Observation pressure probes consisted of shallow, intermediate, and deep probes (Massmann, 1989). The shallow probe was located in the glacial till covering a 6-m (19.7-ft) region while the intermediate and deep probes were in the sand and gravel expanding over a 24-m zone (78.7-ft). The shallow probe responded more slowly than the intermediate probe during the extraction tests. This was expected since the shallow zone consisted of silty-sand materials obviously less permeable than the sand and gravel. The deep probe within the sand and gravel region responded as quickly as the intermediate probe, but 10% less drawdown occurred. The difference in the drawdown was attributed to the position of the lower probe being lower than the screened interval of the extraction well (Massmann, 1989).

Analysis of the data showed an agreement with the Theis (1935) solution for the first 200 minutes of the test yielding

an air permeability of 9.2 X 10^{-8} cm^2 (Massmann, 1989). The data beyond 200 minutes simulated a leaky aquifer solution by Hantush (1956). This leakage was attributed to the till that acted as a confining unit above the sand and gravel region. Using the Hantush solution provided values of $k' = 2.09 \times 10^{-9}$ cm^2 for the confining layer while the sand gravel region had a $k = 1.0 \times 10^{-7}$ cm^2. Massmann's analysis demonstrated that the confined and leaky aquifer solutions for groundwater provide good approximations of the flow of gas.

2.1.3 GMI STUDY: GLACIAL CLAY

The field tests described in the above studies were conducted in soils with high permeability. Until recently, the study of SVE systems in relatively impermeable regions has been an area of little attention. Studies by (Abdul et al., 1990) showed that permeability of clay is usually too low for soil venting. Normally, clay has a permeability of about 1.4 X 10^{-10} cm^2 which is not considered effective in SVE systems. However, tests by Gibson et al. (1993) showed that interaction between organic solvents and clay can actually increase the clay permeability, and soil venting can be a means of remediation in clay regions contaminated by organic solvents.

In the study by Gibson et al. (1993) the area of vapor extraction consisted of a clay zone overlying a bedrock interface. Depths from the surface to the bedrock varied from

0.61 m (2.0 ft) on the outer edges of the zone of influence to 10.97 m (36.0 ft) near the center. Uncontaminated clay served as a medium of low permeability acting as a means of leakage to the confined and fractured clay unit lying 3.05 m (10.0 ft) to 4.57 m (15.0 ft) below the surface. The extraction well was centrally located and consisted of a 4.57-m (15.0-ft) screen interval extending from 4.57 m to 9.14 m (15.0 to 30.0 ft) below the surface. Also, monitoring wells were installed in 30 locations to measure responses in drawdown and to sample vapors.

Gibson et al. (1993) presented data indicating that the confining layer of uncontaminated clay and the porous bedrock stratum beneath the contaminated clay acted as regions of leakage. The leaky aquifer solution by (Hantush and Jacob, 1955) was used to analyze the data. Data from various monitoring wells indicated air pressure drawdown in the 3.05-m to 9.14-m (10.0-ft to 30.0-ft) zone of the fractured clay. Also, within a radial distance of 6.10 m (20.0 ft) from the extraction well steady-state conditions were reached within four minutes. The above leaky aquifer solutions generated air permeabilities on the order of magnitude of 10^{-8} - 10^{-7} cm^2. In addition to the above prediction, the solution for a steady-state radial flow by (Johnson et al., 1990b) was used to analyze the data. The results gave an air permeability of 1 X 10^{-8} cm^2 comparing quite reasonably with the Hantush and

Jacob (1955) solution.

2.2 GENERAL GUIDELINES IN FIELD SITE CHARACTERIZATION

The following information needs to be obtained according to Johnson et al. (1990a): site geology, site hydrogeology, contaminant delineation and temperature variations in the subsurface if SVE is a candidate for remediation. Properties of the geological stratification in conjunction with bore-hole samples aid in the determination of the optimal location for a pilot-scale SVE system. *Ex-situ* bore-hole samples serve as means of determining properties of a medium such as hydraulic conductivity, void ratio, porosity, and contaminant concentrations.

Results from *ex-situ* laboratory tests can act as a basis of comparison of permeabilities from *in-situ* pneumatic tests. According to Massmann (1989) there are three methods for determining the gas permeability: (1) estimating permeability as a function of saturated hydraulic conductivity; (2) estimating permeability as a function of grain size parameters; and (3) estimating permeability from gas extraction tests. The most important parameter generated from pneumatic tests, k_{air}, is highly dependent on moisture content. Furthermore, determination of the air-filled porosity from *ex-situ* tests can serve as an approximation of *in-situ* conditions.

One constraint crucial to the performance of a SVE system is an impermeable surface boundary (Johnson et al., 1990a). The performance of a SVE system can be either reduced or improved as shown in Figures 2.1 and 2.2, respectively. As shown, lack of an impermeable surface above the zone of vacuum can reduce the effectiveness of air flow through the zone of contamination. Johnson et al. (1990a) point out that the surface seal has a significant effect on vapor flow paths for areas of treatment less than 5 m (1.6 ft) below ground surface and can be added or removed to create a desired vapor flow path. However, for treatment 8 m (2.6 ft) below the surface, a seal has little effect on the vapor flow path (Johnson et al., 1990a).

The soil type and stratification of the subsurface are equally important (Johnson et al., 1990a). Previous studies have concentrated on single screen venting wells over layers beneath the subsurface. However, complicated geologic conditions may in some circumstances require alternative means of classifying the subsurface permeabilities. The existence of multi-layered media may require a series of screens to quantify the layer's k_{air}.

Finally, the location of the contaminated soil is crucial. The passage of air flow needs to be directed toward the plume such that maximum vapor extraction rates are achieved. Thus proper location of the impermeable boundary in

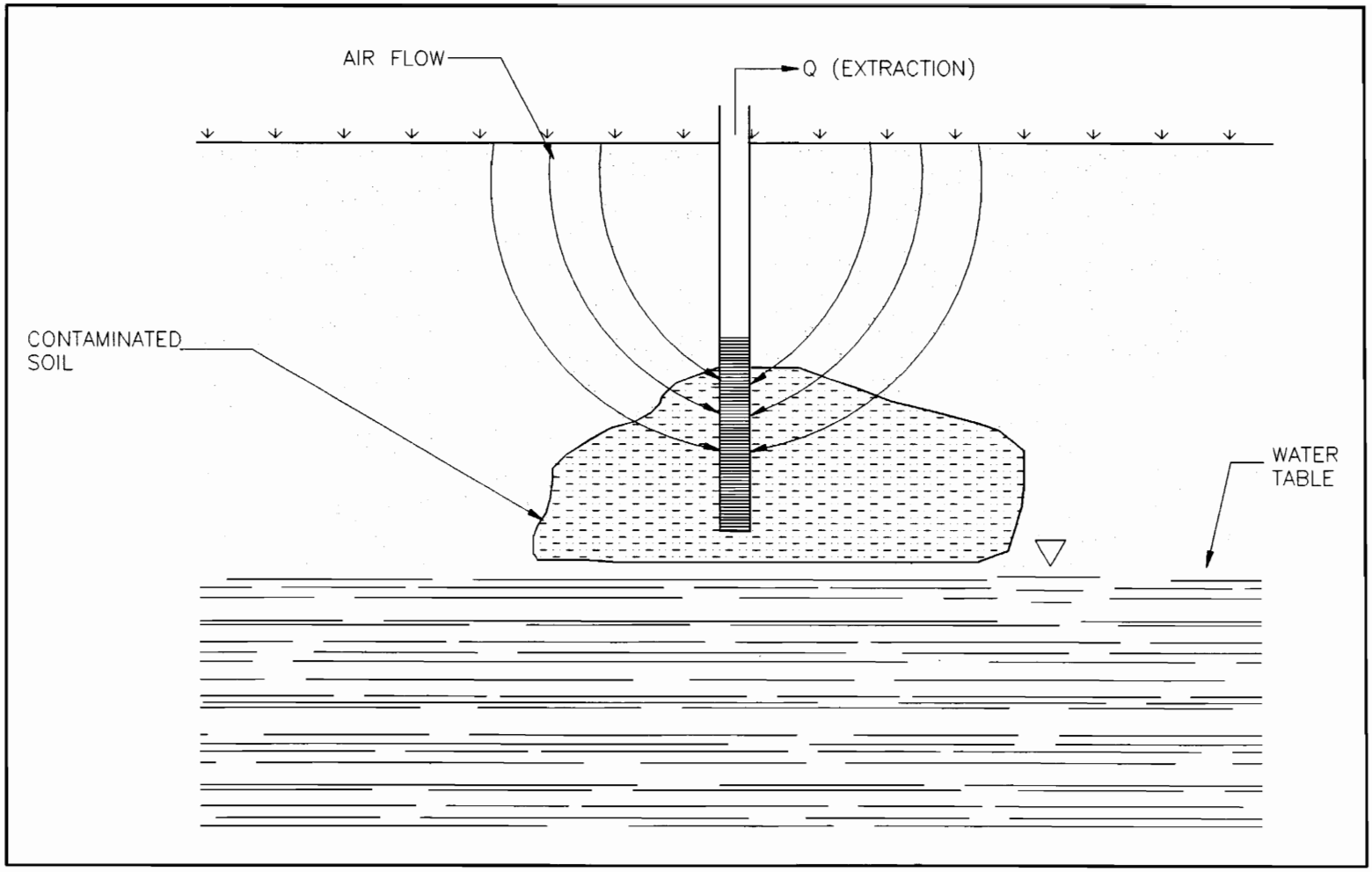

Figure 2.1: Open surface during vapor extraction

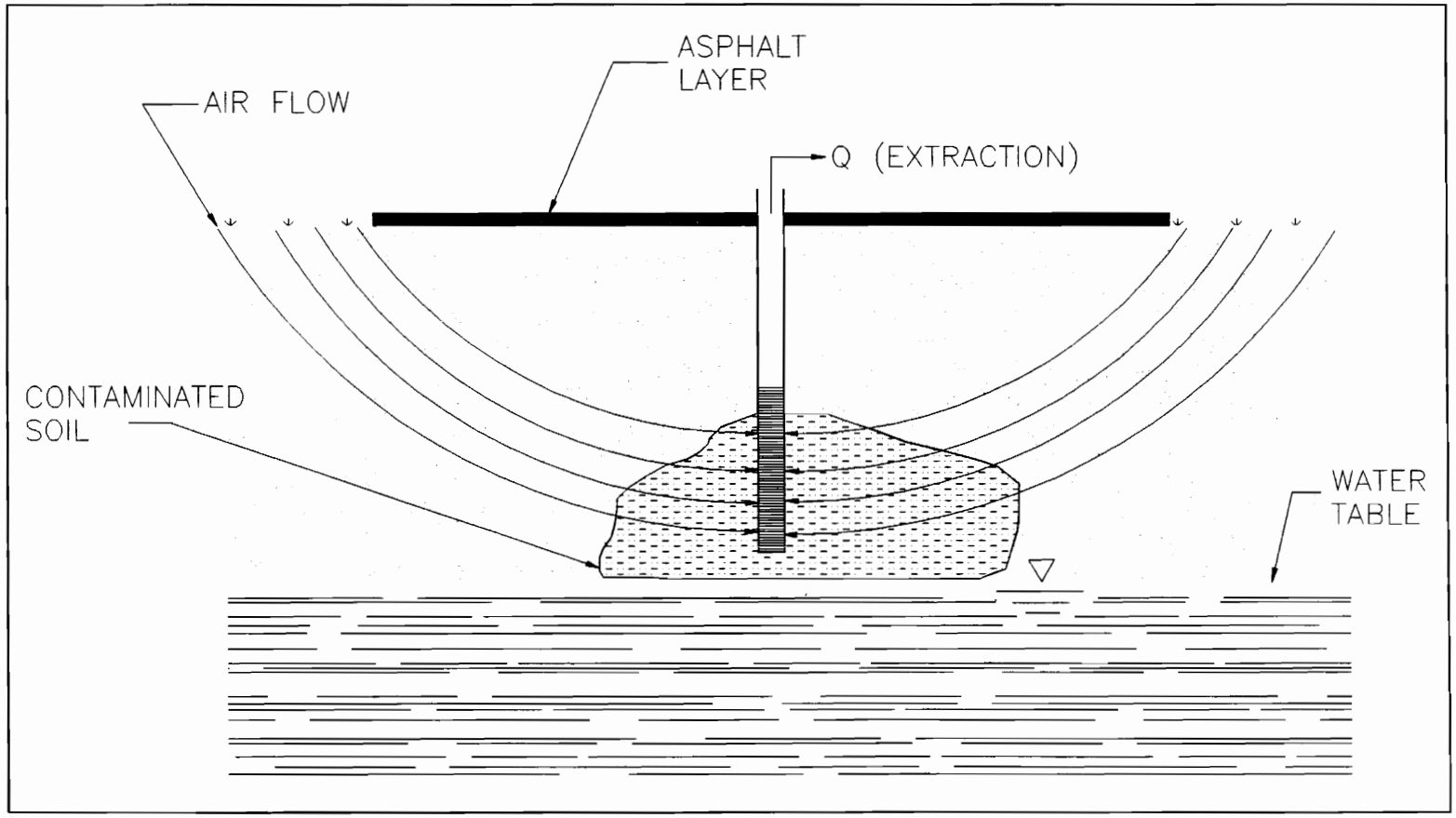

Figure 2.2: Surface seal during vapor extraction

conjunction with the plume and concentration on layers most permeable to vapor transport can ensure the best performance from the system.

2.3 GOVERNING EQUATIONS

Equations for vapor transport differ from that of liquids due to differences in molecules and their interaction with the surroundings (Massmann, 1989). The primary difference is that liquids are dominated by viscous flow, while gas flow may have considerable slip flow. The phenomenon of slip flow (Dullien, 1979) also known as the Klinkenberg effects (Klinkenberg, 1941) is an item of concern. The following expression by Dullian (1979) predicts the molar flux as a function of both viscous and slip flow (Massmann, 1989):

$$F_m = -\left[\frac{r_p^2 P}{8\mu} + \frac{4 r_p RT}{3 W_m V_m}\right] \frac{1}{RT} \nabla P \qquad (2.1)$$

where,

F_m = molar flux (Mole L^{-2} T^{-1})

r_p = average pore radius (L)

P = absolute pressure (M L^{-1} T^{-2})

μ = viscosity (M L^{-1} T^{-2})

R = gas constant (L^2 degree K^{-1} T^{-2} $Mole^{-1}$)

T = absolute temperature (Degree K)

W_m = molecular weight (M $Mole^{-1}$)

V_m = mean molecular velocity (L T^{-1})

∇ = gradient operator (L^{-1})

Slip occurs when the mean free path of the molecules approaches the distance of the pore radii (Baehr and Hult, 1991). The mean free path of gases tends to be much smaller than liquids, therefore slip flow occurs. The effects of slip are most noticed as the pore radii decreases and as air-phase pressure decreases (Baehr and Hult, 1991).

Studies by Massmann (1989) and Baehr and Hult (1991) have identified the slip flow effects in relation to SVE. Massmann (1989) concluded that for pore radii > 10^{-3} mm that slip flow is small compared to viscous flow. Baehr and Hult concluded that slip flow can be significant when the porous media has a intrinsic permeability of 10^{-9} cm^2 or less. These limitations indicate that the effects are most important when dealing with clay or silt materials. Since the viscous flow term in Equation (2.1) is in terms of pore radius squared while slip flow is proportional to the pore radius, the slip flow term (second term in 2.1) may be dropped from the equation, and the molar flux in vapor extraction systems can be described by a form of Darcy's Law where the hydraulic gradient is replaced

by the pressure gradient (Massmann, 1989). However, since Darcy's law assumes viscous flow, slip flow must be minimal as predicted by the type media. Therefore, the velocity of the air-phase in terms of pressure gradient is expressed in the following form (Massmann, 1989):

$$\overline{V}=k_{air}\frac{\nabla P}{\epsilon\mu_{air}} \qquad (2.2)$$

where,

$\overline{V}$ = air-phase velocity (L T^{-1})

k_{air} = soil permeability of air flow (L^2)

ϵ = air-filled soil porosity (dimensionless)

∇P = absolute pressure gradient (M L^{-1} T^{-2} per L of length)

μ_{air} = viscosity of air (M L^{-1} T^{-1})

An important indicator of the validity of Darcy's Law is the Reynolds Number written in terms of air transport. Usually Darcy's Law is valid if $1 < R_e < 10$ for groundwater. Findings of air-flow experiments conducted to determine validity in sand columns by Yu (1985) indicates that Darcy's Law is still valid for $R_e < 6$ (Baehr and Hult, 1991).

The continuity equation is another basic law incorporated by vapor flow models. The continuity equation can be

expressed in the following form (Johnson et al., 1990b):

$$\frac{\partial(\epsilon\rho b)}{\partial t} = -\nabla\cdot(\rho b V) \qquad (2.3)$$

where,

ρ = vapor density (ML^{-3})

V = vapor "Darcy" velocity (LT^{-1})

b = stratum thickness (L)

t = time (T)

The ideal-gas law is considered valid so that soil vapor density can be represented through the pressure and temperature in the following form:

$$\rho = \frac{PW_a}{RT} \qquad (2.4)$$

where,

W_a = average molecular weight (M $Mole^{-1}$)

All of the above mentioned governing processes and laws (slip and viscous flow, Darcy's Law, the continuity equation, and the ideal-gas law) are basic components to governing equations

from which solution techniques are derived.

The equation for transient flow of an ideal gas expressed in terms of the pressure squared is obtained by substituting the density as a function of pressure and Darcy's Law into the continuity equation (Johnson et al., 1990b):

$$\left(\frac{2\epsilon\mu_{air}}{k_{air}}\right)\frac{\partial P}{\partial t}=\nabla^2 P^2 \qquad (2.5)$$

The above equation can be simplified by assuming that the pressure squared term is negligible because the minimum absolute pressure at SVE extraction wells usually varies from 0.80 to 0.90 atmospheres (Massmann, 1989). By definition the pressure drawdown is expressed as follows:

$$P' = P_{atm} - P \qquad (2.6)$$

where,

P' = pressure drawdown (atm)

P_{atm} = prevailing atmospheric pressure (atm)

P^2 in Equation (2.5) is eliminated by the following steps:

$$P^2 = P_{atm}^2 - 2P_{atm}P' + P'^2 \qquad (2.7)$$

Because $(P')^2$ is much less than the other terms, Equation

(2.7) is written as:

$$P^2 = P_{atm}^2 - 2P_{atm}P' \tag{2.8}$$

Incorporating Equation (2.8) into the second spatial derivative and P' into the time derivative of Equation (2.5) yields an equation for radial flow of an ideal gas as a function of P' (Johnson et al., 1990b):

$$\left(\frac{\epsilon\mu_{air}}{k_{air}P_{atm}}\right)\frac{\partial P'}{\partial t} = \frac{1}{r}\frac{\partial}{\partial r}\left(r\frac{\partial P'}{\partial r}\right) \tag{2.9}$$

where,

r = radial distance from the extraction well at a point on the cone of depression (L)

If Equation (2.7) were substituted into Equation (2.5) then, the nonlinear term $(P')^2$ would make it difficult to develop analytical models which describe vapor transport in porous media.

Baehr and Hult (1988) use the same basic governing equations except the P^2 term is implemented by using a change of variable where $\phi = P^2$. Therefore, the following partial differential equation is obtained for radially symmetric geometry (Baehr and Hult, 1989):

$$\mu_{air}\epsilon\frac{1}{\sqrt{\Phi}}\frac{\partial\phi}{\partial t}-(k_r\frac{\partial^2\phi}{\partial r^2}+k_z\frac{\partial^2\phi}{\partial z^2}+k_r\frac{1}{r}\frac{\partial\phi}{\partial r})=0 \qquad (2.10)$$

where,

k_r = radial air permeability (L^2)

k_z = vertical air permeability (L^2)

2.4 SOLUTION TECHNIQUES

Each solution for k_{air} found in the literature has a unique set of assumptions, boundary conditions and simplifications. An awareness of this fact prevents the application of a technique in an inappropriate situation. The purpose of this section is to evaluate several solution techniques for both steady-state and transient conditions.

2.4.1 TRANSIENT SOLUTIONS

Massmann (1989) concluded that the use of groundwater flow models is appropriate for air flow in porous media when certain simplifying assumptions are applied. Note that Equation (2.9) is identical to the governing PDE for radial groundwater flow. Using the assumptions and simplifications presented by Johnson et al. (1988), Massmann (1989) derived the following equation for transient flow of an ideal gas in porous medium:

$$S_{s(air)}\frac{\partial P'}{\partial t}=\nabla\left(\frac{\rho g k_{air}}{\mu_{air}}\nabla P'\right) \qquad (2.11)$$

where,

$S_{s(air)}$ = air specific storage (L^{-1})

g = gravitational acceleration ($L\ T^{-2}$).

The specific storage for transport of gas in porous media is given by Massmann (1989):

$$S_{s(air)}=\frac{g\epsilon W}{RT} \qquad (2.12)$$

The fundamental difference between this equation for the flow of an ideal gas and the governing equation for groundwater flow is the dependence of gas density on pressure. Equation (2.11) compares favorably with the partial differential equation for transient flow of groundwater given by Freeze and Cherry (1979) in which P = h, $S_{s(air)}= S_s$, and K = $(k_{air}\rho g)/(\mu_{air})$ (Massmann, 1989):

$$S_s\frac{\partial h}{\partial t}=\nabla(K\nabla h) \qquad (2.13)$$

Thus, the transient solution for a confined and fully-penetrating well given by Theis (1935) is applicable to gas flow in porous media in the following form:

$$h-h_o=\frac{Q\mu_{air}}{4\pi g\rho_w k_{air} b}W(u) \qquad (2.14)$$

where,

$h_o - h$ = gas drawdown expressed in terms of water column (L) = $P'/g\rho_w$

$W(u)$ = Theis (1935) well function (dimensionless)

ρ_w = density of water ($M\ L^{-3}$)

u = $\frac{r^2\epsilon\mu_{air}}{4tk_{air}P_{atm}}$ (dimensionless)

The procedure for use of the above equation to determine the air permeability is basically a matter of substituting variables obtained from pneumatic tests. The following equation, which is a transformation of the above equation, gives k_{air}:

$$k_{air} = \frac{Q\mu_{air}}{b4\pi\rho_w g s^*} W(u)^* \qquad (2.15)$$

where,

s^* = (P'/γ_w) drawdown obtained from match point (L)

$W(u)^*$ = value of Theis well function obtained from match point (dimensionless)

Data obtained from pneumatic tests are volumetric flow rate (Q), drawdown at a point on a cone of air depression (s^*), and ambient and extraction well temperature (T_{atm} and T). The procedure to determine k_{air} in Equation (2.15) is as follows:

1). measure the volumetric flow rate (Q) and pressure (P_w) at the extraction well,

2). measure the ambient and extraction well vapor temperature (T_{atm} and T),

3). generate a log-log plot of drawdown versus time at an observation well at a distance, r, within the radius of influence of the well,

4). determine properties of vapor density and viscosity as a function of temperature (T) and pressure (P_w),

5). obtain s^* and $W(u)^*$ with a plot of drawdown versus time by matching type curves for the Theis well function.

For the SVE tests conducted at the Midway Landfill, Massmann (1989) used both the Theis (1935) and Hantush (1956) solution for groundwater pumping tests. An example of the application of the latter solution is also cited by Gibson et al. (1993). Analyses of drawdown from pneumatic tests indicate that the later-time pressure drawdown data matches the theoretical curves for a leaky aquifer better match than the Theis solution (Massmann, 1989).

Hantush's (1956) analytical solution for a fully-penetrating well leaky aquifer as applied to pneumatic tests is given by (Baehr and Hult, 1991):

$$k_{air} = \frac{Q\mu_{air}}{4\pi b s^* \gamma_w} W\left(\frac{r^2 S}{4Tt}, \frac{r}{B}\right)^* \qquad (2.16)$$

where,

B = $(k_{air} bb'/k_{air}')$ Hantush leakage factor (L^2)

b' = thickness of domain where leakage occurs (L)

k_{air}' = air permeability of confining unit (L^2)

$W(u,r/B)^*$ = value of Hantush well function obtained from match point (dimensionless)

For pneumatic tests the procedure for determining k_{air} is as follows:

1). measure the volumetric flow rate (Q) and pressure (P_w) at the extraction well,

2). measure the ambient and extraction well vapor temperature,

3). generate a log-log plot of drawdown versus time at an observation well at radial distance, r, within the radius of influence of the well,

4). determine properties of vapor density and viscosity as a function of temperature (T) and pressure (P_w),

5). obtain s^* and $W(u, r/B)^*$ with a plot of drawdown versus time by matching type curves for the Hantush well function,

6). determine the r/B^* value from the type curves to calculate k_{air}',

where,

$$k'_{air} = \left(\frac{r^*}{B}\right)^2 \frac{k_{air} b b'}{r^2} \qquad (2.17)$$

Also, additional means of analysis for using both steady and unsteady state solutions can be derived (Johnson et al., 1990a). The Theis-based solution (2.14) for the infinite confined aquifer can be written in the following form:

$$P' = \frac{Q}{4\pi b\left(\frac{k_{air}}{\mu_{air}}\right)} \int_{\frac{r^2 \epsilon \mu_{air}}{4 k_{air} P_{atm} t}}^{\infty} \frac{e^{-x}}{x} dx \qquad (2.18)$$

The infinite series expression for the well function integral can be approximated for $r_2 \epsilon \mu_{air} / 4 k_{air} P_{atm} t < 0.01$ (Johnson et al., 1990a):

$$P' = \frac{Q}{4\pi b \frac{k_{air}}{\mu_{air}}} \left[-0.5772 - \ln\left(\frac{r^2 \epsilon \mu_{air}}{4 k_{air} P_{atm}}\right) + \ln(t)\right] \qquad (2.19)$$

Note that u was printed as less than 0.10 for approximation of the above infinite series by Johnson et al., (1990a). The procedure for use of the above equation to determine the air permeability is as follows:

1). measure the volumetric flow rate (Q) and pressure at the extraction well (P_w),

2). measure the ambient and extraction well vapor temperature,

3). generate a semi-log plot of drawdown versus

time at an observation well at radial distance, r, within the radius of influence of the well,

4). determine properties of vapor density and viscosity as a function of temperature (T) and pressure (P_w),

5). determine the slope and the y-intercept of the plot,

where,

$$n=slope=\frac{Q}{4\pi b(\frac{k_{air}}{\mu_{air}})} \tag{2.20}$$

$$B=y\text{-}intercept=n\cdot(-0.5772-\ln(\frac{r^2\epsilon\mu_{air}}{4k_{air}P_{atm}})) \tag{2.21}$$

6). use the slope of the plot to determine the air permeability (Johnson et al., 1990a),

where,

$$k_{air}=\frac{Q\mu_{air}}{4n\pi b} \tag{2.22}$$

An alternative to determining the air permeability without use of the volumetric flow rate is to arrange Equation (2.21) in the following form (Johnson et al., 1990a):

$$k_{air} = \frac{r^2 \epsilon \mu_{air}}{4 P_{atm}} \exp\left(\frac{B}{n} + 0.5772\right) \qquad (2.23)$$

2.4.2 STEADY-STATE SOLUTIONS

Baehr and Hult (1991) derived an equation for air flow using the basic assumptions discussed above except air compressibility was incorporated. The assumptions made were Darcy's law for gas transport is valid for soil venting, soil gas temperature distribution is steady-state, and soil vapor acts as an ideal gas. In the case of compressible gases the change of variable of $\phi = P^2$ generates the equation for gas transport in linear terms. Hence, using the assumption that vapors act as an ideal gas, conservation of mass, and Darcy's Law for gas transport, the following partial differential equation in terms of cylindrical coordinates is given by (Baehr and Hult, 1991):

$$\mu_{air} \epsilon \frac{1}{\sqrt{\phi}} \frac{\partial \phi}{\partial t} = k_r \frac{\partial^2 \phi}{\partial r^2} + k_z \frac{\partial^2 \phi}{\partial z^2} + \left(\frac{\partial k_r}{\partial r} + \frac{1}{r} k_r\right) \frac{\partial \phi}{\partial r} \qquad (2.24)$$

$$+\left[2k_z\frac{Wg}{RT}+\frac{\partial k_z}{\partial z}-k_z\left(\frac{1}{T}\frac{\partial T}{\partial z}+\frac{1}{\mu_{air}}\frac{\partial \mu_{air}}{\partial z}\right)\right]\frac{\partial \phi}{\partial z}$$

$$+2\left[\frac{Wg}{RT}\left(\frac{\partial k_z}{\partial z}-k_z\frac{1}{\mu_{air}}\frac{\partial \mu_{air}}{\partial z}\right)-2k_z\frac{Wg}{RT}\frac{1}{T}\frac{\partial T}{\partial z}\right]\phi$$

Steady-state air-water distribution and only vertical soil temperature variation are additional assumptions. Baehr and Hult (1991) investigated estimations for Klinkenberg effects for hypothetical homogeneous and isotropic porous media. Nonlinear terms, which preclude the development of analytical solutions, are generated if the Klinkenberg effect (1941) is substituted into Equation (2.24). However, omitting Klinkenberg effects results in the elimination of nonlinear terms.

Equation (2.24) can be further simplified if the terms $\partial k_r/\partial r$ and $\partial k_z/\partial z$ are set equal to zero. Setting $\partial k_r/\partial r = 0$ would be justified only if lateral heterogeneity is present; meaning water redistribution caused by air transport would be neglected (Baehr and Hult, 1991). Also, setting $\partial k_z/\partial z = 0$ would be valid only if layered strata and moisture variation with depth were neglected (Baehr and Hult, 1991). Furthermore, the viscosity of an ideal gas is dependent on temperature in

the following form (Noggle, 1985; Baehr and Hult, 1991):

$$\frac{1}{\mu_{air}}\frac{\partial \mu_{air}}{\partial z} = \frac{1}{2T}\frac{\partial T}{\partial z} \qquad (2.25)$$

The above assumptions are incorporated into Equation (2.24) to generate the following partial differential equation describing steady-state, two-dimensional, axisymmetric air flow (Baehr and Hult, 1991):

$$\mu_{air}\epsilon\frac{1}{\sqrt{\Phi}}\frac{\partial \phi}{\partial t} = k_r\frac{\partial^2 \phi}{\partial r^2} + k_z\frac{\partial^2 \phi}{\partial z^2} + k_r\frac{1}{r}\frac{\partial \phi}{\partial r} \qquad (2.26)$$

$$-\left[\left(3/2k_z\left(\frac{1}{T}\frac{\partial T}{\partial z}\right)\frac{\partial \phi}{\partial z} + \left(5\frac{Wg}{RT}k_z\frac{1}{T}\frac{\partial T}{\partial z}\right)\phi\right] + \left(2k_z\frac{Wg}{RT}\right)\frac{\partial \phi}{\partial z}\right.$$

Additional assumptions include omitting temperature gradients and the elevation component of the total head (i.e., setting $\partial T/\partial z = 0$ and $\partial \phi/\partial z = 0$). Therefore, Equation (2.26) can be reduced to a form from which an analytical solution can be generated describing unsteady air flow in the following form (Baehr and Hult, 1989):

$$\mu_{air}\epsilon\frac{1}{\sqrt{\Phi}}\frac{\partial \phi}{\partial t} = \left(k_r\frac{\partial^2 \phi}{\partial r^2} + k_z\frac{\partial^2 \phi}{\partial z^2} + k_r\frac{1}{r}\frac{\partial \phi}{\partial r}\right) \qquad (2.27)$$

Furthermore, the leaky aquifer term after Hantush (1964) can be implemented to obtain the following differential equation (Baehr and Hult, 1989):

$$\mu_{air}\epsilon\frac{1}{\sqrt{\phi}}\frac{\partial\phi}{\partial t}=k_r\frac{\partial^2\phi}{\partial r^2}+k_z\frac{\partial^2\phi}{\partial z^2}+k_r\frac{1}{r}\frac{\partial\phi}{\partial r}-\frac{k'}{bb'}(\phi-P_{atm}) \qquad (2.28)$$

Baehr and Hult use Equations (2.27) and (2.28) with $\partial\phi/\partial t$ to derive analytical solutions for the evaluation of steady-state axisymmetrical air flow in porous media. The two analytical solutions consider the case of a domain in direct contact with atmospheric pressure and a domain separated from the atmosphere by a confining unit with land surface as an upper boundary in both cases, respectively (Baehr and Hult, 1991). A domain that is separated by a confining unit is the primary analytical solution of interest in this thesis. The following equation is the analytical solution to Equation (2.28) for a partially-penetrating extraction well (Baehr and Hult, 1991):

$$\phi=P_{atm}^2+\frac{aQ*}{\pi k_r r_w}\left(\frac{k_o(M_o\frac{r}{a})}{bM_o k_1(M_o\frac{r_w}{a})}+\frac{2}{\pi(1-d)}\sum_{n-1}^{\infty}\frac{1}{n}\left[\frac{\sin(\frac{n\pi 1}{b})-\sin(\frac{n\pi d}{b})}{M_n K_1(M_n\frac{r_w}{a})}\right]\right.$$

$$\left.\cdot K_o(M_n\frac{r}{a})\cos(\frac{n\pi z}{b})\right) \qquad (2.29)$$

where,

r_w = effective radius of well (L)

ϕ = air-phase pressure squared $(M\ L^{-1}\ T^{-2})^2$

$a = (k_r/k_z)^{1/2}$

$Q^* = (Q\mu RT)/W$

K_o = zero-order Bessel function of the first kind

K_1 = first-order Bessel function of the second kind

d = distance from lower confining unit to top of well screen (L)

l = distance from lower confining unit to bottom of well screen (L)

$M_n = [(m\pi/b)^2 + k'/bb'k_z]^{1/2}$

m = n - 1/2 (dimensionless)

Equation (2.29) incorporates other boundary conditions which include (Baehr and Hult, 1991):

$$\partial\phi/\partial z(r,0) = \partial\phi/\partial z(r,b) = 0,$$

$$\lim_{r\to\infty} \partial\phi/\partial z(r,z) = P^2_{atm}$$

and at $r = r_w$

$$\partial\phi/\partial r = 0 \text{ for } 0 < z < d,$$

$$\frac{\partial\phi}{\partial r} = \frac{-Q^*}{\pi k_r (l-d) r_w} \quad \text{for } d < z < l\ ,$$

$\partial\phi/\partial r = 0$ for $l < z < b$.

The analytical solution was implemented by Joss and Baehr (1993) in AIRTEST version 3.1; a Fortran program which determines the air permeabilities through a least squares analysis using pneumatic test data (see Appendix A). The procedure for using AIRTEST to determine air permeabilities is as follows:

1. select option to create a new data file in the main menu,
2. choose option to analyze full-scale permeability data,
3. substitute data into program obtained from pneumatic tests.

Another steady-state solution technique of interest in this discussion is posed by Johnson et al. (1990b). The model assumes radial, nonleaky flow, and steady-state conditions. The assumptions, as shown in previous techniques, use the basic continuity equation and Darcy's law as governing equations. Other assumptions made are that pressures are not significant enough to affect the soil matrix, changes in air permeability due to liquid removal are neglected, and vapors act as an ideal gas Johnson et al. (1990b).

If the left-hand side of Equation (2.9) is set equal zero

for steady-state conditions and the boundary conditions of P = P_w and P = P_{atm} at r = r_w and r = r_I, respectively, are incorporated, then the following equation is generated (Johnson et al., 1990b):

$$P^2(r) - P_W^2 = (P_{atm}^2 - P_W^2) \frac{\ln(\frac{r}{R_W})}{\ln(\frac{R_I}{R_W})} \qquad (2.30)$$

Johnson et al. (1990b) also expressed the solution in terms of the volumetric flow rate for homogenous media in the following form:

$$Q = b(\frac{\pi k_{air}}{\mu_{air}}) \frac{P_W[1 - (\frac{P_{atm}}{P_W})^2]}{\ln(\frac{R_W}{R_I})} \qquad (2.31)$$

Equation (2.31) is transformed into the following form to determine the air permeability for pneumatic test data:

$$k_{air} = (\frac{\mu_{air} Q}{b\pi}) \frac{\ln(\frac{R_W}{R_I})}{P_W[1 - (\frac{P_{atm}}{P_W})^2]} \qquad (2.32)$$

For pneumatic tests, the procedure for determining k_{air} is as

follows:

1). measure the volumetric flow rate (Q) and pressure at the extraction well (P_w),

2). measure the ambient and extraction well temperature,

3). generate a semi-log plot of drawdown versus radial distance to determine a radius of influence (R_I),

4). use the temperature to determine properties of the vapor density and viscosity as a function of the temperature (T) and pressure (P_w),

5). solve for k_{air} using Equation (2.32).

CHAPTER 3

FIELD SITE

The field site, owned by Ermo Marketing Company, is located in Columbia, S.C. at Port Oil Station No. 288 in the northeast corner of the intersection of Interstate 20 and Broad River Road (Figure 3.1). This region is in a northeast trending zone known as the Carolina Slate Belt; a region of low grade metamorphic rocks along a fall line which extends from Georgia through the Carolinas to Virginia (Johnson, 1972). The source of contamination at the site was a leaky underground storage tank. The following sections provide a history of site assessments, description of site topography, site geology, and site soil characteristics.

3.1 BACKGROUND

Several stages of a detailed site assessment have been conducted. A preliminary site assessment was submitted by Westinghouse Environmental and Geotechnical Services on December 12, 1989 (Law Environmental, Inc., 1991). Next, Law Environmental, Inc. was retained by Ermo Marketing Company to conduct a Phase II Site Assessment which began on February 18, 1991. Afterward, the gas station was closed on February 20, 1991 for reasons other than environmental concerns (Law Environmental, Inc., 1991). Recently, Law Environmental, Inc.

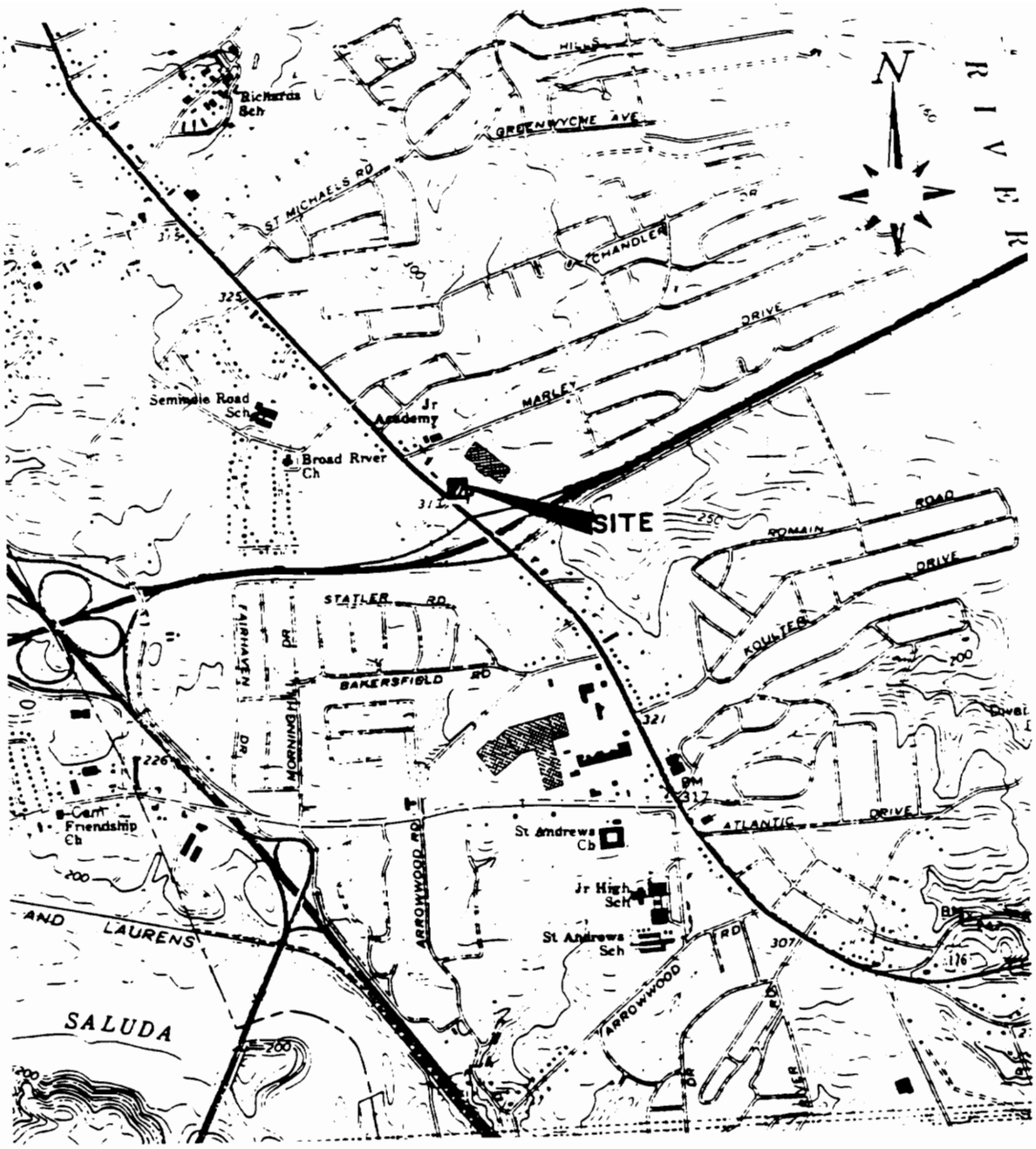

SOURCE: USGS 7.5 SERIES TOPOGRAPHIC QUANDRANGLE: COLUMBIA NORTH 1972

Figure 3.1: Topographic location of field site

carried out a Phase III assessment which was summarized in a report on April 16, 1992. Then, in September, 1992 a joint effort between USC/VT was initiated for investigation of the effective application of SVE-based technologies in Piedmont soil for VOC removal. The research in this thesis is part of an on-going extended site assessment which concentrates on the quantification of physical properties crucial to the full-scale SVE system (Widdowson et al., 1993).

3.2 SITE TOPOGRAPHY

The site is located on top of a ridge at an elevation of approximately 95.4 m (313 ft) above mean sea level (see Figure 3.1). Directly to the east is a parking lot which slopes downgradient and to the west is the Broad River Road on the ridge plateau. Southeast of the site is an Exxon Station. The Broad River is located 2134 m (6000 ft) east, and the Saluda River is located 2438 m (8000 ft) south.

3.3 SITE GEOLOGY

In a study of the Carolina Slate Belt, Johnson (1972) identifies geological conditions at the field site in Figure 3.2. The Carolina Slate Belt is a region of low grade metamorphic rock flanked on both sides by belts of medium grade metamorphic rock and is covered by Triassic basin red beds and Cretaceous and younger coastal plain sediments

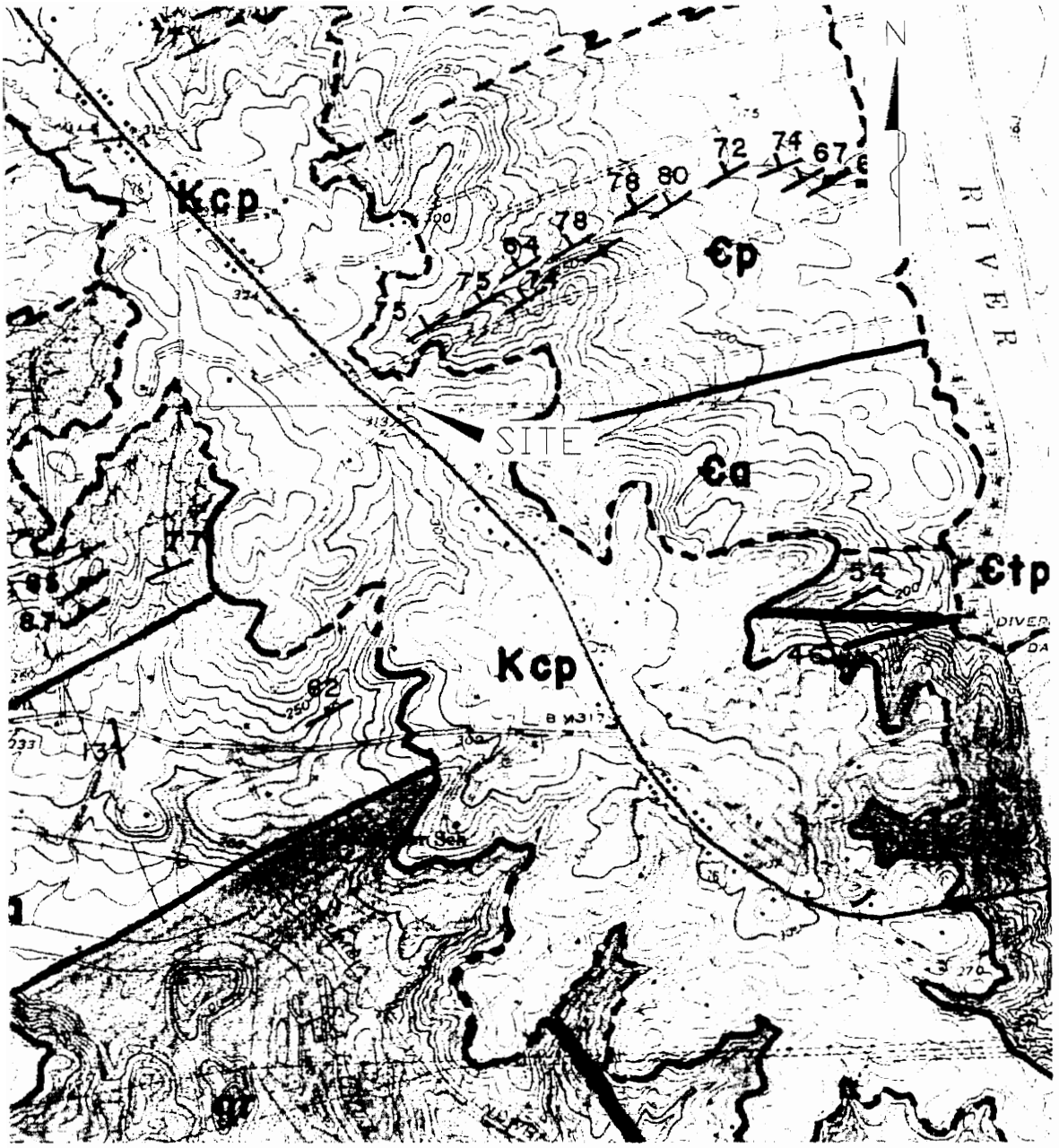

SCALE 1:24000

EXPLANATION:

Kcp - Coastal Plain Sediments	**gr** - Granite
ϵp - Evenly Laminated Phyllite	**ϵtp** - Tuffaceous Phyllite
ϵa - Amphibolite and Greenstone	

Figure 3.2: USGS map indicating field site geology (Johnson, 1972)

(Johnson, 1972). However, Law Environmental, Inc. (1991) describe subsurface soils encountered as indicative of those most likely associated with alluvium from the Broad and Saluda Rivers and the Tuscaloosa formation (Coastal Plain). The field site is located in an area of evenly laminated phyllite overlain by coastal plain sediment (Johnson, 1972). Evenly laminated phyllite in this region appears to have been originally deposited as alternating layers of silt and clay characterized by long continuous bedding laminations that vary from 1 mm to 1 cm in thickness (Johnson, 1972). At the location of pneumatic tests the laminated phyllite coarsens upward with increasing fine sand portions until there is an eventual change to a flaser bedded phyllite producing alternating layers of clay and fine sand (Johnson, 1972). Furthermore, quartz veins as quantified by Widdowson et al. (1993) are characteristic of the evenly laminated phyllite in numerous, but small quantities (Johnson, 1972).

3.4 SITE SOIL CHARACTERISTICS

As part of the extended site assessment Widdowson et al. (1993) identify the subsurface in terms of three distinct strata with increasing permeability with depth (Figure 3.3). The upper stratum (4.57 m or 15.0 ft) consists of mainly clay and silt intermixed in sand with a dark-red color. Also, quartz nodules of 6 to 7 mm (0.24 to 0.28 in.) in diameter,

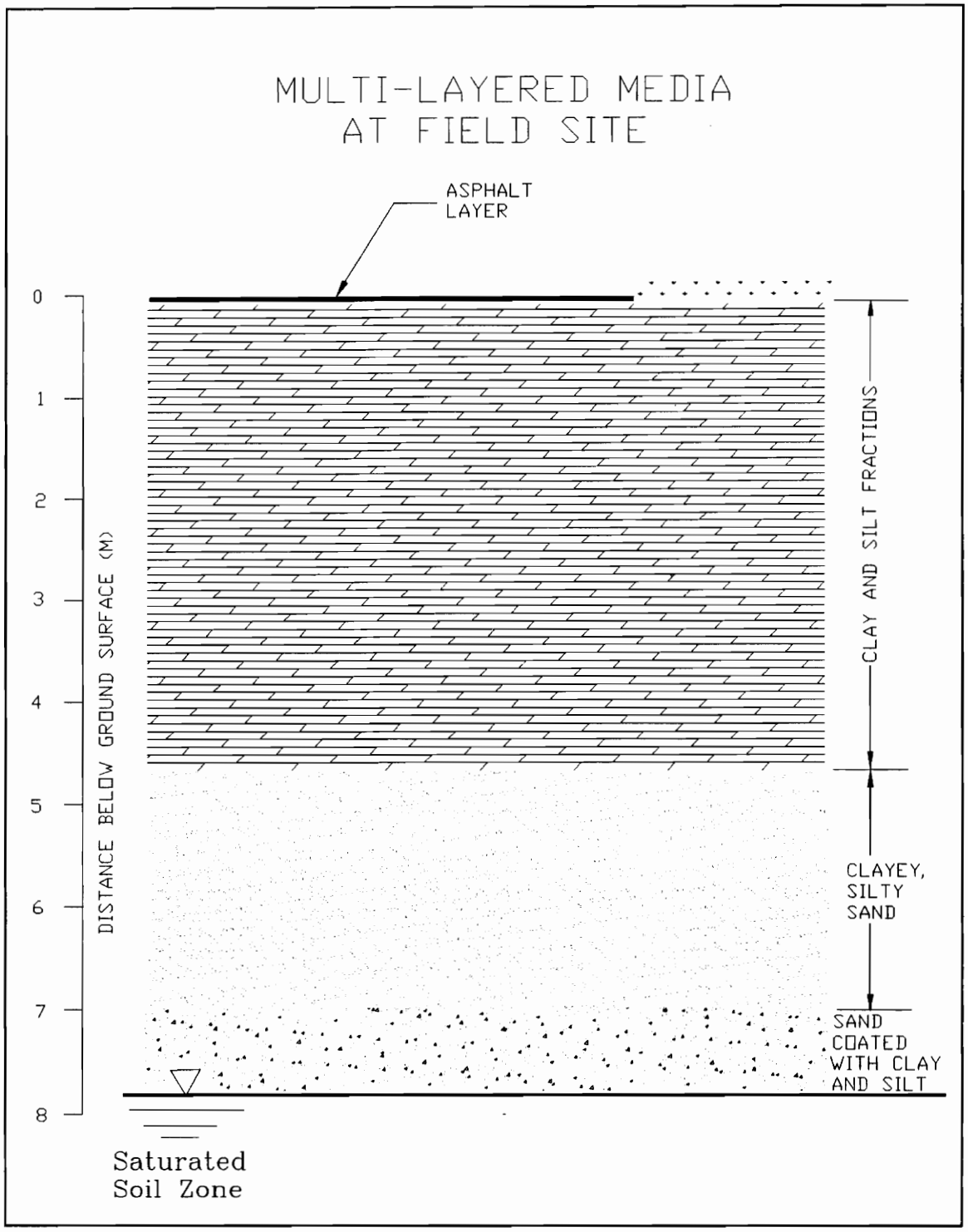

Figure 3.3: Multi-layered media in Carolina Slate Belt

increasing in number with depth, are distributed in the upper stratum. In the middle stratum (4.57 - 7.01 m or 15.0 - 22.0 ft.) sand particles increase, and the texture changes to a yellowish-red medium. Beyond 7.01 m (22.0 ft.) sand dominates the soil matrix and is coated with clay and silt. At approximately 9.14 m (30.0 ft.) gravel layers become noticeable and are intermixed with sand. The water table varies between 6.71 to 7.25 m (22.0 to 23.8 ft.) below the subsurface (Law Environmental Inc., 1991). Quartz veins of thickness ranging from 2.5 to 5.0 cm were encountered throughout the strata (Widdowson et al., 1993).

3.5 PHYSICAL PROPERTIES

Soil samples were collected by Widdowson et al. (1993) by means of a 5.72-cm (2.25-in) diameter drive-tube sampler inserted through a 15.9-cm (6.25-in.) hollow stem auger. Samples obtained were from 6.1 to 10.7 m below ground surface at 0.76-m (2.5-ft) intervals from bore holes labeled in Figure 3.4. Four 5.1-cm (2.0-in.) long brass sleeves were stacked within the drive-tube sampler; approximately 25-cm (10-in) samples were obtained by two of the four parts were utilized to obtain the saturated permeability along with other physical properties.

The following permeabilities were calculated from saturated hydraulic conductivities obtained from laboratory

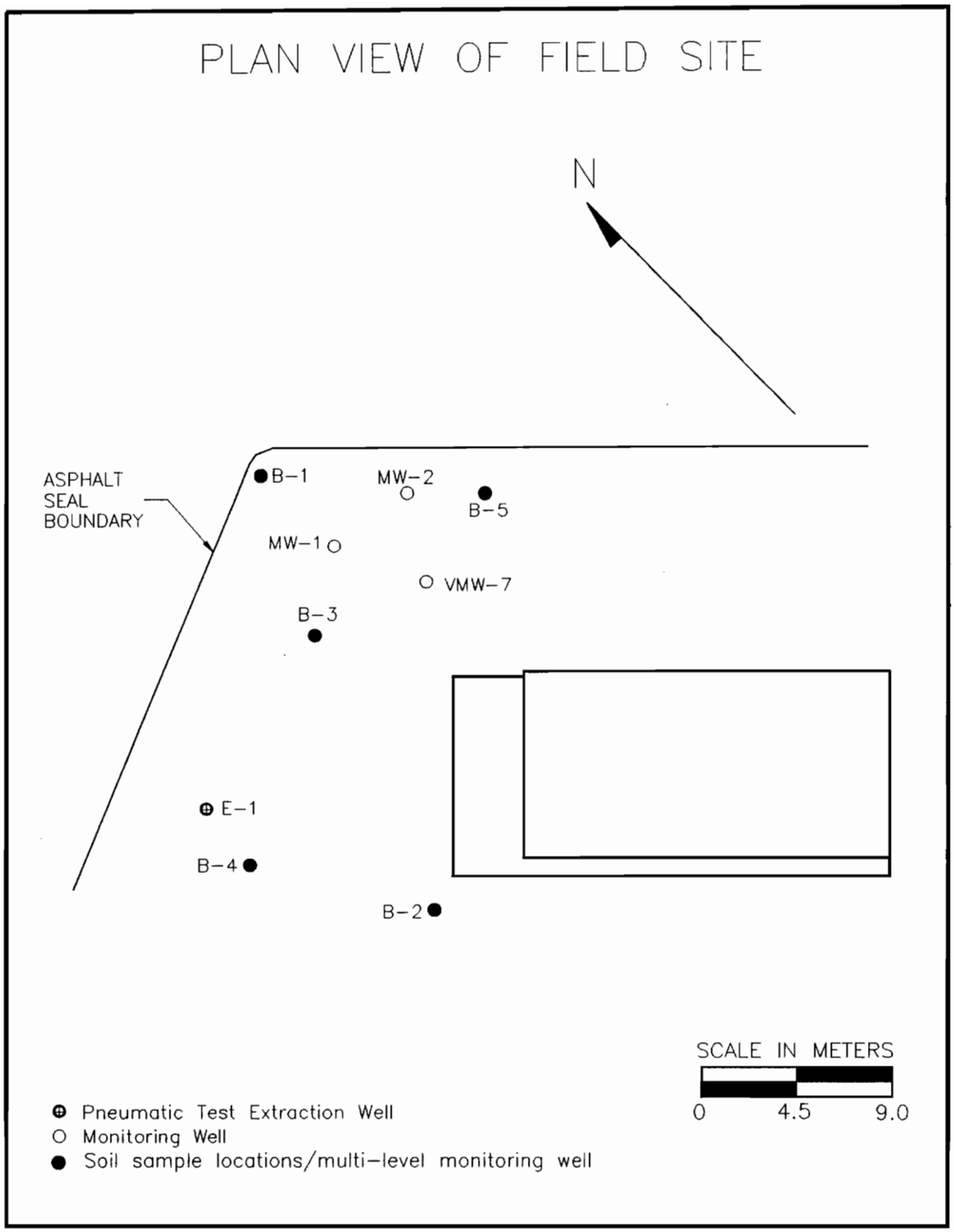

Figure 3.4: Plan view of field site

tests conducted on drive tube samples (see Table 3.1): k = 3.60×10^{-12} to 1.79×10^{-11} cm^2 for the clay and silt region (Widdowson et al., 1993). For the middle stratum permeabilities range from k = 1.79×10^{-11} to 1.79×10^{-9} cm^2. The lower stratum has permeabilities ranging from k = 3.60×10^{-10} to 3.60×10^{-9} cm^2. The range of the permeabilities were highly variable within each stratum; however, the middle stratum is the most variable.

The conversion factor to convert the saturated hydraulic conductivity to the gas permeability in dry soils is as follows (Massmann, 1989):

$$k_{air} = 1.04 \times 10^{-5} K_{sat} \qquad (3.1)$$

where,

k_{air} = air permeability in (cm^2)

K_{sat} = saturated hydraulic conductivity (cm s^{-1})

The above equation was used to convert K_{sat}, obtained from laboratory tests, to the intrinsic air permeability as a basis of comparison to those values from pneumatic tests presented in Chapter 7. Values obtained for the intrinsic air permeability are shown in Table 3.1.

Table 3.1: Saturated hydraulic conductivities and intrinsic air permeability

STRATUM NUMBER	DEPTH (m)	K_{SAT} (cm/s)	k_{air} (intrinsic) (cm^2)
1.0	4.57	3.52×10^{-7} to 1.75×10^{-6}	3.66×10^{-12} to 1.82×10^{-11}
2.0	4.57 to 6.71	1.75×10^{-6} to 1.75×10^{-4}	1.82×10^{-11} to 1.82×10^{-9}
3.0	6.71 to 10.67	3.53×10^{-5} to 3.53×10^{-4}	3.67×10^{-10} to 3.67×10^{-9}

A series of tests were conducted in the laboratory to determine specific characteristics of the lower stratum and the interface between the middle and lower stratum (Widdowson et al., 1993). Soil samples, obtained from the drive-tube sampler at bore hole #4 (B-4), at approximately 4.3 m (14.0 ft) southeast of the vacuum extraction well (E-1, see Figure 3.4) and 6.10 m (20.0 ft) below the ground surface provided the following physical properties: n = 0.407 - 0.456, k = 2.47 X 10^{-9} to 3.23 X 10^{-9} cm^2, and e = 0.687 - 0.837 (see Figure 3.4). The porosity, (n), indicates that voids make up close to half the total volume of the solid.

Since the volume of voids is made of both the volume of

air and water, there can be a high intrinsic air permeability according to the degree of saturation. Furthermore, weather conditions can have an effect on the degree of saturation. Therefore, the presence of moisture in the soil pores will cause the air porosity to be less than the total porosity Massmann (1989). The following relationship is used to relate air porosity to the total porosity (Massmann, 1989):

$$\epsilon = n_t(1-S) \qquad (3.2)$$

where,

n_t = total porosity

S = the degree of saturation

Tests conducted by Widdowson et al. (1993) in the laboratory determined the source of a wide range of conductivities in the same soil stratum. A possible explanation was identified by variations in minerals. Also, it was noticed by Widdowson et al. (1993) that the middle stratum had misaligned seams which may explain discontinuity in high-conductivity soils. The middle stratum is of specific interest due to the fact that the variation in the conductivities were widely variable (Widdowson et al., 1993). Causes for variations in this stratum are attributed to discontinuous seams and variation in mineral content. Furthermore, according to the previous description of soil

characteristics within each stratum, deviations in hydraulic conductivities make sense.

CHAPTER 4

EXPERIMENTAL APPARATUS AND PROCEDURE

The test setup consists of the following components: multi-level extraction well, multi-level (ML) pressure monitoring wells, the vacuum system, and data acquisition components. Compatibility and accuracy of system components are of significance. Compatibility ensures that the measuring devices can relay a signal that can be accepted by the data acquisition system. Accuracy is achieved by properly identifying the tolerance of the measuring devices of data acquisition components. Taking into account these considerations can ensure the most accurate data on conditions during pneumatic tests. The following sections of this chapter will concentrate on detailed description of test design, system components, and procedural methods.

4.1 OVERVIEW OF TEST DESIGN

The first step in the design process was the choice of location for the extraction well as discussed in Chapter 3. Site-specific soil stratifications and boundary conditions were obtained from bore hole analyses as discussed in Chapter 3. Figure 4.1 displays the position of the extraction well with ML pressure monitoring wells in the multi-layered media at the field site. The extraction well was located in a

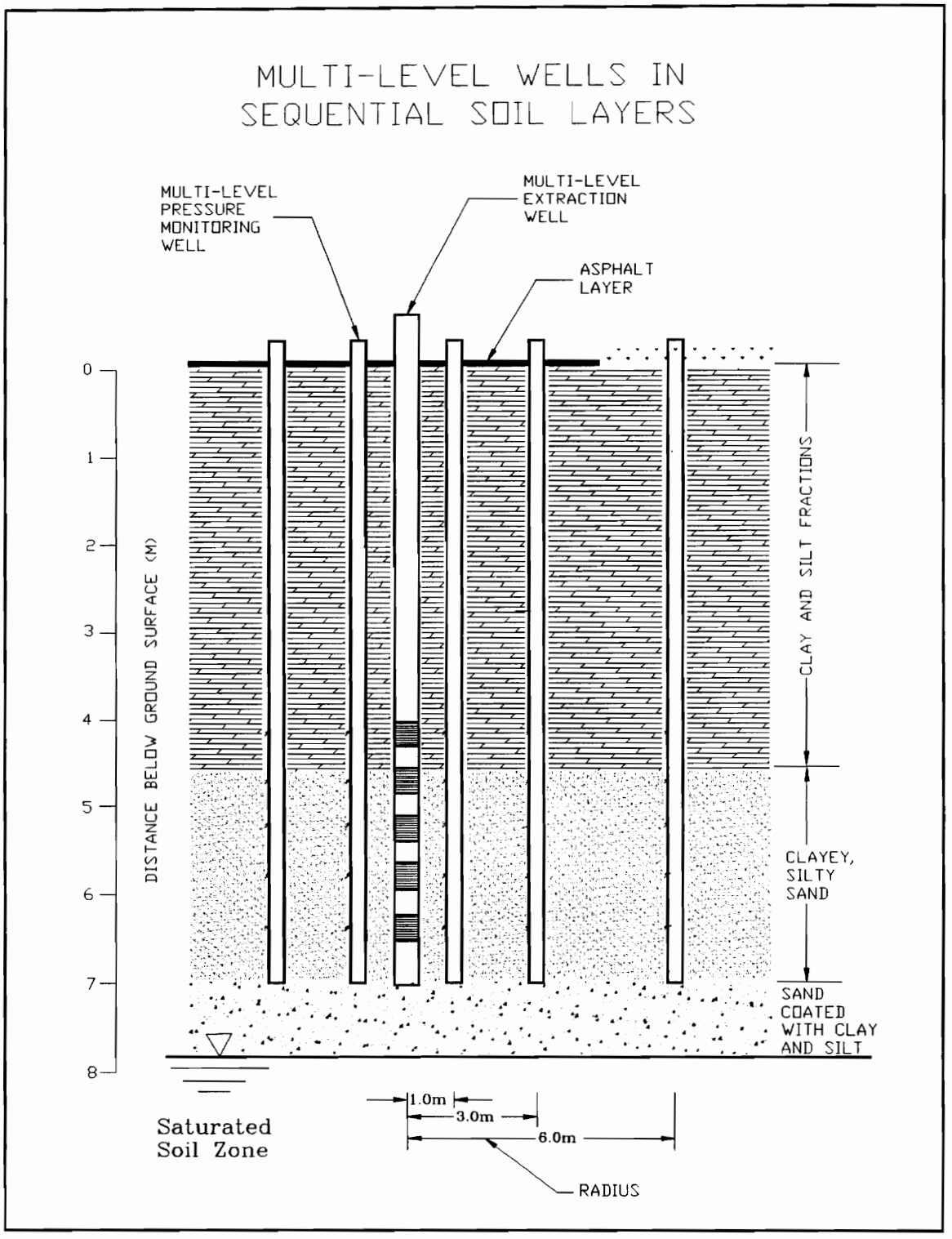

Figure 4.1: ML extraction and pressure monitoring wells in multi-layered media in Carolina Slate Belt

11.43-cm (4.5-in.) bore hole near the surface seal, as shown in Figure 4.2, so that air flow through and from outer the edges of the surface seal could be modeled, but also at a sufficient distance to avoid extraction of heavily-contaminated soil vapors. As noted by Widdowson et al. (1993) variations in soil composition caused hydrodynamic properties to vary; however, the characteristics tend to even out over a large scale. Thus, it is assumed that air-phase permeability measured at the extraction well was indicative of air permeabilities characteristics of the site source area.

Intermittent layers of filter sand and bentonite at the extraction well were designed to allow for multi-level extraction in the vadose zone. Pneumatic packers (Aardvark Corporation, Inc.) were utilized to isolate the screens within the extraction well and allow individual layers of the subsurface to be investigated. The vacuum system setup consisted of two different packer arrangements. The single packer arrangement was utilized to investigate the lowest screen (screened interval #1). The second arrangement consisted of a double packer assembly to allow pneumatic tests to be conducted in the remaining screened intervals. The packers were arranged in the extraction well according to the sequential soil layer under investigation and connected to a system of pipes which lead from the uppermost packer to the vacuum pump.

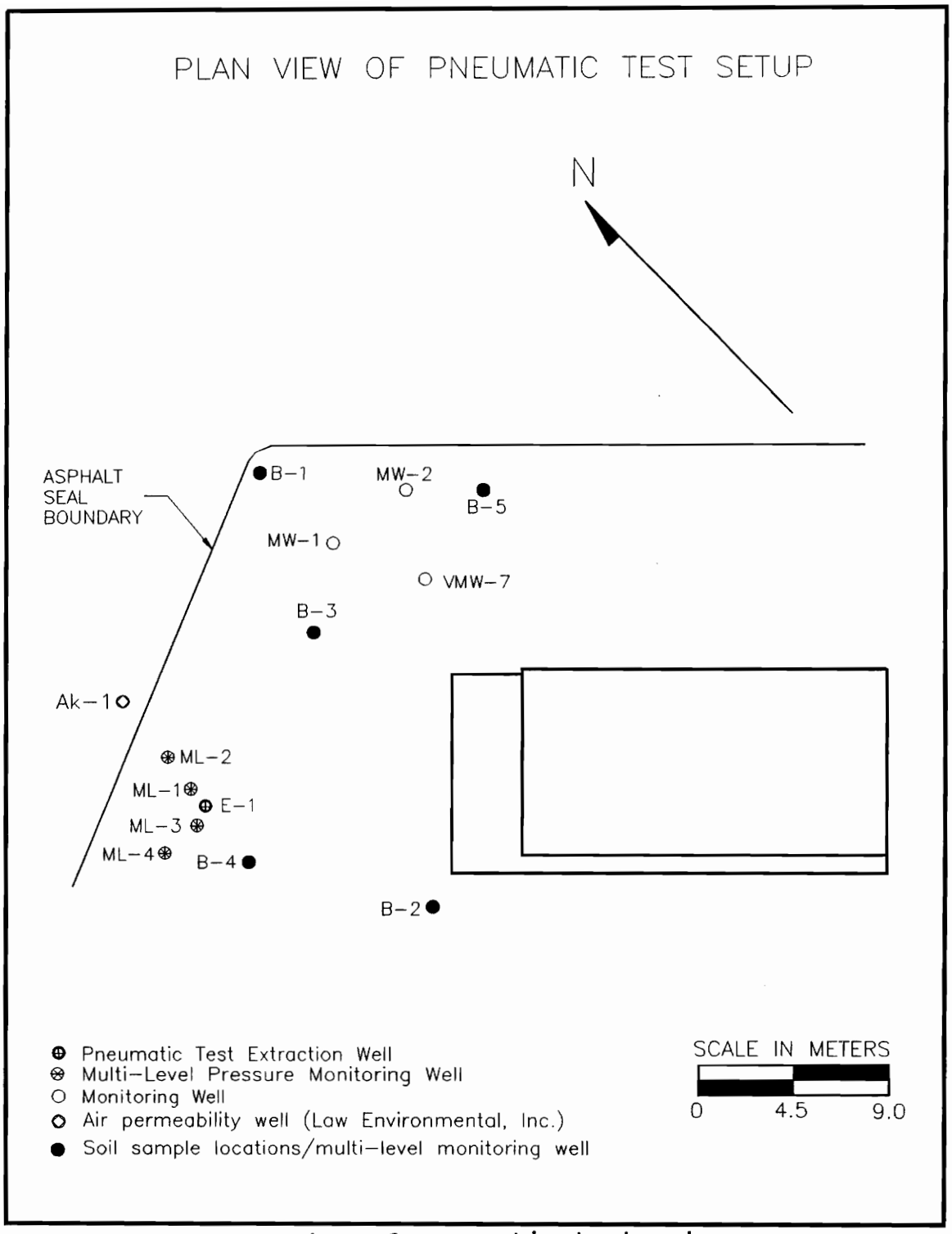

Figure 4.2: Plan view of pneumatic test setup

Five multi-level pressure monitoring wells were installed to monitor pressure drawdown during tests. Nanjunjeswar et al. (1989) suggested multi-level monitoring wells be spaced at the following radial intervals according to the soil types: in silt/clay 1.5, 3.0, and 4.5 m; in silty sand 3.0, 6.0, and 9.0 m; and in sandy soils 6.0, 12.0, and 18.0 m. According to field site soil characteristics, the suggested radial distance were utilized to determine the spacing of monitoring wells. Pressure monitoring wells were placed along three radii with two monitoring wells on each of the inner (1.0 and 3.0 m) radii and one well on the outer radius (6.0 m). Two axes, located 90^0 apart, were identified in order to detect leakage of air through the surface seal and passage of air from the outer edges of the sealed perimeter.

The implementation of the data acquisition system with the vacuum system was achieved through a series of ports tapped into the vacuum line. The ports tapped for the measurement of velocity and temperature were specially fabricated. Since both measuring devices required that a probe be inserted into the stream of air flow, a thermocouple fitting supplied by Smith and Brooks, Inc. (part #FH4BZ) was utilized. This type connection provided easy removal of a probe while at the same time providing an air tight connection. For the measurement of pressure at the extraction well head a Parker brass part #68P4-4 (Smith and Brooks, Inc.)

fitting was screwed into a hole that was tapped into the vacuum line.

4.2 WELL CONSTRUCTION DETAILS

The extraction well was constructed with Tri-Loc Schedule 5 stainless steel pipe. As shown in Figure 4.3, the well consisted of a 5.08-cm X 45.72-cm (2-in. X 18-in.) sump with a 5.08-cm (2-in.) male cap. A series of five slotted 5.08-cm X 30.48-cm (2-in. X 12-in.) screens with standard slot openings of 0.05-cm (0.02-in.) were separated by four 5.08-cm X 30.38-cm (2-in. X 12-in.) solid stainless steel sections. Connections between sections were Tri-Loc threaded with flush joints and rubber o-rings used as a sealant. The total depth of the screened and solid sections made up 3.12 m (10.25 ft.) of the total 7.67-m (25.2-ft.) extraction well length. The remaining casing consisted of three 5.08-cm X 1.52-m (2-in. X 5-ft.) sections. Puregold Chip (Part # T-21910) was used as a sealant between the bore-hole wall and the extraction well in layers between screened intervals (Figure 4.3). An appropriate sand filter was identified to act as a filter between the bore hole wall and well screen. The first 0.86-m (2.83-ft) sand filter was added in the well annulus between the first screen and bore-hole bottom. A tag line was lowered down into the well annulus to determine if proper portions of

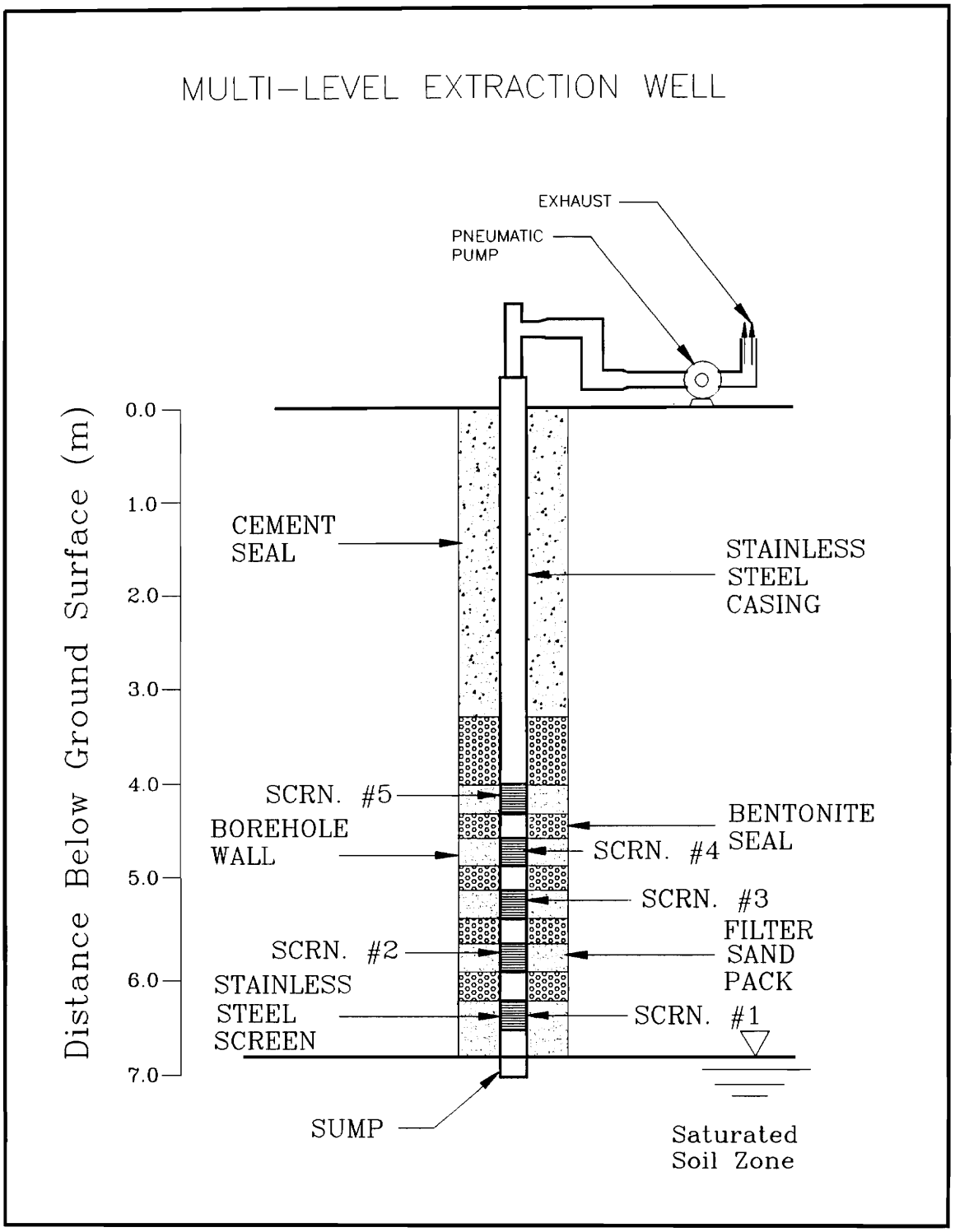

Figure 4.3: Multi-level extraction well

either bentonite or sand filter were added. Bentonite seals and sand filters between screened intervals were typically 0.33 m (1.1 ft) and 0.34 m (1.13 ft), respectively. Proper portions of the bentonite chip were added taking into consideration volumetric expansion upon addition of water. Additionally, a cement seal was added at the top of the grout seal above multi-level screen #5 to reduce infiltration of surface runoff. Dimensions of the Puregold Chip and sand filter can be found on Figure 4.3. The extraction well extended 0.61 m (2.0 ft.) above the ground surface and was capped with a stainless steel cap to prevent rainfall or objects from entering into the extraction well.

Multi-level pressure monitoring wells were constructed with 2.54-cm (1.0-in.) O.D. solid Tri-Loc PVC pipe, 0.64-cm O.D. (1/4-in.) polyethylene tubing, geotextile fabric, duct tape, and plumber's putty (Figure 4.4). Monitoring points within the multi-level wells were spaced at approximately 60.96-cm (2.0-ft.) intervals and situated adjacent to extraction well screened intervals at specified radial distances. An exception was monitoring point #6 (Figure 4.4) which was situated approximately 0.61-m (2.0-ft.) above the extraction well screened interval #5. The following procedure was used to construct a single monitoring point:

(1) a single hole was drilled in the PVC pipe at a desired location (e.g., monitoring point #1);

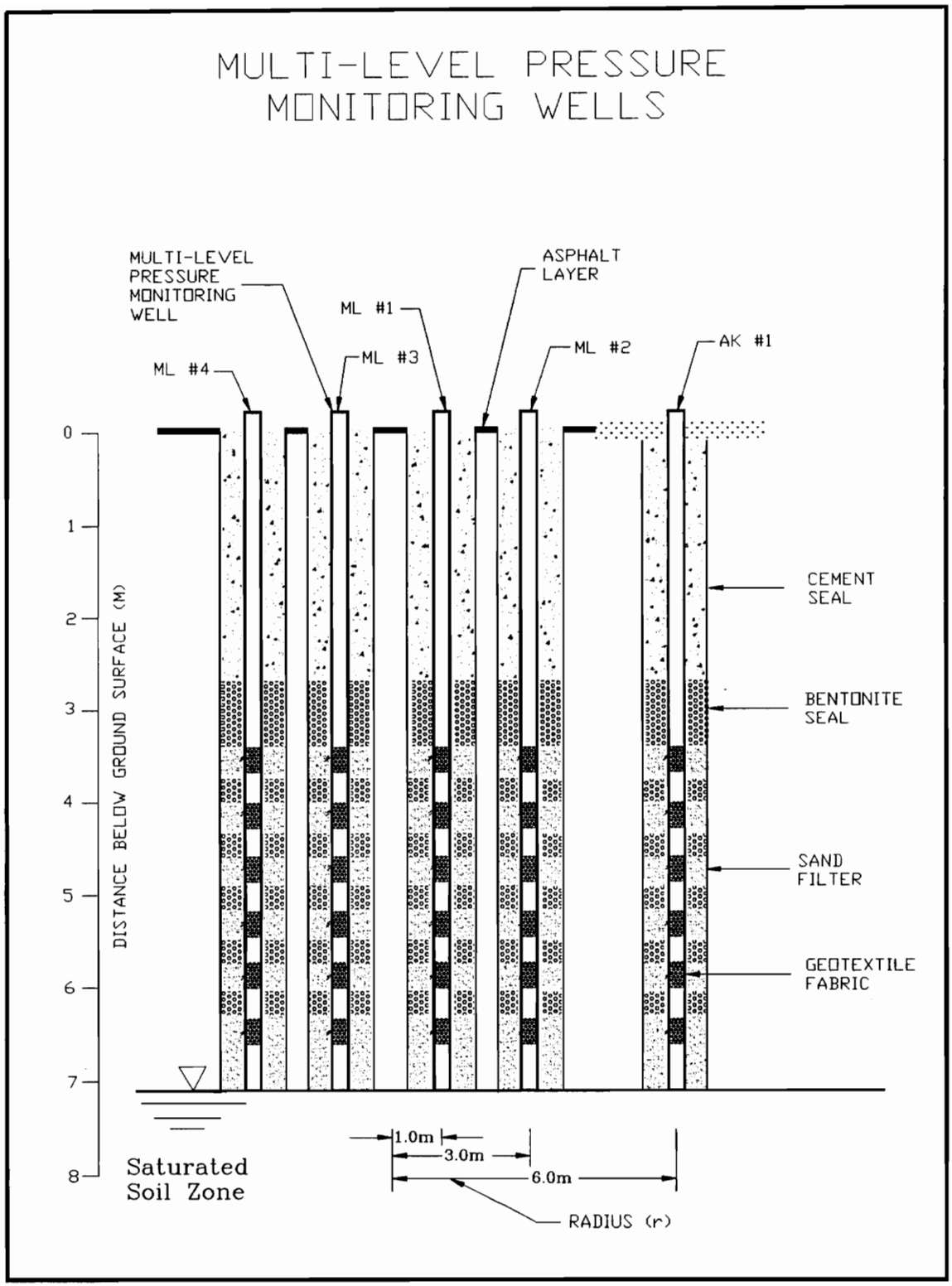

Figure 4.4 Multi-level pressure monitoring wells

(2) the 0.64-cm (1/4-in.) O.D. polyethylene tubing was then inserted through the hole in the PVC pipe;

(3) tubing was pushed through the drilled hole and out the end of PVC pipe that would extend above the ground surface (well head) until approximately 0.61 m (2.0 ft) was extending out;

(4) the polyethylene tubing was then clipped at the monitoring point so that 2.54 cm (1.0 in)of tubing was projecting out;

(5) plumber's putty was used to seal the annulus between the tubing and drilled hole;

(6) to avoid possible clogging of tubing by debris, the extending polyethylene tube (probe) was wrapped in an approximately 10.16-cm wide X 5.08-cm long strip of geotextile fabric;

(7) duct tape was used to affix the geotextile in place without hindering the passage of air flow;

(8) the pressure monitoring probe was completed by adding a Swage-Loc fitting to the 0.61-m (2.0-ft.) piece of tubing extending out of the well head;

(9) repeat the above procedure for the remaining five pressure monitoring locations to complete one multi-level pressure monitoring well.

After completion, the multi-level pressure monitoring well was

placed in the bore hole and set so that monitoring points were the proper distance from the ground surface. Filter sand was added in the well annulus to a desired thickness above the first monitoring point. Next, bentonite seals and sand filters between and adjacent to monitoring points were added sequentially, typically 0.30-m (1-ft) and 0.34-m (1.12-ft) in thickness, respectively (see Figure 4.4). To complete the multi-level pressure monitoring wells a cement seal was added on top of the grout seal above pressure monitoring point #6.

4.3 DATA ACQUISITION

The most critical concern was compatibility between the measuring instruments and datalogger, i.e., programmability and data transfer. The CR10 datalogger (a product of Campbell Scientific, Inc.) was chosen to log data. The CR10 allows real-time measurement of up to six channels of data. For the pneumatic tests this included: the well head temperature, two multi-level pressure monitoring-wells and extraction-well vacuum pressures, and air velocity of the air stream flowing out of the extraction well.

4.3.1 SETUP

In addition to monitoring the layers most influenced by the vacuum system, gauges were installed to measure any pressure readings above and below sequential soil layers

(Figure 4.5). Magnehelic vacuum gauges of various ranges were installed to monitor pressure in these layers. Also, a slack tube manometers model #1211-200 and #1211-50 (Dwyer Instruments, Inc.) served as means to check vacuum pressures obtained from the pressure transducers.

Electronic and manual measurement of vacuum pressures within layers of influence at ML pressure monitoring wells #1 and #3 was accomplished using two Omega (model #PX236-005G V) pressure transducers with a 0 to 34.5-KPag (0 to 5-psig) range and two magnehelic gauges (model #2000-25CM, Dwyer Instruments, Inc.) with a 0 to 25-cm range, respectively. For the pneumatic test conducted at screened interval #1 (710.18 cm below the ground surface) the following setup was used to monitor drawdown:

(1) at ML #1-1 (ML pressure monitoring well #1 at monitoring point #1) a 0.64-cm O.D. piece of polyethylene tubing with a Swage-Loc nut and ferrule on each end was connected to the extending piece of tubing at the well head representing monitoring point #1;

(2) the tubing was then branched off using a Smith and Brooks, Inc. part #164C-4 union tee, with one line leading to the magnehelic gauge (0-25 cm) and the other to the pressure transducer;

(3) the same procedure was then used to setup ML #3-1 to measure pressure drawdown;

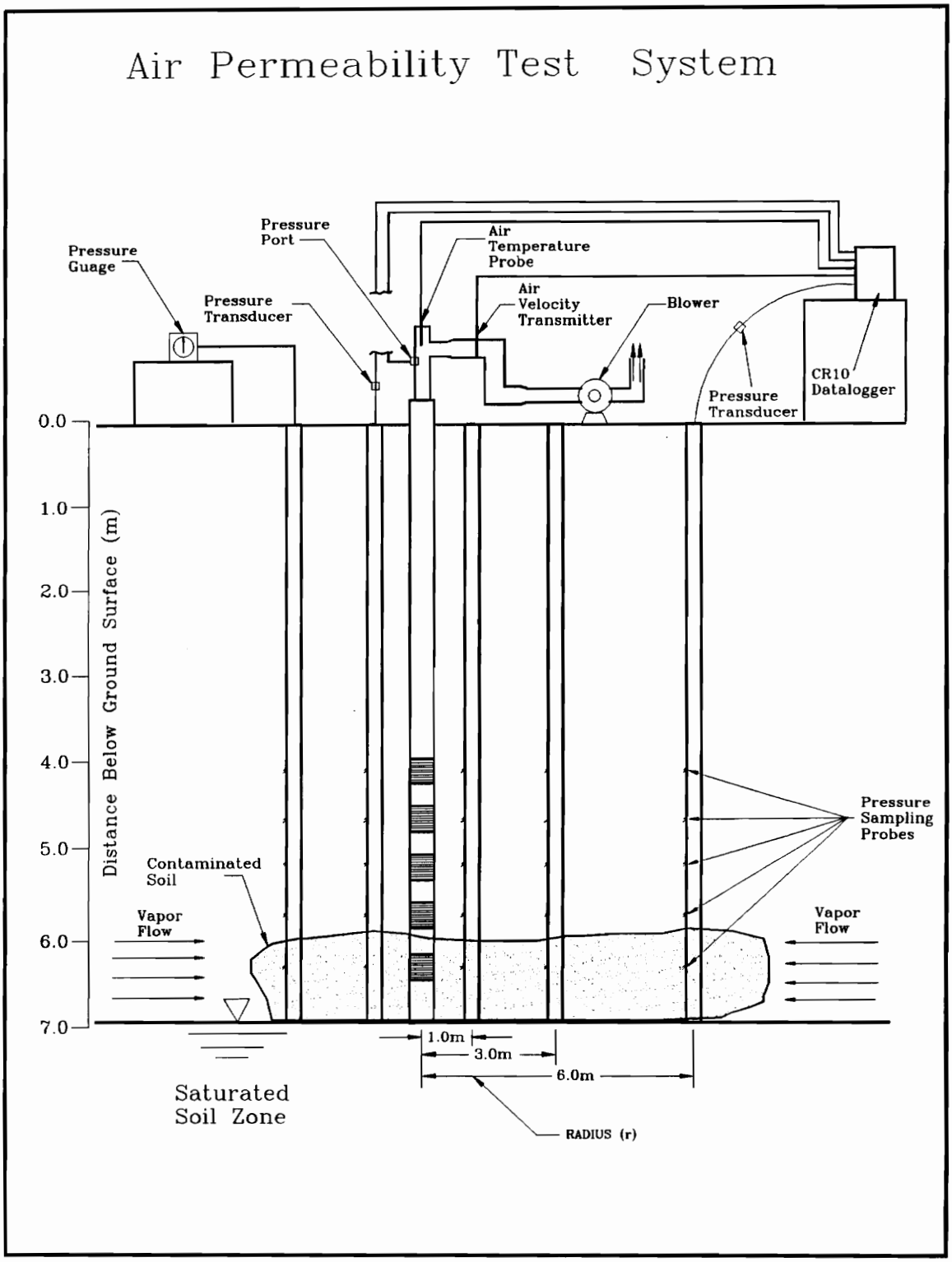

Figure 4.5 Pneumatic test arrangement

(4) drawdown data in adjacent sequential layers were measured using specified magnahelic gauges (Dwyer Instruments, Inc.) and strands of 0.64-cm O.D. polyethylene tubing cut in appropriate lengths;

(5) the following ML location were monitored with listed magnahelic gauges: ML #1-2 (model #2000-100MM, 0-100mm), ML #1-3 (model #2000-50MM, 0-50mm), ML #3-2 (model #2000-100MM, 0-100mm), ML #3-3 (model #2000-50MM, 0-50mm);

(6) also, ML #4-1 pressure drawdown was monitored using a slack tube manometer model # 1211-50 with a 25-0-25-cm range.

Pressure at the extraction well was measured by taking an appropriate length of 0.64-cm O.D. polyethylene tubing with a Swage-Loc nut and ferrule on one end and connecting it to the air tight port in the vacuum line (see Figure 4.6). Then the tubing was branched off with one line leading to a magnehelic gauge model #2210 (0-68.95 KPag or 0-10 psig) and the other leading to an Omega model #PX6303-30VAC5V pressure transducer.

An Air Velocity Transmitter (Series 640, by Dwyer Instruments, Inc.) was used to measure velocity. The probe attached to the transmitter was connected to the thermocouple fitting on the vacuum line, set in place, and sealed off. Finally, temperature was measured using a model #107-U air temperature probe supplied by Campbell Scientific, Inc. This

temperature probe was inserted in the other thermocouple fitting in the vacuum line.

4.3.2 WIRING AND PROGRAMMING

Because the CR10 has a limitation of 2.5 volts for the maximum input and excitation voltage, adjustments were required according to the device. Since the output voltage of the Omega model #PX6303-30VAC5V pressure transducer was 5.0 volts, a voltage divider was added to reduce the input voltage to the CR10. Also, the velocity transmitter provided a 4-20-mA output signal that was converted to a differential voltage by means of a 125-ohm resister with a 0.01% tolerance. After making these adjustments to the measuring devices, each component was wired to a channel in the CR10 interface.

An input program (see Appendix B) to be downloaded to the CR10 was then designed to read various devices and convert voltage readings to appropriate units of measurement. Calibration of each transducer was conducted to define an offset and multiplier. These values were inserted into an instruction in the program. For the Omega model #PX236-005G V pressure transducers a program instruction for a full bridge voltage was added to the program. A differential voltage instruction was added to the program to establish communication with the Omega model #PX6303-30VAC5V pressure transducer. The single-ended voltage output from the

temperature probe was converted to a reading of degrees fahrenheit or celsius by means of another instruction in the program. Also, according to the range of velocity transmitter, a differential voltage instruction was added to the program to read the voltage output.

4.4 VACUUM SYSTEM

The layout of the vapor extraction system was unique in its setup as shown in Figures 4.6 and 4.7. The pneumatic packer assembly (model #23B-30-510) consisted of two sliding heads that expanded radially and contracted axially as pneumatic pressure was applied. The packer glands were very practical since the expanded rubber elements covered irregularities in the venting well (Aardvark Corporation, Inc.). Location of the screened interval in the multi-level extraction well was important in determining the packer assembly setup, either single or straddle packer. Regardless of the packer assembly a perforated tube threaded on each end was needed to allow passage of air through the bottom of the upper packer (single packer) or in between the upper and lower packer (straddle packer); upper packer being the packer above the screened interval during pneumatic tests.

Packers were connected a 30.48-cm (12-in.) long perforated 0.95-cm (3/8-in.) O.D. tube fabricated to provide a means for air flow through the screened intervals. Pressure

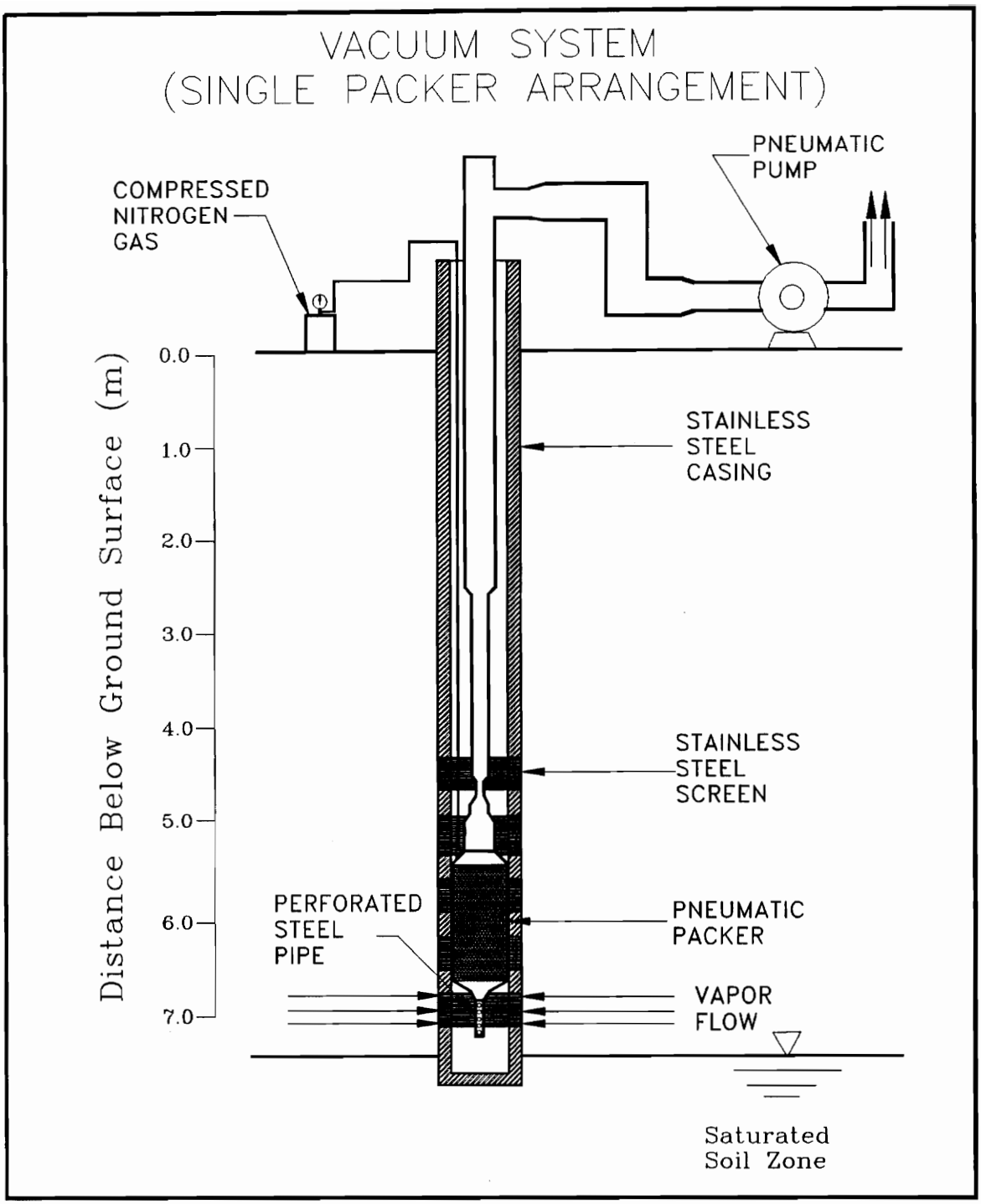

Figure 4.6: Single packer vacuum system arrangement

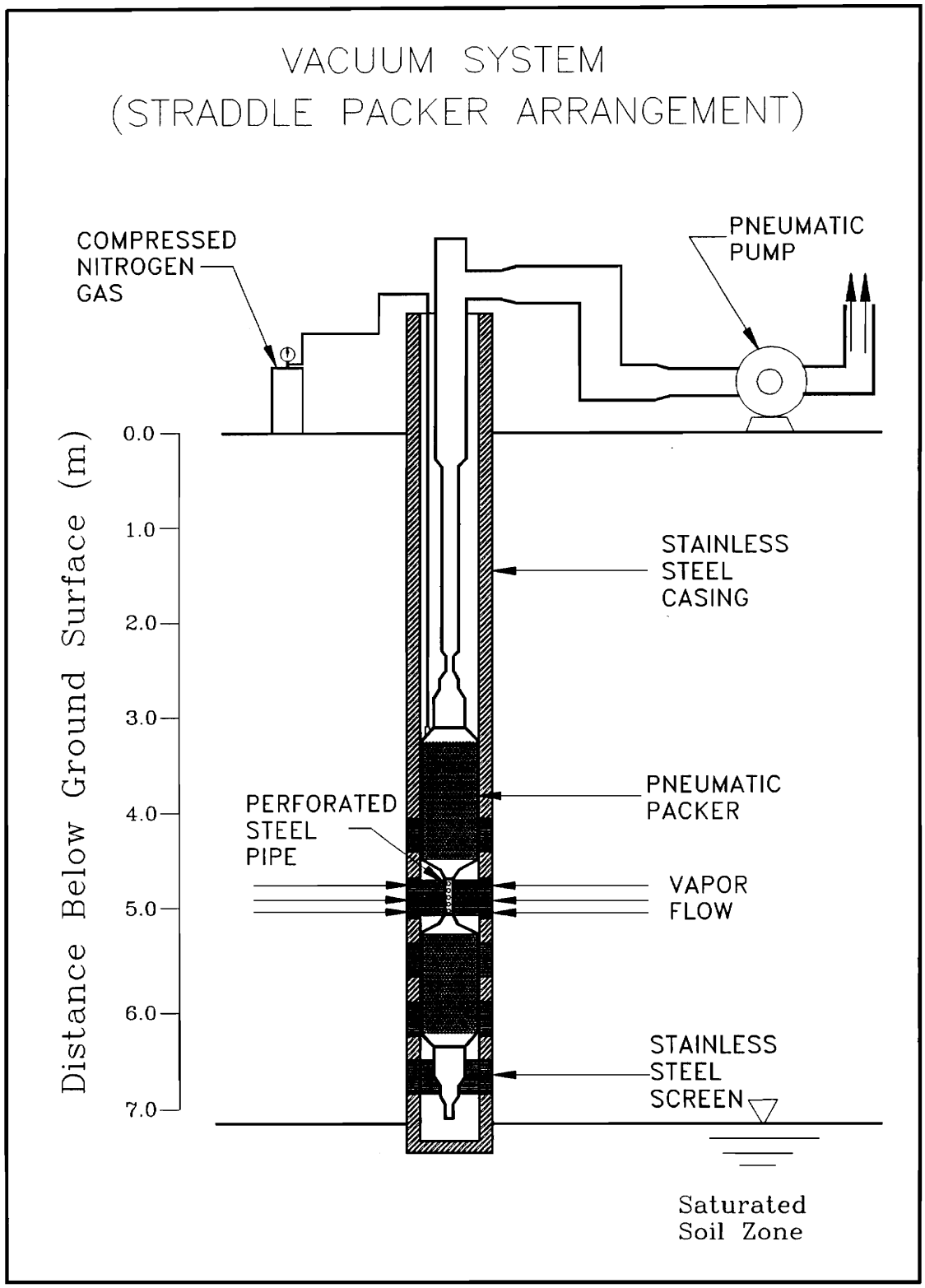

Figure 4.7: Straddle packer vacuum system arrangement

was applied to the packers by means of a compressed nitrogen tank with a regulator (0-10342 KPa or 0-1500 psi range). A quick disconnect valve was attached to the regulator to allow easy connecting and disconnecting of the nylon tubing leading to the top packer. The 0.48-cm (3/16-in.) O.D. nylon inflation tubing rated at a maximum pressure of 17237 KPa (2500 psi) was used to convey pneumatic pressure to the packers. A piece of 0.48-cm (3/16-in.) O.D. nylon tubing approximately 0.30-m (1.0-ft.) with nut and ferrules on each end was connected to fittings on the top and bottom of the upper and lower packer, respectively. In case of single packer operation the bottom end of nylon tubing was capped off. The tubing was attached to the upper packer before lowering the packer assembly down into the well. Connections between nylon tubing and the packers were made using air tight nut and ferrule fittings.

At the top of the uppermost packer a 0.95-cm (3/8-in.) male steel tube was connected to a 2.54-cm (1.0-in.) O.D. schedule 40 PVC pipe by means of several steel reducers. The length of this section was approximately 3.05-m (10.0-ft.) (Figure 4.7). When additional length was needed, as in the case of the lower screens, an adapter was used to change the 2.54-cm (1.0-in.) nominal diameter PVC pipe to 3.18-cm (1.25-in.) schedule 40 PVC pipe. In either case, the PVC section extended up to a PVC 90° elbow at the well head.

Approximately 0.13-m (0.43-ft.) below the elbow the Parker brass part #68P4-4 (Smith and Brooks, Inc.) was screwed into a tapped hole in the PVC pipe wall to allow monitoring of vacuum pressure (see Figure 4.5). At the top of the elbow a 0.64-cm (0.25-in.) hole was tapped and the thermocouple fitting supplied by Smith and Brooks, Inc. (part #FH4BZ) was screwed into place. Also, a plastic ferrule identical to the metal ferrule from the manufacture was used in the thermocouple fitting to obtain a better seal. The air temperature probe was inserted through the fitting.

At the well head a series of PVC couplings were used to increase the pipe size to 5.08-cm (2.0-in) to accommodate the blower inlet and to allow monitoring of air flow. Approximately five feet downstream of the 5.08-cm PVC pipe, an additional 0.79-cm (5/16-in.) thermocouple fitting was screwed into a tapped hole in the pipe line. This distance was designed to allow the formation of fully developed flow after the elbow. Afterward, the air velocity probe was inserted inside the fitting and sealed off.

4.5 TEST PROCEDURE

Proper test procedure was essential in generating results that accurately depicted conditions during the tests. The first step was to check and insure equipment was functioning properly. For a check list of pneumatic test equipment refer

to Appendix C. The next step was the assembly of the vacuum system. An initial check of air tight connections was important to prevent inaccurate measurements during the test. The desired depth of extraction was determined, and the packer(s) were assembled for either single or straddle packer operation. Then a 9.14-m long X 0.48-cm (3/16-in.) O.D. steel cable and the 0.48-cm (3/16-in.) nylon inflation tubing was connected to the packer(s). The 0.48-cm (3/16-in.) steel cable was used as a secondary means of pulling the vacuum system in case of packer failure. The 1.27-cm (1/2-in.) O.D. male threaded expansion joint was connected to the upper packer to increase the pipe size to 2.54-cm (1.0-in.) O.D. Tri-Loc PVC pipe. The number of 2.54-cm (1.0-in.) and 3.18-cm (1-1/4-in.) PVC sections were determined according to length needed to reach the extraction well head. The packer assembly was lowered into the extraction well by connecting 1.52-m (5-ft.) pipe sections to either 2.54-cm (1.0-in.) O.D. or 3.18-cm (1.25-in.) Tri-Loc PVC pipe. After reaching the desired depth with the packer assembly, the packers were inflated to specified pressure with a supply of compressed nitrogen gas. Next the 3.18-cm (1-1/4-in.) elbow was joined to the 3.18-cm (1-1/4-in.) PVC section at the well head. The expansion joint was connected to the elbow to increase pipe size to 5.08-cm (2-in.). Then a 50.8-cm X 1.52-m (2-in. X 5-ft.) PVC section was linked to the expansion joint at the well-head elbow.

Afterward, the vacuum pump was joined with the 5.08-cm (2-in.) vacuum line.

The data acquisition station was set up, and pressure transducers were calibrated for site conditions. According to temperature conditions, an offset had to be determined in the field for the two Omega (model #PX236-005G V) pressure transducers. This was accomplished by producing a vacuum pressure and relating an output voltage to vacuum pressure on the magnehelic gauges in the field. Then, pressure transducers were connected to multi-level wells with the previously described polyethylene tubing. An air velocity transmitter range was selected, and the heat sensor probe was set in the port on the 5.08-cm (2-in.) PVC. Afterward, the transmitter was linked up with the CR10 datalogger. Finally, the thermistor was connected to the thermocouple fitting in the elbow and linked up with the datalogger. Then a system check was initiated by powering up the measuring devices and downloading a program to the CR10. If measuring devices were improperly responding then adjustments were made. Otherwise, the system was powered down and the air permeability system was prepared for a test.

The CR10 was programmed to collect data at a desirable interval, and the program was initiated. Multi-level locations, not linked up with the pressure transducers, were monitored with previously described magnehelic gauges. In

addition to the above parameters, the exhaust can be monitored using a GC-PID/FID or organic vapor analyzer and/or explosimeter. The test remained at a constant vacuum at the well head until the vacuum readings began to level off at the multi-level wells. The test was completed by down-loading the data, disconnecting all monitoring points, vacuum line assembly, and electrical connections.

CHAPTER 5

PNEUMATIC TESTS PERFORMANCE AND RESULTS

A series of tests were conducted to quantify pressure, and velocity ranges, evaluate system performance, and collect data to determine k_{air} for sequential soil layers. Three specific tests were conducted in the following order:

1). preliminary tests to determine adequate blower or vacuum pump specifications and evaluate system components,

2). tests to collect drawdown at multi-level wells,

3). laboratory tests to determine the effects of energy losses during the field tests.

Law Environmental, Inc. monitored vacuum pressures, vapor mass extraction and volumetric flow rate during a 2-hour vapor extraction test on December 8, 1992, which served as a preliminary estimate of system parameters (Widdowson et al., 1993). Additionally, results of *ex-situ* tests, as discussed in Chapter 3, also helped to determine initial measurement device ranges and blower specifications for preliminary tests. During pneumatic tests, data were taken to quantify vacuum pressures, temperatures, and air mass extraction for a given blower. Each test was conducted at a multi-level layer using a different blower or pump to determine the above parameters.

Then data from tests was used to determine the blower size as well as range of additional measurement devices. Also, laboratory tests were conducted to determine head losses within the pneumatic pipe line as a means of determining pressure at multi-level well screen intervals.

5.1 PRELIMINARY TESTS

For a given motor speed each blower or pump has an expected performance relating pressure to the volumetric flow rate at a standard temperature. A number of performance curves help identify the operating conditions for each blower. Since the multi-level approach identifies zones of varying permeability, a blower may need to operate in low or high permeable layers. As suggested in Figure 3.3 the subsurface at the site has increasing permeability with depth. Thus, the pump and blower produced different vacuum pressures and flow rates at each layer in the subsurface (Table 5.1).

The first step was to identify a suitable blower or pump. Normally, it is standard to start with the 88 CFM blower (Spatco Inc., personal communication). The Gast R7 series, Rotron DR 707 or liquid ring vacuum pump can be used for tighter or very permeable sediments (Spatco Inc., personal communication). Likewise, the above blower and pump models can be used with heterogenous media. The specifications for each of the above blowers or pumps vary and can be obtained

Table 5.1: Performance of blower or pump in multi-level media

SCREEN # model pump/blower	FLOW RATE			PRESSURE					
	MIN	MAX	TIME AVG.	MIN		MAX		TIME AVG.	
	(CM^3/S)			ATM	PASCALS	ATM	PASCALS	ATM	PASCALS
SCRN. #1 Gast Blower model R5	1270	3859	2174	0.82	-18001	0.84	-16119	0.83	-17072
SCRN. #1 Vacuum pump	704	5671	4577	0.44	-57115	0.97	-3394	0.64	-36953
SCRN. #2 Gast Blower model R5	784	875	834		-		-		-
SCRN. #2 Vacuum pump	660	1547	1166	0.10	-90804	0.19	-81703	0.16	-85106
SCRN. #3 Gast Blower model R5	917	1888	1304	0.84	-16119	0.85	-15053	0.85	-15603
SCRN. #4 Gast Blower model R5	699	2327	1251	0.81	-18748	0.85	-14705	0.84	-15954
SCRN. #5 Gast Blower model R5	236	3306	1547	0.82	-18524	0.90	-10517	0.84	-16646

from vendors. Performance curves supplied by companies were reviewed to determine motor limitations.

During field tests both a Gast Blower model R5 series and Cenco vacuum pump were utilized to determine their performance with the multi-level extraction well. The corresponding maximum vacuum pressures and flow rates were measured to prevent permanent damage resulting from ruining the motor under high vacuum pressures with low flow rates. Before operation, motor limitations were closely examined to avoid excessive damage to equipment. Specifically, in relatively impermeable media, pumps and blowers typically generate high vacuum pressures with low extraction flow rates. A relief valve to the vacuum line was added to allow adjustment of pressure within the extraction well in the case of low flow rates.

Preliminary tests consisted of testing the blower and pump in sequential soil layers to identify the most permeable layers. The first test was conducted in the least permeable layer at screened interval #5. As shown in Table 5.1, the Model R5 Gast Blower performed poorly. Next, the blower was set up to initiate a pneumatic test at screened interval #4 and a decrease in mass extraction was measured. Screened interval #3 was tested using the Gast R5 Blower, and again, the mass extraction rate was out the range of ideal conditions. At screened interval #2 the flow rate decreased

with the blower, and the vacuum pressure exceeded the range of the pressure transducer. Thus, the assumption of increasing permeability with depth was not completely valid. A second test conducted at screen #2 with a vacuum pump generated vacuum pressures and flow rates shown in Table 5.1. Screened interval #1 was tested with the Gast R5 Blower, and the extraction rate increased significantly relative to previous layers. At this stage the vacuum pump was connected to the vacuum system and generated an average flow rate and vacuum pressure of 4577 cm^3/s and 0.64 atmospheres.

Johnson et al. (1990a) identify ideal flow conditions with flow rates ranging from (47200 - 472000 cm^3/s) 100-1000 scfm. As determined by Widdowson et al. (1993), the permeability of the field site tends to fall short of these ideal conditions. However, existence of heterogeneities in the subsurface may in some circumstances provide moderate, but acceptable, vapor flow rates (Widdowson et al., 1993). Observation of Table 5.1 supports the deduction that heterogeneities within the subsurface generate varying flow rates. For example, the vacuum pump generated an average flow rate of 4577 cm^3/s for a well pressure (P_w) of 0.64 atm at screen #1 while only producing 1166 cm^3/s for P_w = 0.16 atm at the adjacent screen #2.

5.2 PERFORMANCE CHARACTERISTICS OF EXTRACTION WELL

The pressure and flow rate at the well head were modified by means of an adjustable valve to determine performance characteristics of the extraction well using the vacuum pump. More specifically, these tests were conducted in the field to determine the relationship between P_w and the corresponding flow rates. As shown in Figure 5.1, drawdown as a function of flow rate at the well head for screen #1 can best be described by an exponential function. By regression analysis and with a $R^2 = .89$ the following expression was derived:

$$P_{wi} = -2944 + 4127316 Q_w + 1776954112 (Q_w^2) \qquad (5.1)$$

where,

Q_w = flow rate (m^3/s)

P_{wi} = pressure drawdown at the extraction well-head (pascals)

Also, the data can be analyzed to determine variations in the stabilized pressure at the well head caused by energy losses due to the well and formation. In Chapter 6 a quadratic equation predicting the relationship between the vacuum pressure and flow rate at the extraction well head is used to determine pressure variations caused by energy losses.

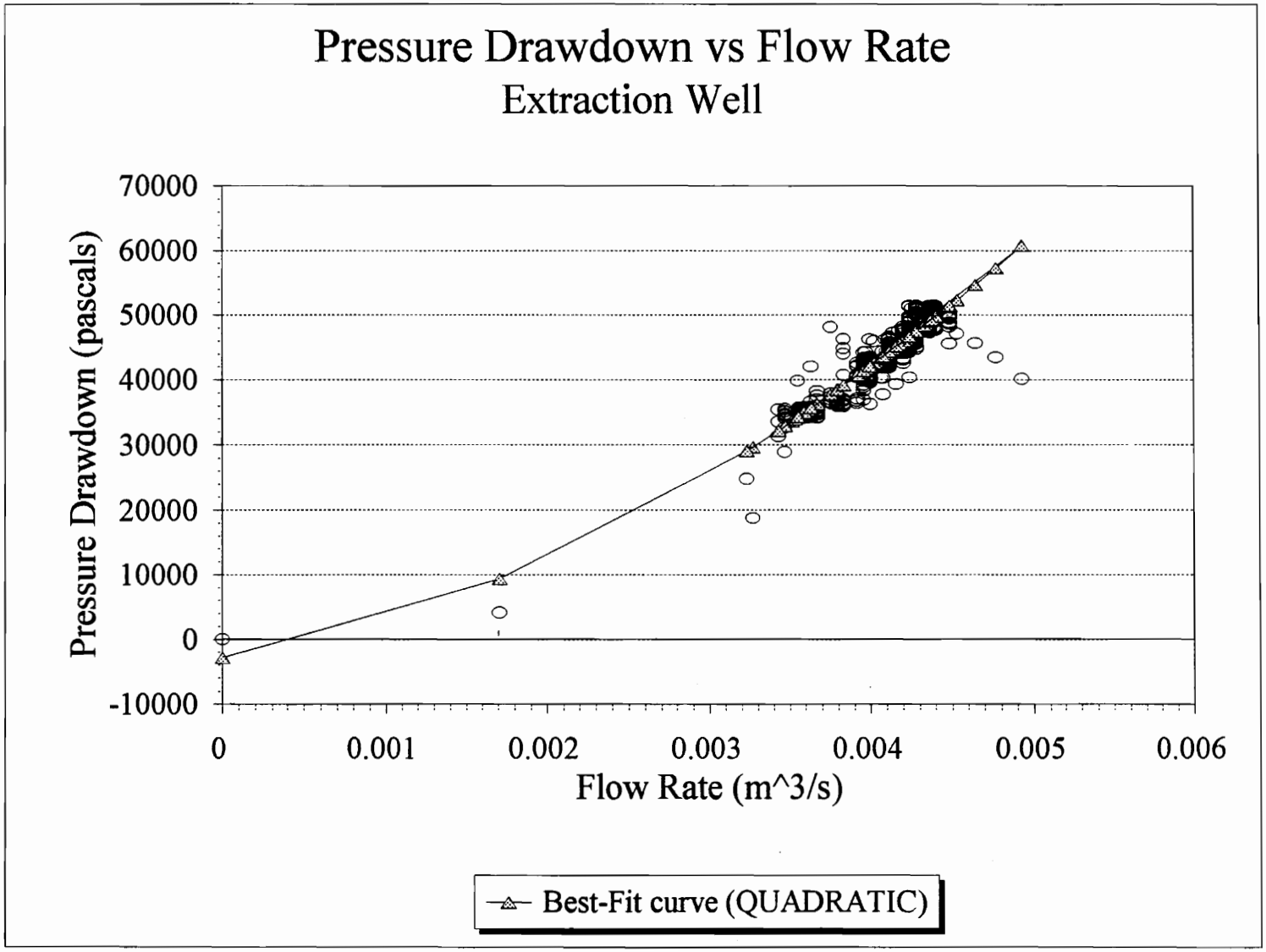

Figure 5.1: Drawdown versus flow rate at the extraction well

5.3 AIR PERMEABILITY TESTS

Three tests were conducted at the site over a thirty-eight day period to collect data necessary to calculate air permeabilities. Parameters monitored at the extraction well were temperature, flow rate, and vacuum pressure. Additionally, pressure drawdown was monitored at multi-level pressure monitoring wells along both radii. Mass flow rate was calculated by utilizing the ideal gas law. Due to lack of availability of proper equipment, pressure at the extraction well was not measured on August 26, 1993 (see Figure 5.3).

An important parameter in the determination of the mass extraction rate was the temperature. Figure 5.2 depicts the gradual decrease in temperature with time as extracted air continued to travel through the subsurface until an equilibrium was reached. The higher initial temperature reflected ambient atmospheric conditions. The exponential variation in temperature can be predicted as a relationship between the flow path of transported air in relation to subsurface temperature gradients. Figures 5.3 and 5.4 show that pressure and flow rate at the extraction well reached steady-state rapidly. The flow rate was determined from the velocity and cross-sectional area of the pipe line. This rapid steady-state condition was indicative of the absence of large initial storage of air in the media. Furthermore, the consistent steady-state condition was important in

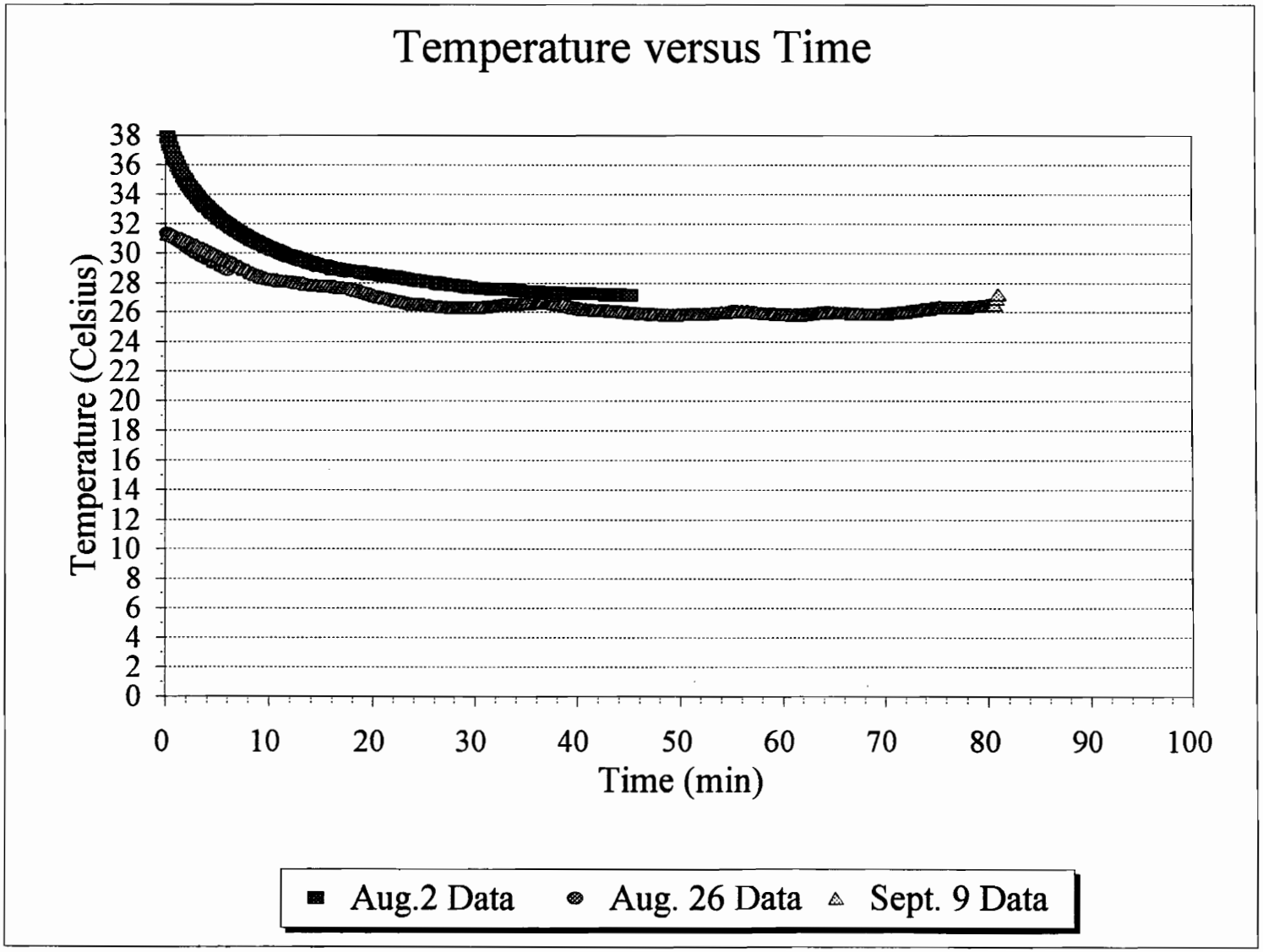

Figure 5.2: Temperature as a function of time in extraction well

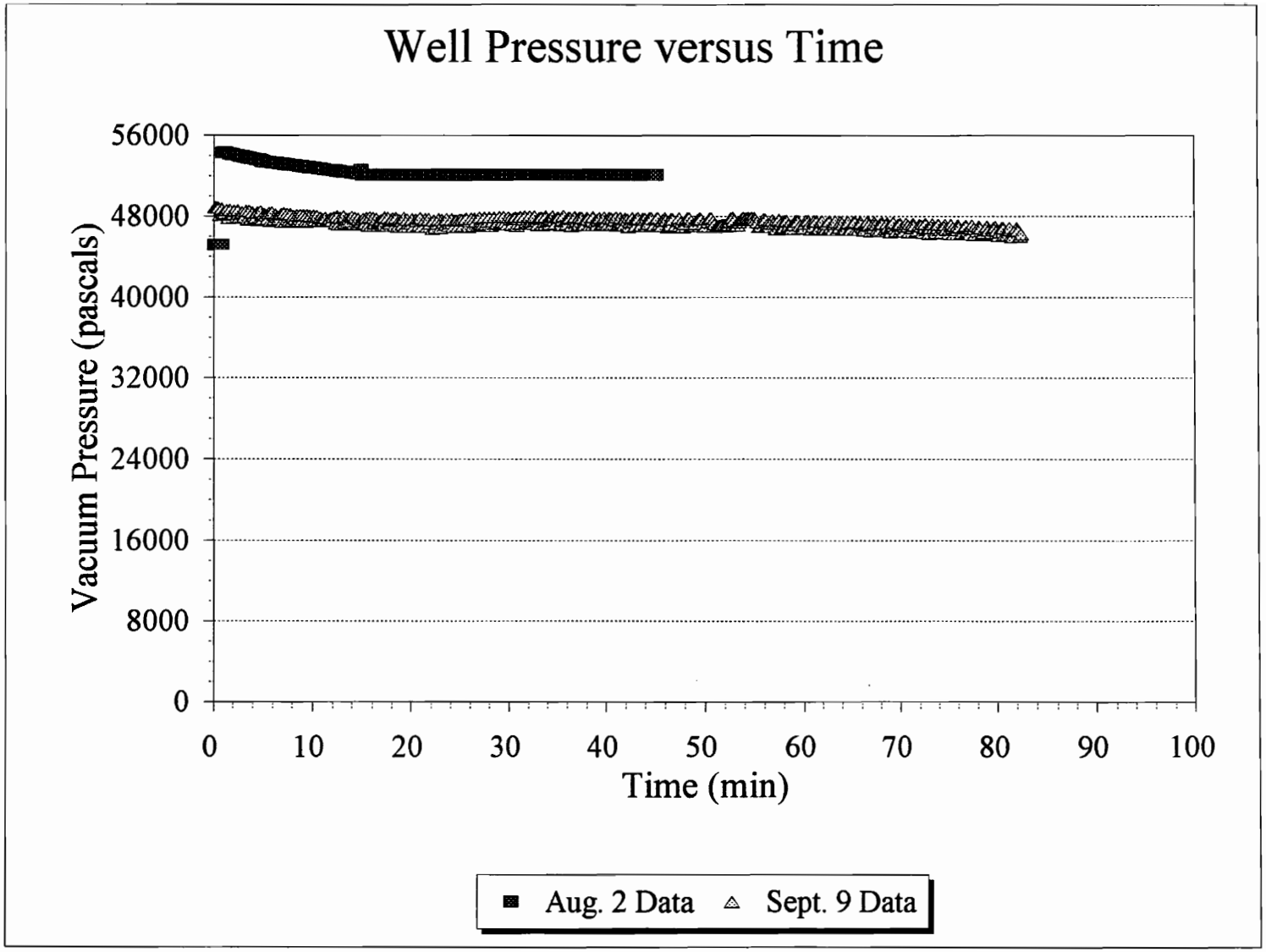

Figure 5.3: Extraction well pressure as a function of time

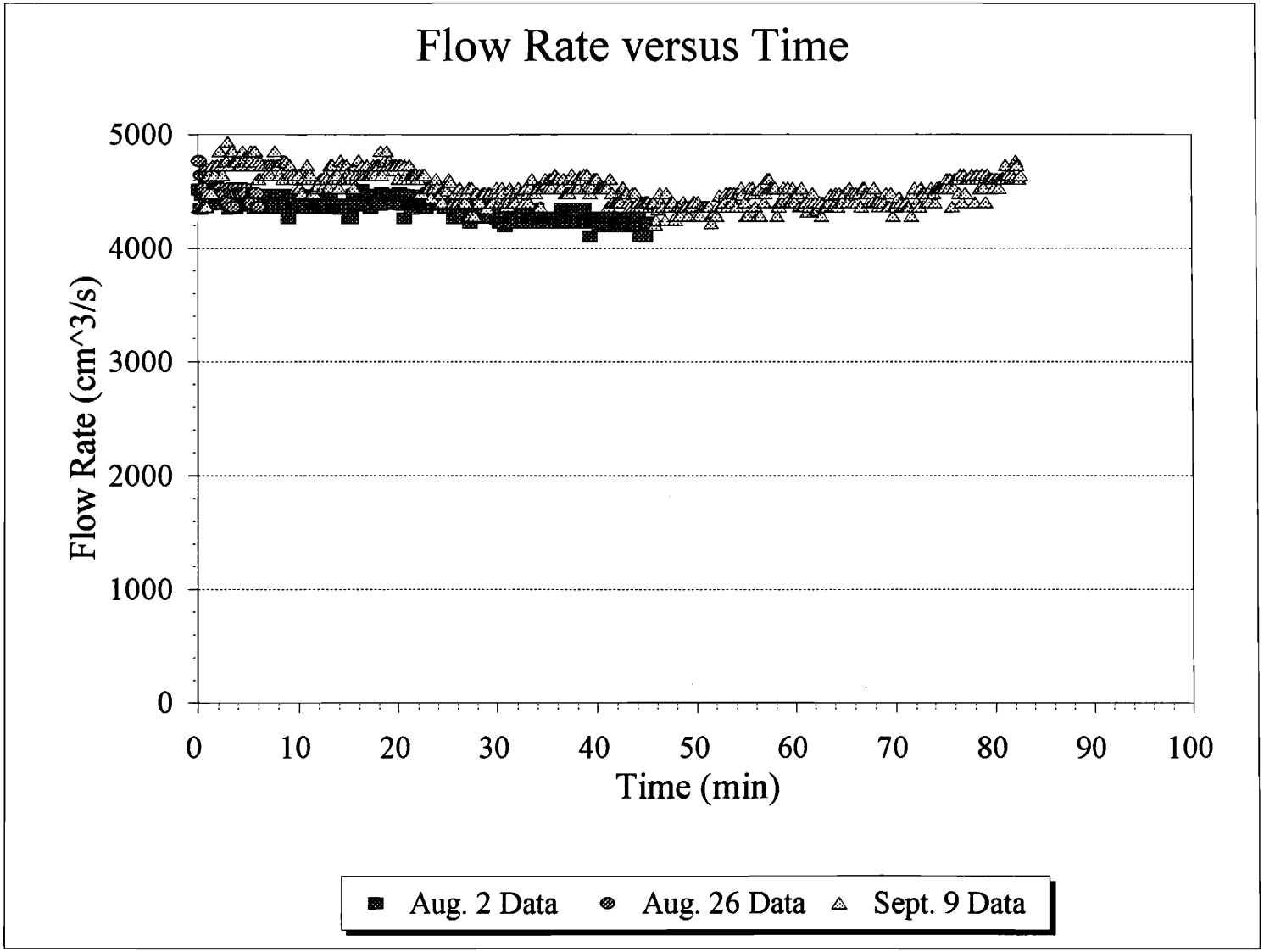

Figure 5.4: Flow rate as a function of time in extraction well

supporting the theory that the formation was not damaged due to air transport during tests. By use of the volumetric flow rate, the mass extraction rate can be calculated using the density of the air determined by the Ideal Gas Law (see Figure 5.5). The mass extraction rate was important in determining the soil air composition.

Multi-level pressure drawdown data is presented in Figures 5.6-5.8. At ML #1-1 pressure drawdown reached a steady-state condition after about twenty minutes with a corresponding vacuum pressure of approximately 19.0 cm of water column (Figure 5.6). The steady-state vacuum pressure for ML #3-1 was 13.33 cm of water column after about two minutes (Figure 5.7). ML #3-1 was at the same radial distance of 1.0-m as ML #1, but on a different axis. Vacuum pressure at ML #2-1, at a radial distance of 3.0-m, was not detected during the first two tests with Magnehelic gauges. After analysis of pressure drawdown at ML #1-1 and #2-1, it was determined that a radius of influence exceeded 3.0 m (9.8 ft.). Magnehelic gauges were selected to detect mm of water column vacuum pressures and monitor pressure at the 3.0-m monitoring wells. For the test conducted on September 9, 1993 the drawdown depicted in Figure 5.8 was monitored for ML #2-1. Only a slight amount of drawdown (0.10 cm) was detected at ML #4-1 (along the same radius as ML #2, but on a different axis) or at other locations monitored: ML #1-2, 1-3, 3-2, 3-3, and

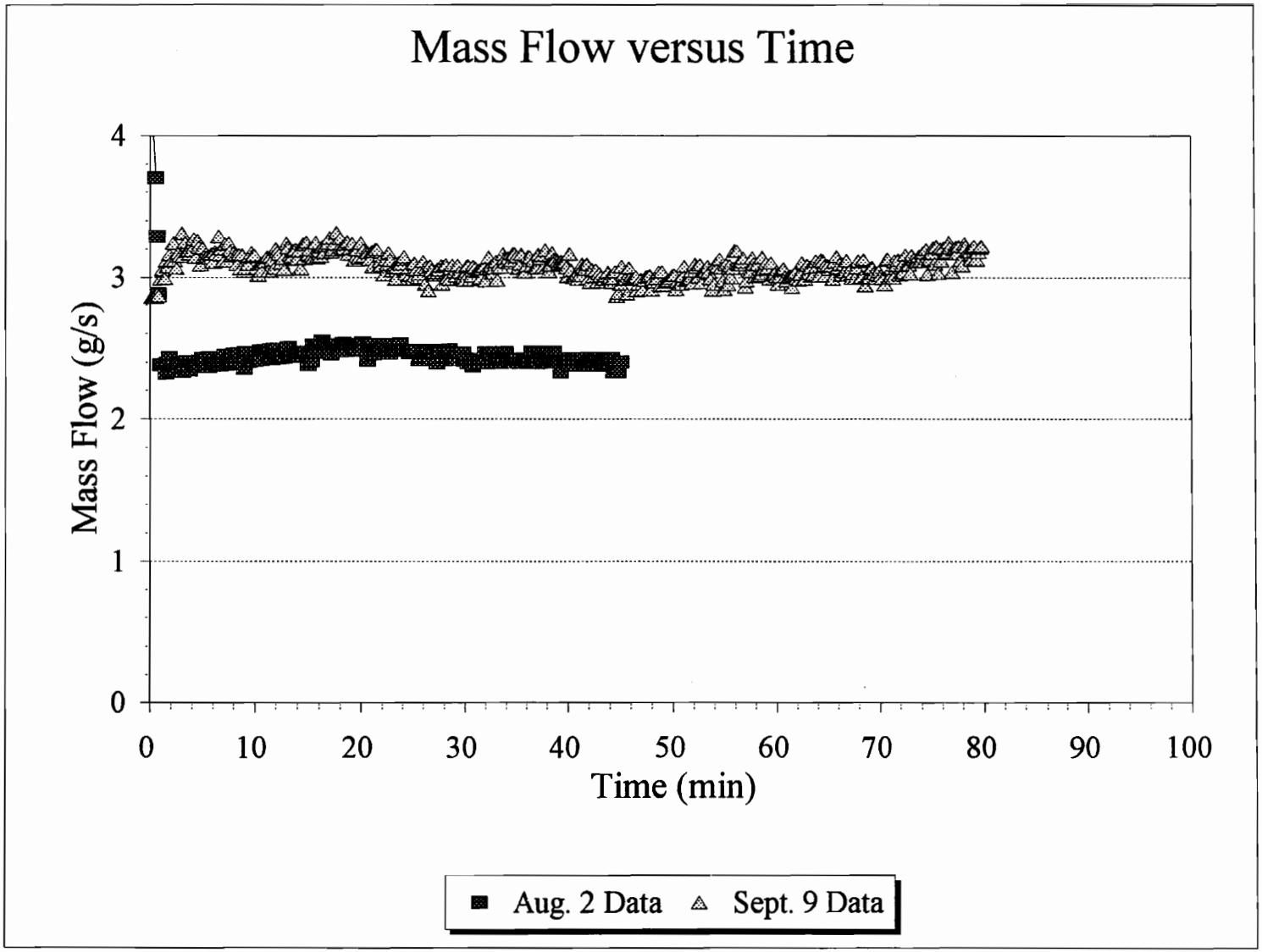

Figure 5.5: Mass flow rate as a function of time in extraction well

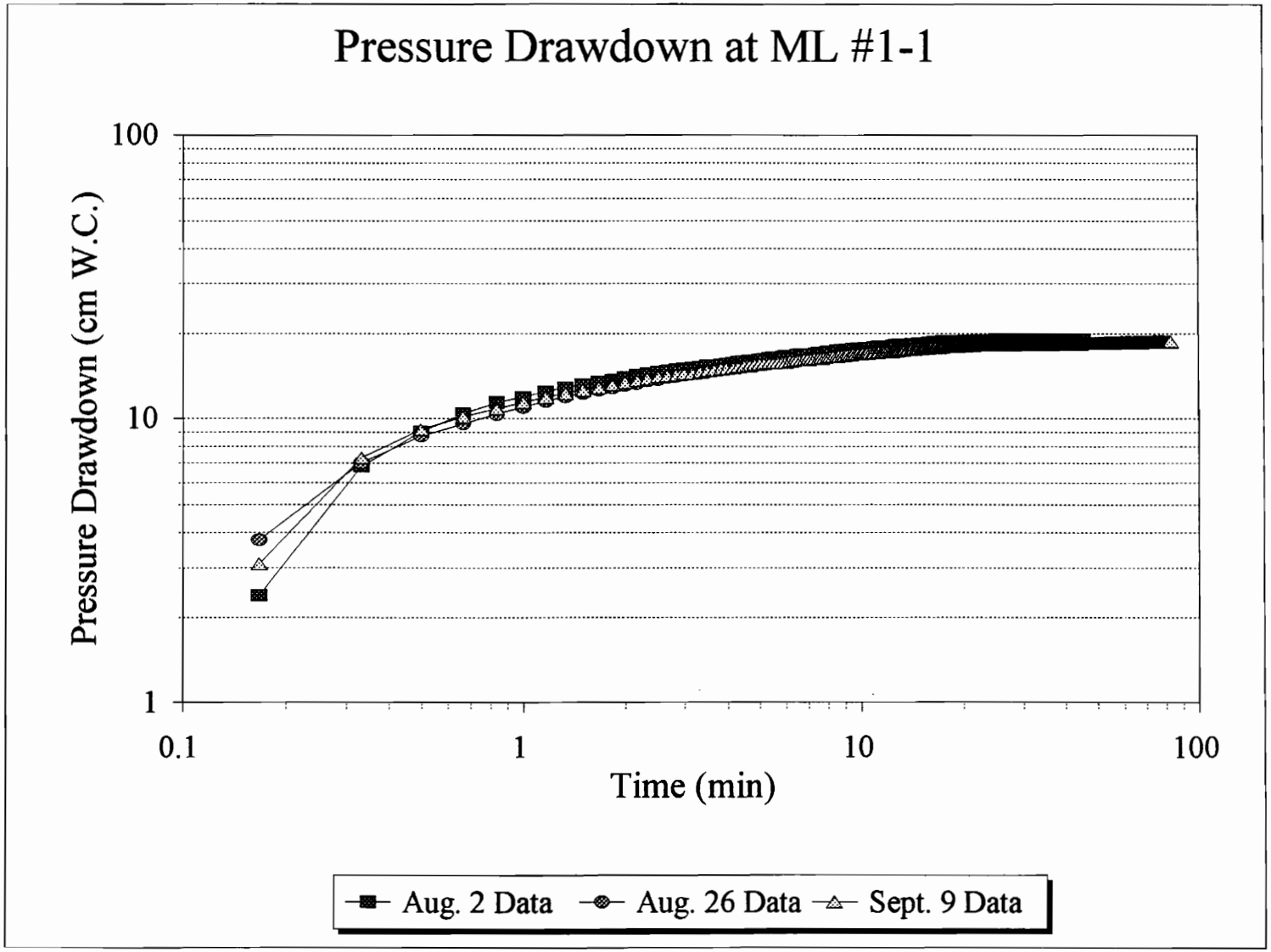

Figure 5.6: Drawdown in multi-level well #1-1

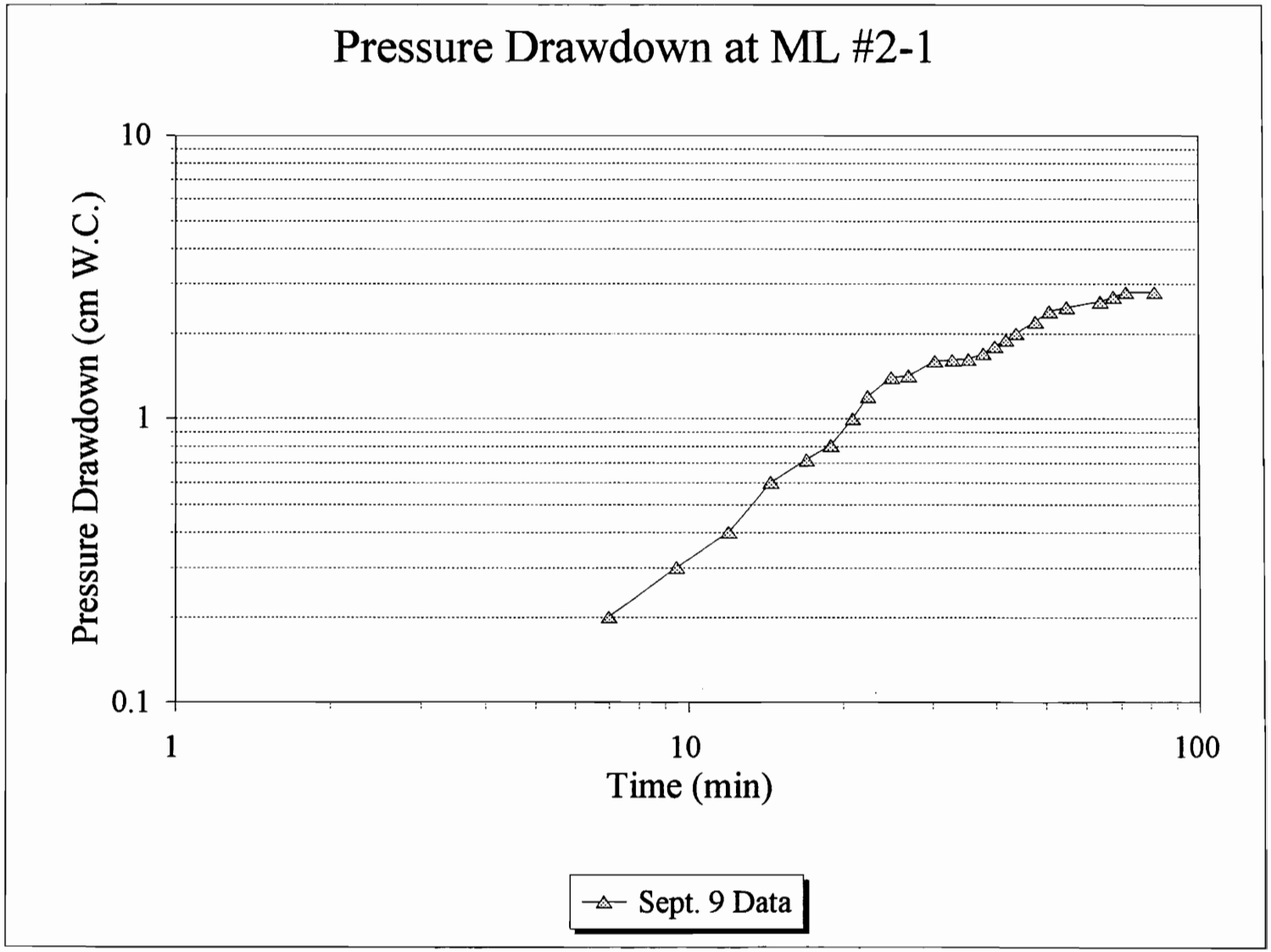

Figure 5.7: Drawdown in multi-level well #2-1

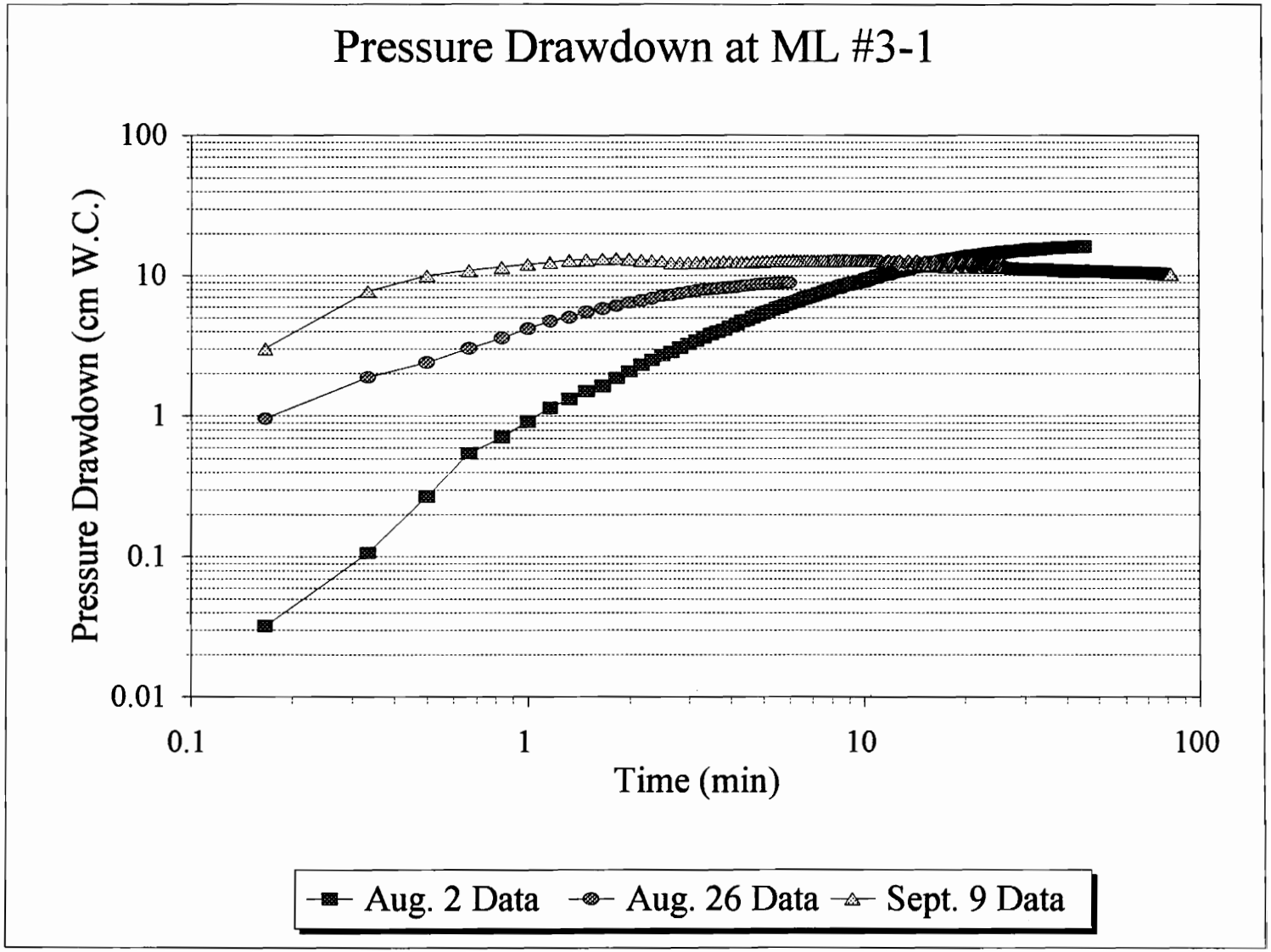

Figure 5.8: Drawdown in multi-level well #3-1

2-2 no drawdown was detected. The steady-state drawdown data with corresponding average pressure, flow rate, and mass flow rate is summarized in Table 5.2

Since repeatability of data is important in field tests, air permeability tests were conducted on three separate occasions. As shown in Figures 5.2-5.5, parameters monitored at the extraction were consistent taking into consideration temperature variations in ambient atmospheric temperatures. Likewise, pressure drawdown data for ML pressure monitoring wells was consistent except for ML #3-1 (see Figure 5.7). The cause of this incongruity was discovered after the second test (August 26, 1993). The source of the variation was identified as a double ferrule design nut was that was mixed with a single ferrule, producing a source of leakage into the line under vacuum. The problem was corrected, and on September 9, 1993 a third test was conducted.

Table 5.2: Results from multi-level tests

	Q_{avg} (CM^3/S)	P_{avg} (PASCAL)	M_{avg} (g/S)	STEADY-STATE DRAWDOWN cm W.C.		
				ML#1-1	ML#2-1	ML#3-1
AUGUST 2	4345	-52305	2.46	19.15	-----	16.18
AUGUST 26	4519	-----	-----	-----	-----	-----
SEPTEMBER 9	4524	-47404	3.10	18.75	2.8	13.33

5.4 ENERGY LOSSES WITHIN VACUUM SYSTEM

Laboratory tests were conducted to examine the effects of energy losses within the vacuum system. The setup of the vacuum system consisted of a single packer arrangement as shown in Chapter 4 (see Figure 4.6). Components used during pneumatic tests such as: data acquisition equipment, measuring devices, PVC casing, connections, and wiring were identical to those utilized during laboratory tests. In order to reproduce mass extraction rates produced at the field site during pneumatic tests, a gate valve was attached to the 3.2-cm (1.25-in.) line leading to a Gast R4 Blower, and the flow rate was modified by means of adjusting the gate valve to allow outside air into the line downstream of the 90^0 elbow. During execution of the test, the valve was adjusted and the pressure was recorded for a given time. Since pressure at the well head was monitored before the elbow, energy losses after this point were not measured. Parameters monitored at the well head were temperature, flow rate, and vacuum pressure. Two arrangements were investigated: one setup with the packer system alone, and the packer system inflated inside of a 5.08-cm (2.0-in.) PVC well screen. The purpose of two arrangements was to quantify the effects of both the packer system and the well screen in terms of energy losses.

Well-head data was analyzed to determine the percentage of the pressure differential due to friction and

hydrodynamics. The following "extended" Bernoulli Equation, which accounts for head losses, was utilized to calculate pressure changes (Munson et al., 1990):

$$\Delta P = P_s - P_{wi} = \frac{V_{wi}^2}{2}\rho_{wi} + h_L \qquad (5.3)$$

where,

P_s = absolute pressure ($M\ L^{-1}\ T^{-2}$)

V_{wi} = velocity at well head ($L\ T^{-1}$)

ρ_{wi} = density of air at well head ($M\ L^{-3}$)

h_L = head loss due to vacuum system ($M\ L^{-1}\ T^{-2}$)

Pressure and velocity head were determined for two points along a stream line. Point #1 was chosen at a point beyond the entrance of air flow into the packer where pressure was atmospheric and velocity was zero. For point #2, at the well head, velocity, vacuum pressure, and temperature were measured by devices described in Chapter 4. For example, during the test at a time equal to 0.50 minutes, the following parameters were measured: $\Delta P = P_1 - P_{wi} = -11.62$ KPascals, $V_{wi} = 11.35$ m/s, and $\rho_{wi} = 1.054 \times 10^{-3}$ g/cm^3

where,

ΔP = pressure differential through vacuum system due to hydrodynamics and friction (Kpascals)

Substitution of the above parameters into Equation (5.3)

showed that the frictional losses made up 99.4% of the total pressure change. Flow rates and corresponding pressures were adjusted using the gate valve to determine an applicable range of pressure differentials and head losses. Since pressures differentials are related to vapor extraction rate, the volumetric extraction rates were converted to mass rates by using the ideal gas law and temperature variations. Plots of pressure differential versus mass flow rate and head loss versus mass flow rate are shown in Figures 5.9 and 5.10, respectively, for the tests configuration without the well screen.

Head losses and pressure differentials were determined for the field-test mass flow rates. Using regression analysis, best-fit curves were generated to quantify pressure differential and head loss as functions of mass flow rate (Figures 5.9 and 5.10), respectively. For an average mass flow rate of 3.10 g/s (Table 5.2) the pressure differential and head loss was -547 pascals (0.005 atm) and -449 pascals (0.004 atm), respectively. The addition of the well screen produced insignificant differences in pressure (ΔP). With the addition of the well screen and a mass flow rate of 3.10 g/s the pressure differential and head loss was -598 pascals (0.006 atm) and -507 pascals (0.0050 atm), respectively.

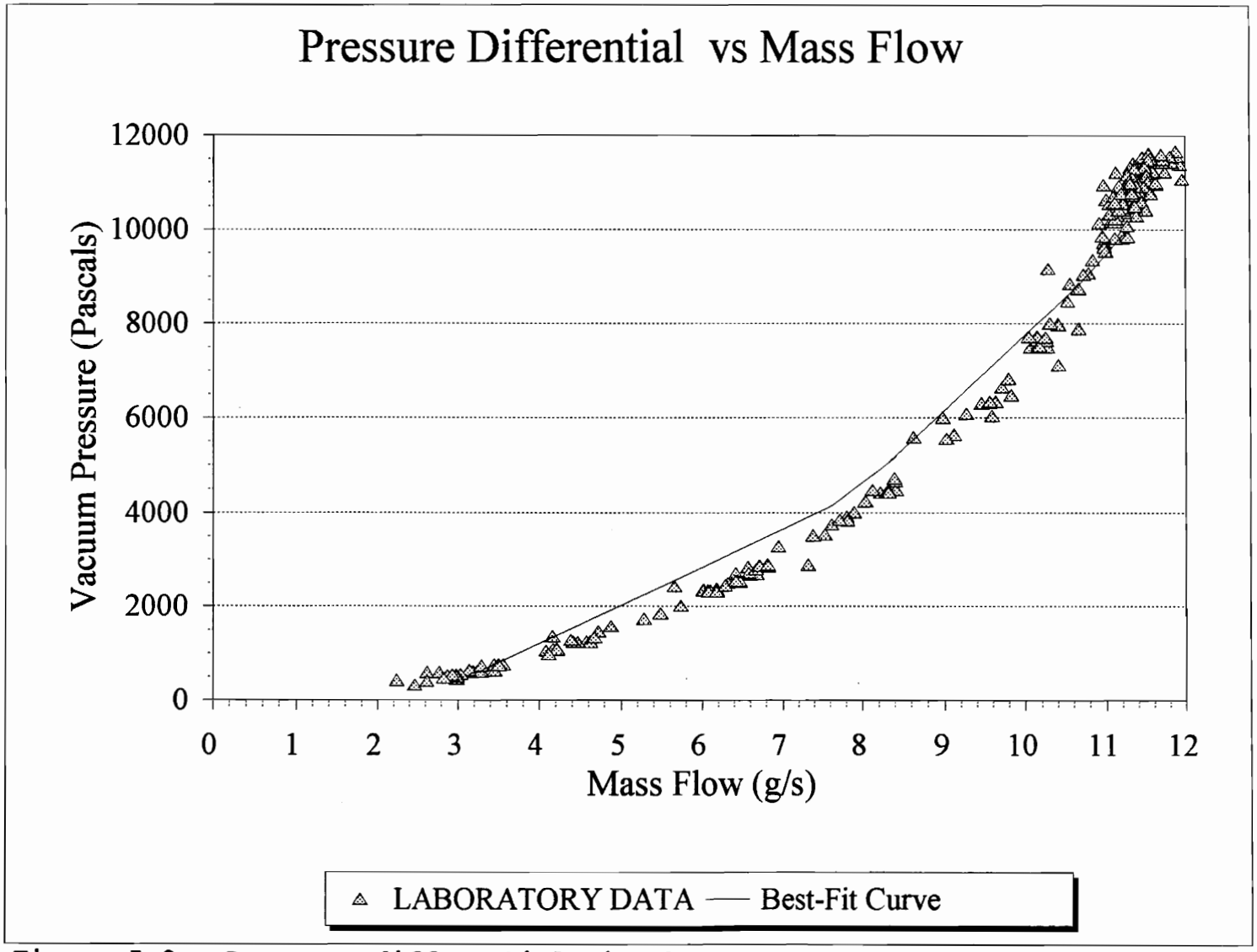

Figure 5.9: Pressure differentials in the vacuum system

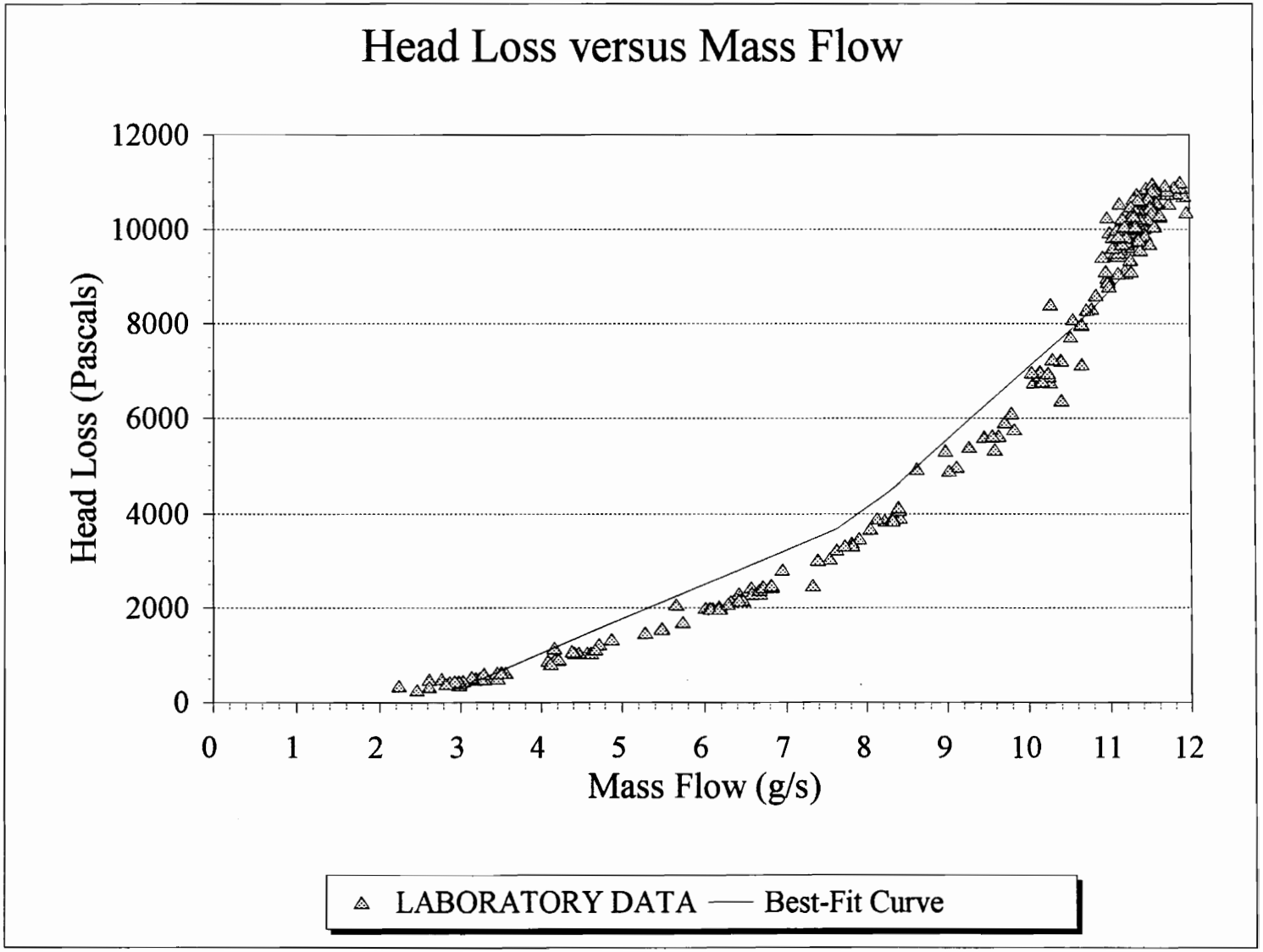

Figure 5.10: Head losses in the vacuum system

CHAPTER 6

DATA ANALYSIS

In this Chapter steps are given to obtain air permeabilities from pneumatic test data for each method of solution. Steady-state and transient data obtained from pneumatic tests were analyzed with solution techniques described in Chapter 2 to obtain air permeabilities. Laboratory tests to determine pressure drop through the packer system presented in the previous chapter indicate head loss within the vacuum system is measurable, but is not significant for the Q values measured during air permeability tests. Further analysis is presented here. Because the centerline velocity was measured in the 5.08-cm (2.0-in.) PVC pipe at the well head, an analysis is presented to find the average velocity as required in the solution methods.

6.1 ANALYSIS OF PRESSURE AT EXTRACTION WELL

Pressure at the well head was measured as 0.53 atmospheres during pneumatic tests conducted; however, this was the pressure drawdown without taking into consideration energy losses due to the vacuum system, well, and formation. In Chapter 5 the pressure differential due to the vacuum system was calculated as 547 pascals (0.006 atmospheres). As a result of these differentials, the pressure at the well

screen (P_s) was 0.536 atmospheres. From extrapolation of pressure drawdown data at ML #1 and #2, the pressure at the well screen was approximately 0.92 atmospheres for a flow rate if 3551.66 cm^3/s (Figure 6.1). If 0.92 atmospheres was the pressure at the extraction well, then 0.40 atmospheres would be attributed to the well and formation losses for P_w = 0.536 atmospheres. A quadratic form of the head losses which predicts variations in the stabilized pressure drawdown at the well screen as a function of the flow rate is given by (Todd, 1980):

$$P_s = BQ + CQ^2 \qquad (6.1)$$

where,

BQ = formation loss

CQ^2 = well loss

Data obtained from adjustment of the flow rate was analyzed to determine above head losses by plotting P_{wi}/Q vs. Q (Figure 6.2). The following expression was derived from a regression analysis with an R^2 = 0.68:

$$P_s = 1727596 \cdot (Q) + 2188002625 \cdot (Q^2) \qquad (6.2)$$

where,

B = 1727596 (kg m^{-4} s^{-1})

C = 2188002625 (kg m^{-7})

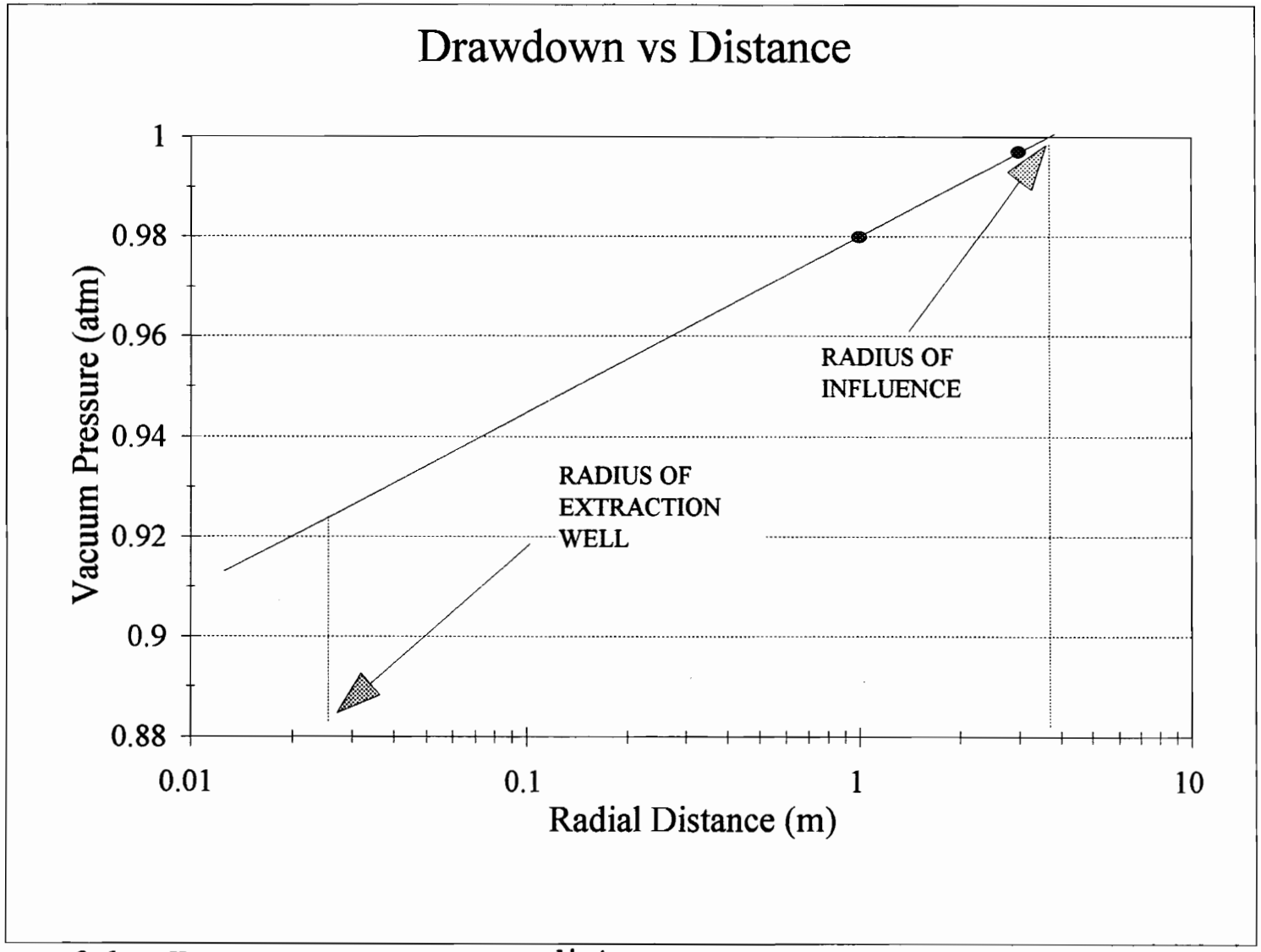

Figure 6.1: Vacuum pressure versus distance

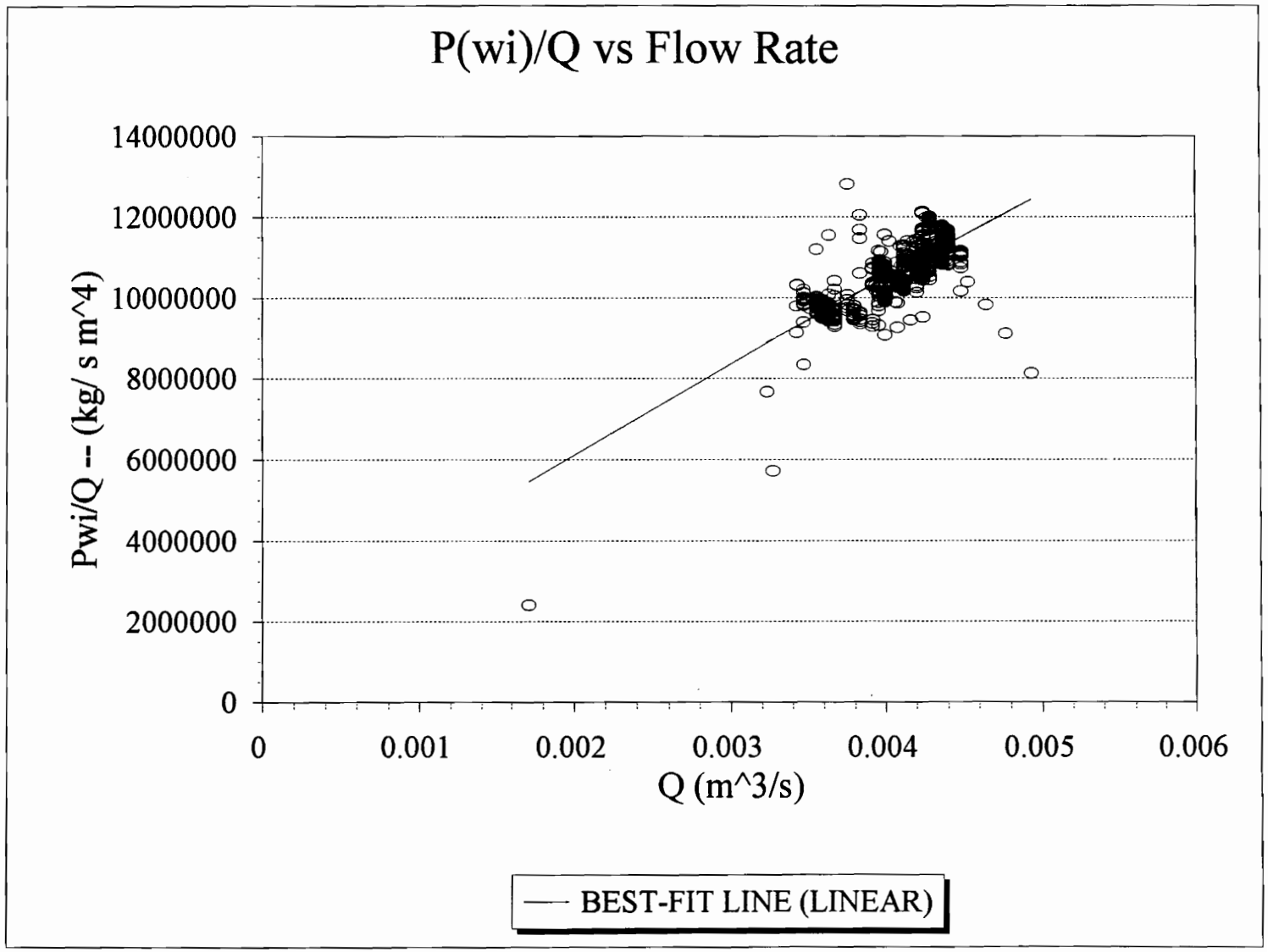

Figure 6.2: Analysis of well and formation losses

For an extraction flow rate typical of the air permeability tests, (0.0035 m^3/s or 3551.66 cm^3/s) the total losses due the well and formation were 0.26 and 0.06, respectively. Taking into consideration these losses and using the pressure at the well screen as 0.536 atmospheres, the pressure at the well screen was 0.86 atmospheres. This approximation of the pressure at the well screen compares reasonably with the pressure of 0.93 atmospheres obtained from extrapolation taking into consideration the R^2 obtained from the regression analysis. Additionally, a plot was generated to emphasize the percentage of the head losses due to laminar flow (BQ). The following expression was utilized to determine the percentages of pressure drawdown due to laminar head loss as a function of the discharge (Driscoll, 1986).

$$Lp = \frac{BQ}{BQ + CQ^2} \qquad (6.3)$$

where,

L_p = fraction of pressure drawdown due to laminar flow

Equation (6.2) was utilized to produce a plot which predicts the percentage of head losses due to the formation or laminar flow (see Figure 6.3). For a discharge of 3551.66 cm^3/s the

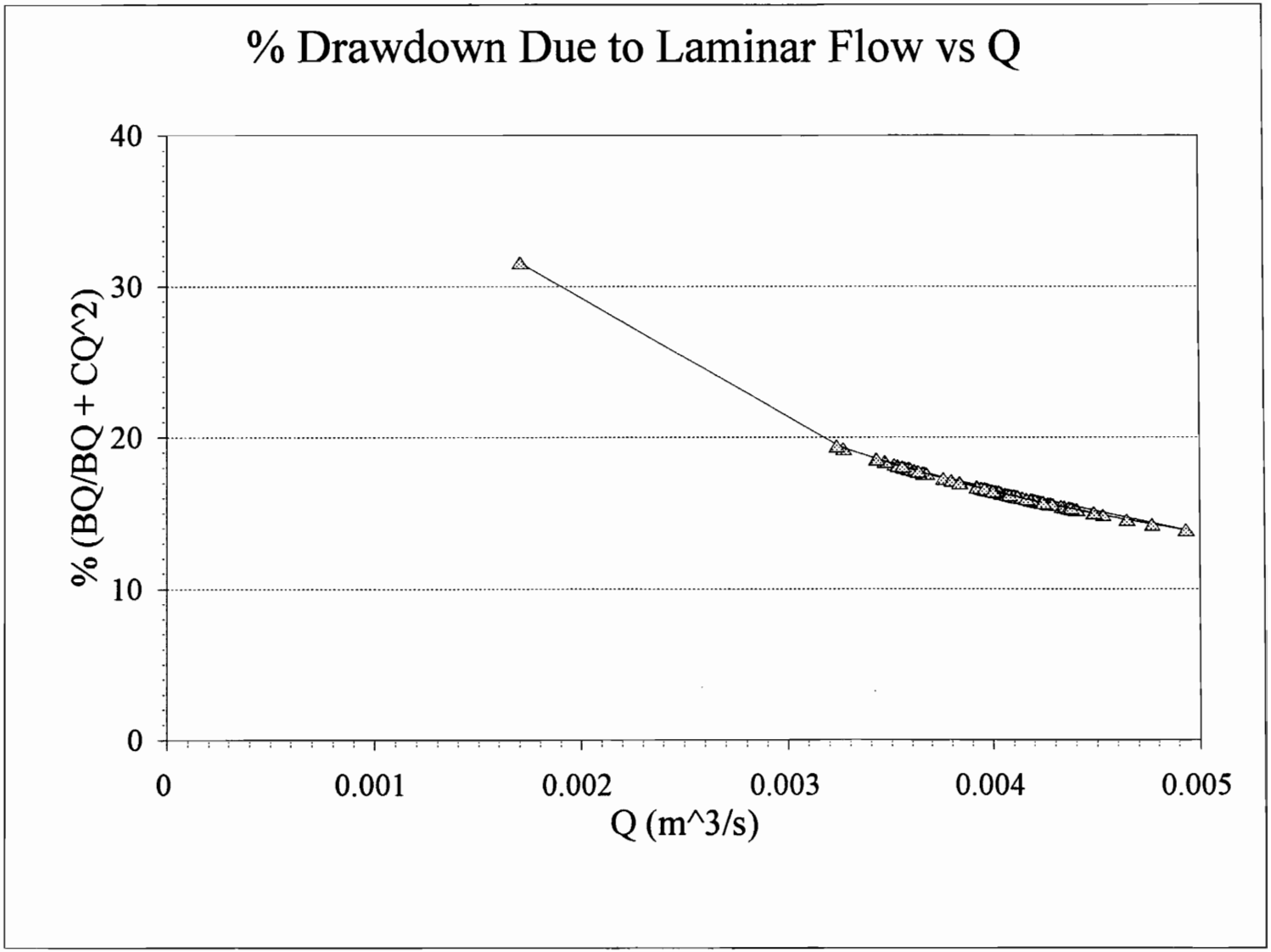

Figure 6.3: Percentage drawdown due to laminar flow versus discharge

percentage of losses due to laminar flow was approximately 18%, meaning 82% of the losses were attributed to turbulent flow.

6.2 EVALUATION OF CENTERLINE VELOCITY

Because the velocity transmitter measured the centerline velocity of the air stream, a means of determining the average was required. Calculation of the Reynolds number (R_e) in the range of 3000-4000 region indicates flow in the region of transition between laminar and turbulent flow. A means of relating the Reynolds number to the friction factor for $3000 < R_e < 10^5$ is given by (Blasius, 1913):

$$f = \frac{.316}{R_e^{.25}} \tag{6.4}$$

where,

f = moody friction factor (dimensionless)

$$R_e = \frac{VD}{\nu} \tag{6.5}$$

and,

V = average velocity of air stream ($L\ T^{-1}$)

D = effective diameter of pipe line (L)

ν = kinematic viscosity of air ($L^2\ T^{-1}$)

The equation which relates the average velocity to the maximum

velocity in terms of the friction factor is given by (Sabersky et al., 1989):

$$\frac{V}{U_{max}} = \frac{1}{1+1.33\sqrt{f}} \qquad (6.6)$$

where,

U_{max} = centerline velocity (L T^{-1})

6.3 SOLUTION TECHNIQUES

Four solution techniques were used as means of analysis of the air permeability: Johnson's steady-state solution for radial flow in porous media (Johnson et al., 1990b), Cooper and Jacob (1946) modified Theis for radial flow in a confined aquifer (Johnson et al., 1990a), Hantush's leaky aquifer solution (Gibson et al., 1993), and AIRTEST Version 3.1 (Joss and Baehr, 1993); a fortran program that implements the analytical solutions given by Baehr and Hult (1991) for steady, two dimensional, axisymmetric air flow.

The following sections detail the application of procedures for the determination of k_{air} using the above mentioned solution techniques. In the case of transient solutions the pressure drawdown as a function of time is presented for multi-level wells 1, 2, and 3. The first

pneumatic test was conducted in the most permeable zone at screened interval number #1 (see Figure 4.2). Tests were also conducted in screened intervals #2 and #3; however, after a hundred and twenty minute duration in both screened intervals, no pressure drawdown was detected. Therefore, analysis in the following sections will concentrate on determining air permeabilities in the screened interval between 633.98 - 656.84 cm (screen #1).

6.3.1 STEADY-STATE RADIAL FLOW

Equation (2.32), which is a steady state solution for air flow through porous media, was directly applied to raw data from pneumatic tests. The steps included in the evaluation are as follows:

1). determine radius of influence using Figure 6.1 (R_I = 374 cm);

2). use Equation (6.4) to determine the average velocity and calculate the average flow rate (Q = V·A(area of pipe) = 3551.66 cm^3/s);

3). determine the effective radius of the extraction well (R_w = 5.71 cm) based on bore hole diameter;

4). substitute pressure at the extraction well from Table 5.2 (P_w= 474160 $g/cm \cdot s^2$);

5). determine prevailing atmospheric pressure (P_{atm} = 1.0 X 10^6 $kg/m \cdot s^2$);

6). determine the length of the screened interval (b = 30.48 cm);

$$7).\ k_{air} = \left(\frac{\mu_{air} Q}{b\pi}\right) \frac{\ln\left(\frac{R_W}{R_I}\right)}{P_W\left[1 - \left(\frac{P_{atm}}{P_W}\right)^2\right]} = 2.02 X 10^{-8} cm^2$$

Additionally, substitution of pressures within the well of 0.86 and 0.92 atmospheres (871395 and 932190 $g/cm \cdot s^2$, respectively) were utilized to calculate the air permeability. These pressures in the extraction well were obtained by extrapolation and analysis of head losses. Air permeabilities calculated were 9.10 X 10^{-8} and 3.99 X 10^{-7} cm^2, respectively.

6.3.2 COOPER-JACOB TRANSIENT SOLUTION FOR RADIAL FLOW

Figures 6.1 through 6.3 present drawdown data for multi-level wells 1-1, 2-1, and 3-1 utilized to predict air permeabilities. The procedure for the evaluation of data for multi-level well #1-1, using Equation (2.17), is summarized below:

1). find the slope from the drawdown data (n = $\Delta P'/\Delta \log(t)$ = 4.63);

2). calculate the average flow rate (Q = 3551.66 cm^3/s) as described above;

3). determine the length of the screened interval (b =

30.48 cm);

4). $k_{air}=\frac{Qu_{air}}{4n\pi b}=1.58X10^{-7}cm^2$;

5). check u < 0.01 (or 0.10 as described by Johnson et al., (1990a) for an estimated air-filled porosity, ϵ,

where,

$$u=\frac{r^2\epsilon\mu_{air}}{4tk_{air}P_{atm}} \qquad (6.7)$$

With a porosity and moisture content of 0.407 and 0.15 as determined by Widdowson et al. (1993), Equation (3.2) was utilized to estimate the air-filled porosity. Substituting u = 0.01 and solving for t in Equation (6.7), the time, t, is greater than 1.20 minutes. In order to meet the condition that u be less than 0.01, the air-filled porosity must be 0.041 or 10% or the porosity. De Marsily (1986) points out that the air phase may reach 10-15% of the porosity for a soil medium close to maximum water saturation.

Air permeabilities determined for multi-level wells 1, 2,

and 3 are presented in Table 6.1. Also, the slope, n, determined from semi-log plots generated for drawdown at multi-level is included from the straight-line portions of data in Figures 6.4, 6.5, and 6.6.

Table 6.1: Results from Cooper-Jacob method of solution

Multi-level pressure monitoring well #	$\Delta P'/\Delta \log(t)$ (n = slope)	Air permeability k_{air} (cm^2)
1	10.8	3.64×10^{-7}
2	3.16	1.26×10^{-6}
3	14.5	2.71×10^{-7}

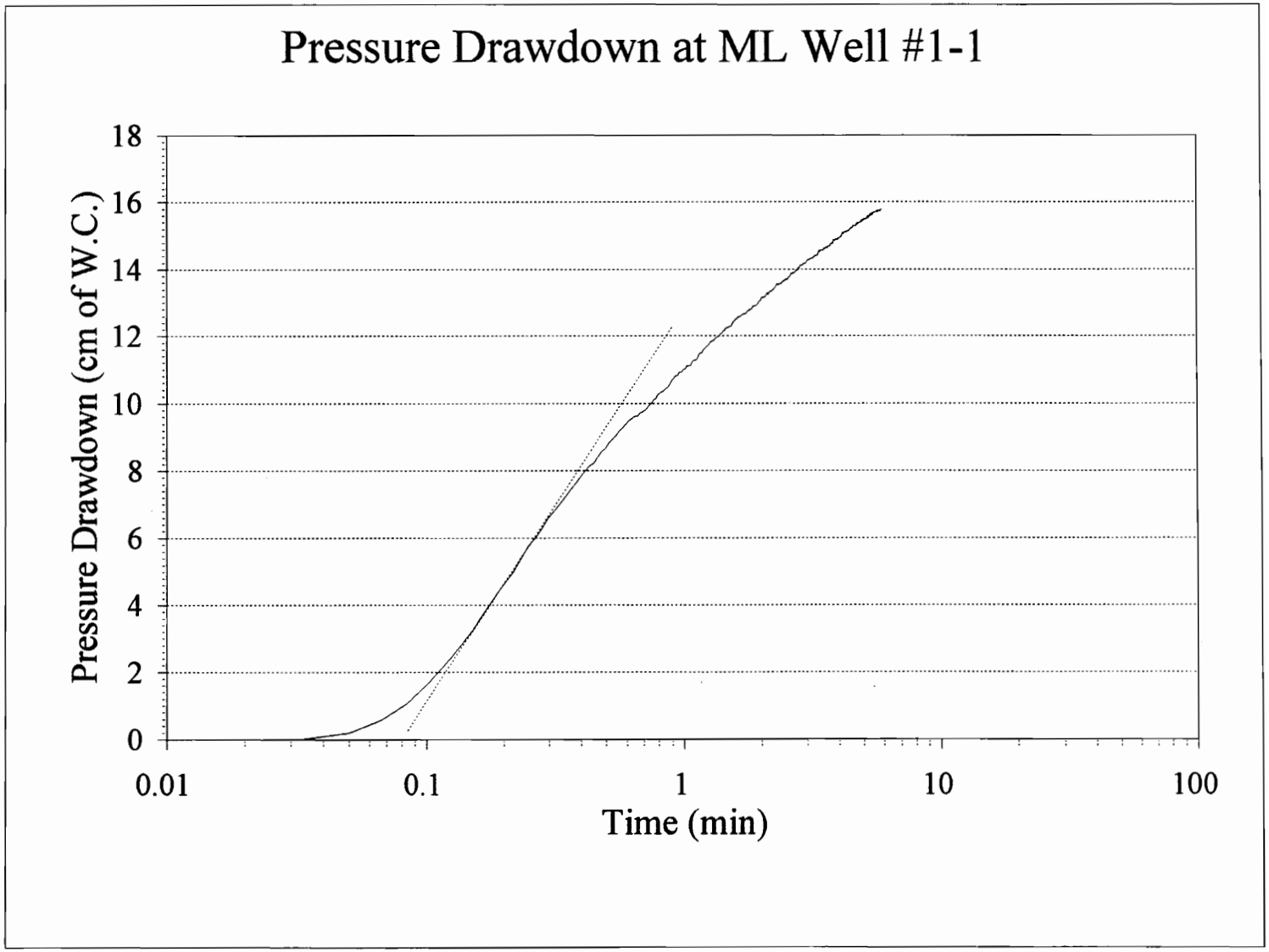

Figure 6.4: Pressure drawdown at multi-level well #1-1

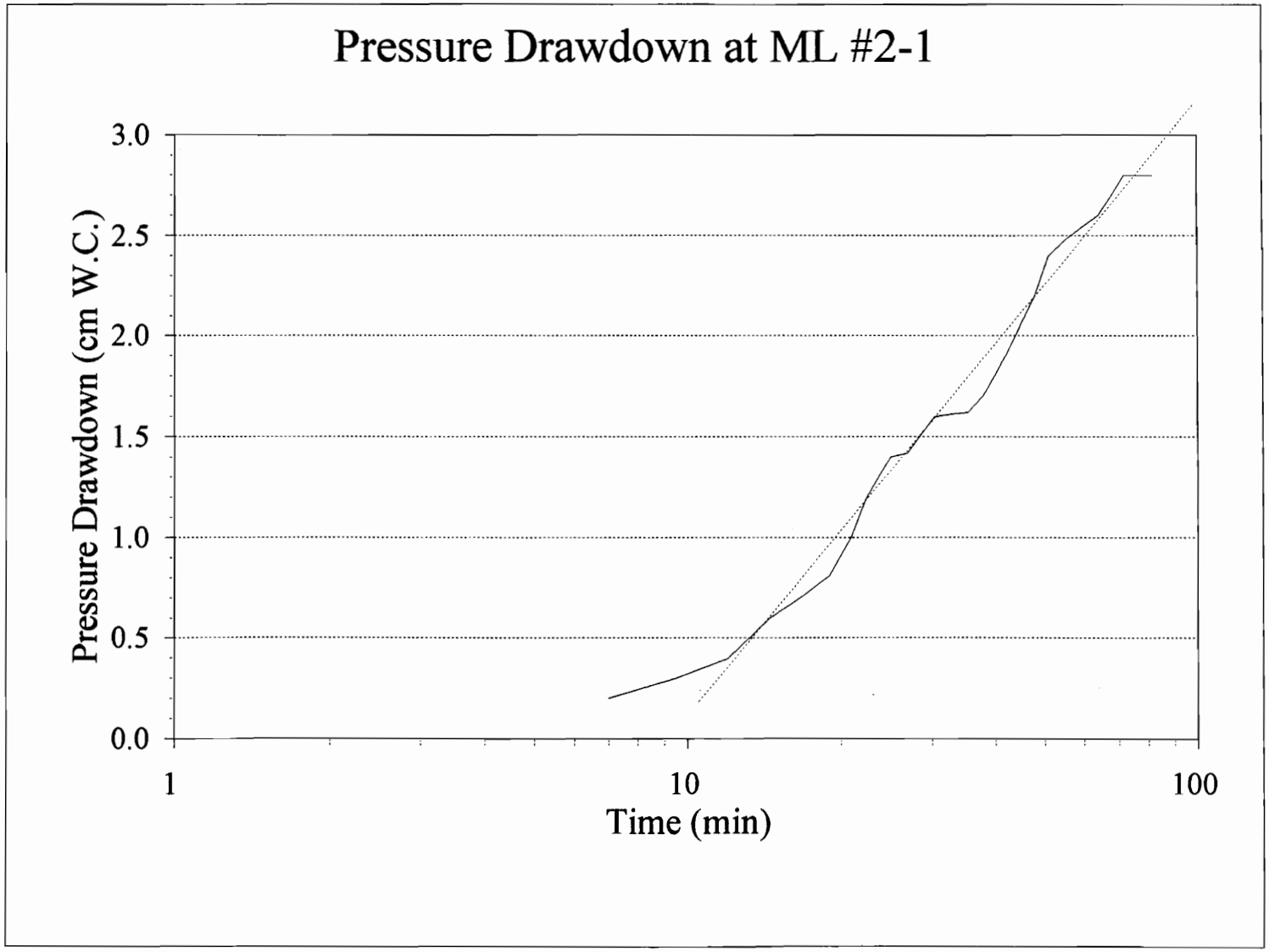

Figure 6.5: Pressure drawdown at multi-level well #2-1

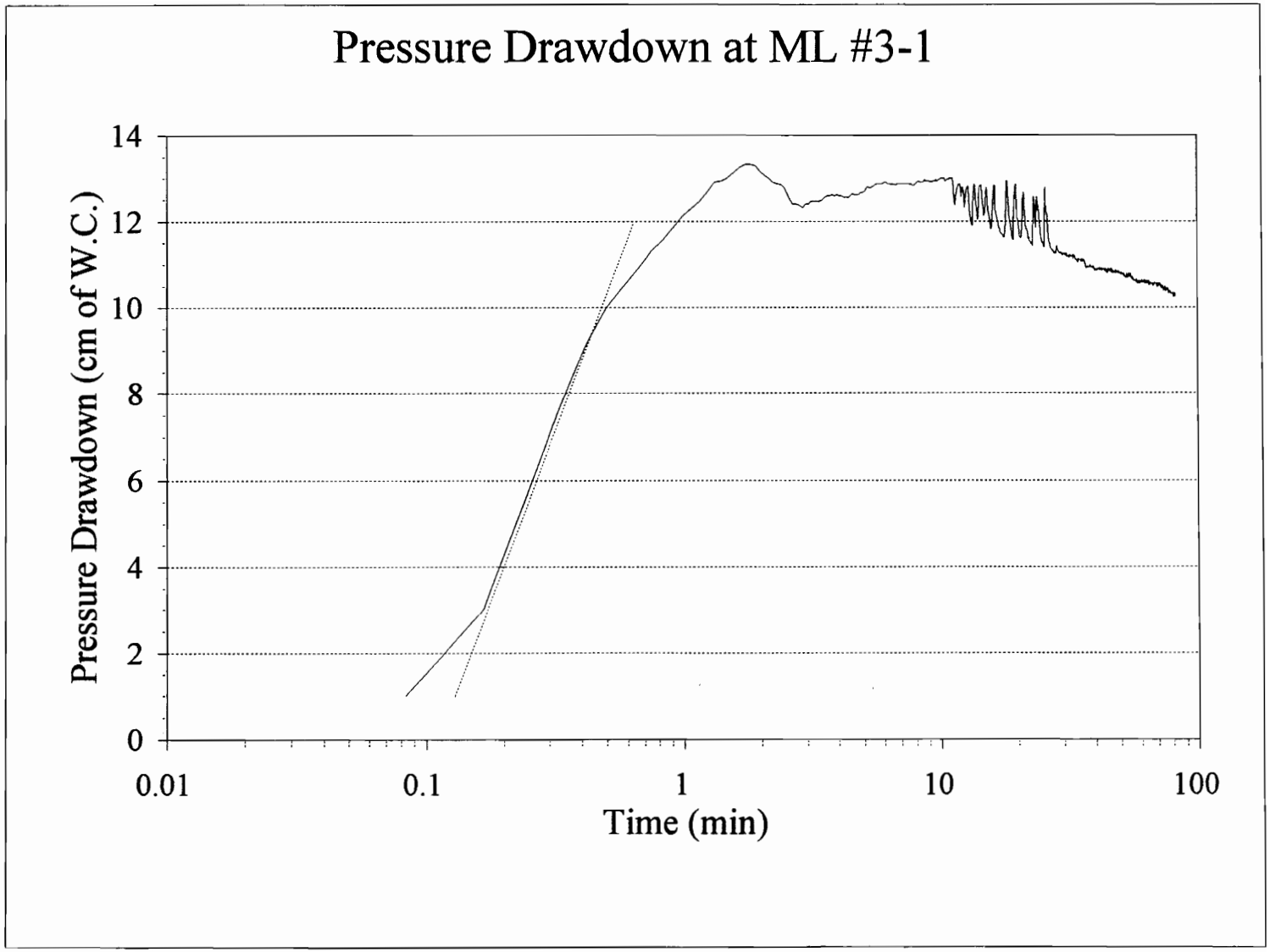

Figure 6.6: Pressure drawdown at multi-level well #3-1

6.3.3 HANTUSH'S LEAKY AQUIFER METHOD OF SOLUTION

Observation of log-log plots from pressure drawdown in the field show signs of leakage. This is apparent if drawdowns are predicted by using the Theis solution. Matching drawdown curves with the Theis well function showed that leakage occurred. The silt and clay region (0 to 457-cm) described in Chapter 3 can be considered as the confining layer or unit of leakage. However, analyses consider the entire region above the screened interval #1 as a region of leakage, i.e., a fully-penetrating well. This is a reasonable assumption considering multi-level layers above screened interval #1 failed to respond after a 120 minute duration during pneumatic tests.

The procedure for applying Hantush's leaky aquifer method of solution to pressure drawdown data was presented in Chapter 2. Figures 6.4 through 6.6 provide drawdown data necessary to conduct the superposition as discussed in Chapter 2. Each pressure drawdown curve includes a match point for the points $1/u^* = 1.0$ and $W(u, r/B)^* = 1.0$ on the type curves for leaky aquifers (after Walton, 1960). The steps included in the evaluation of data for multi-level well #1-1 are as follows:

1). calculate the average flow rate ($Q = 3551.66$ cm^3/s) as described above;

2). determine length of the screened interval ($b = 30.48$ cm);

3). use superposition to determine r/B^* from type curves ($r/B^* = 0.40$);

4). determine s^* from superposition for pressure drawdown data ($s^* = 8.0$ cm of water column);

5). $$k_{air} = \frac{Q\mu_{air}}{4\pi bs^*\gamma_w} W\left(\frac{r^2 S}{4Tt}, \frac{r}{B}\right)^* = 2.14X10^{-7} cm^2;$$

6). $$k'_{air} = \left(\frac{r^*}{B}\right)^2 \frac{k_{air} bb'}{r^2} = 7.25X10^{-8} cm^2.$$

Match points determined from superposition and air permeabilities for each multi-level well are presented in Table 6.2. Furthermore, match points used to determine parameters from type curves are shown in Figures 6.7, 6.8, and 6.9 for ML wells #1 through #3, respectively.

Table 6.2: Results from Hantush method of solution

Multi-level pressure monitoring well #	r/B^*	s^* (cm W.C.)	Radial air permeability k_{air} (cm^2)	Air permeability of confining unit k'_{air} (cm^2)
1	0.40	8.0	2.14×10^{-7}	7.25×10^{-8}
2	1.0	3.6	4.75×10^{-7}	1.11×10^{-7}
3	1.0	17.0	1.01×10^{-7}	2.14×10^{-7}

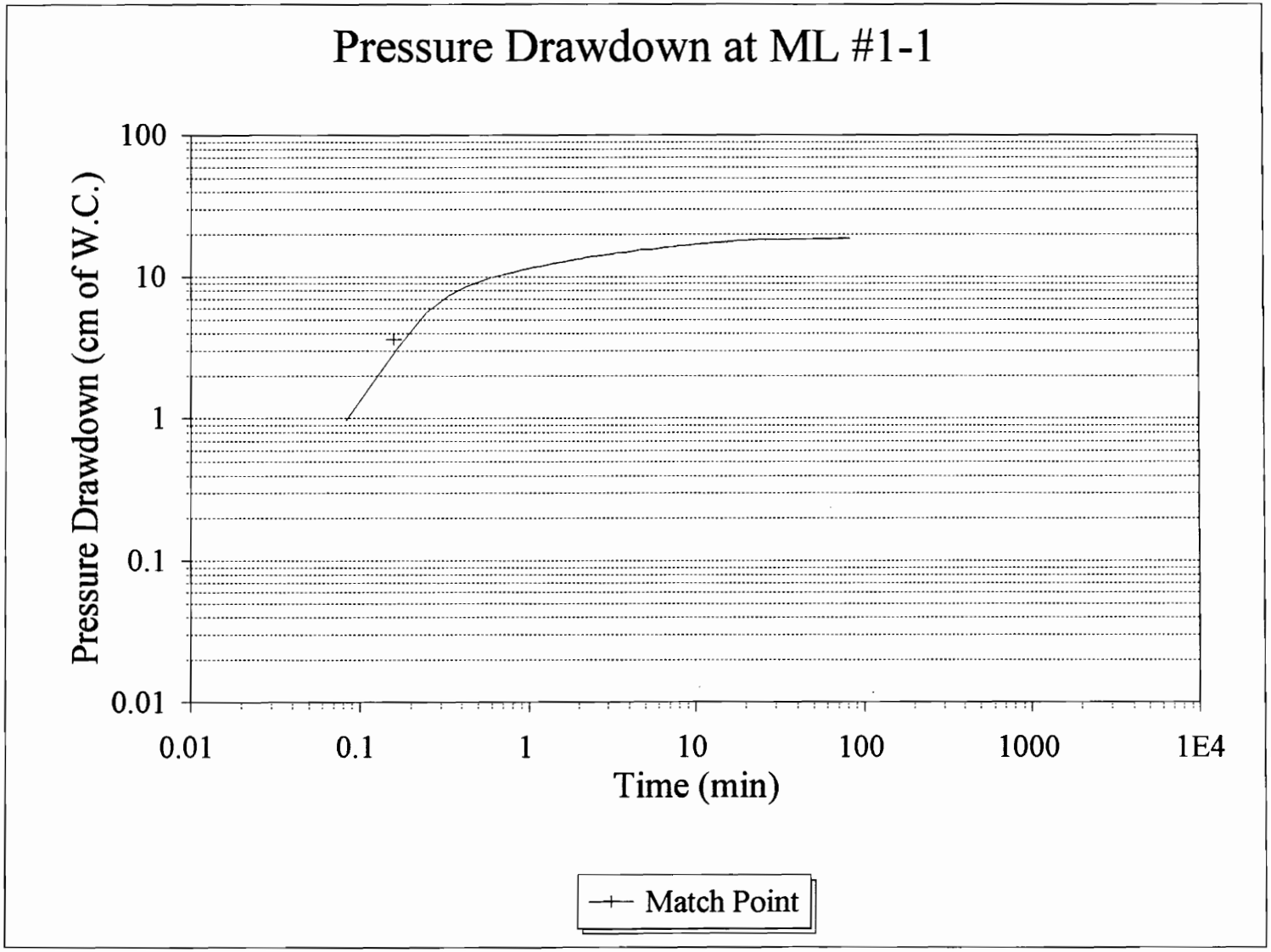

Figure 6.7: Pressure drawdown at multi-level well #1-1

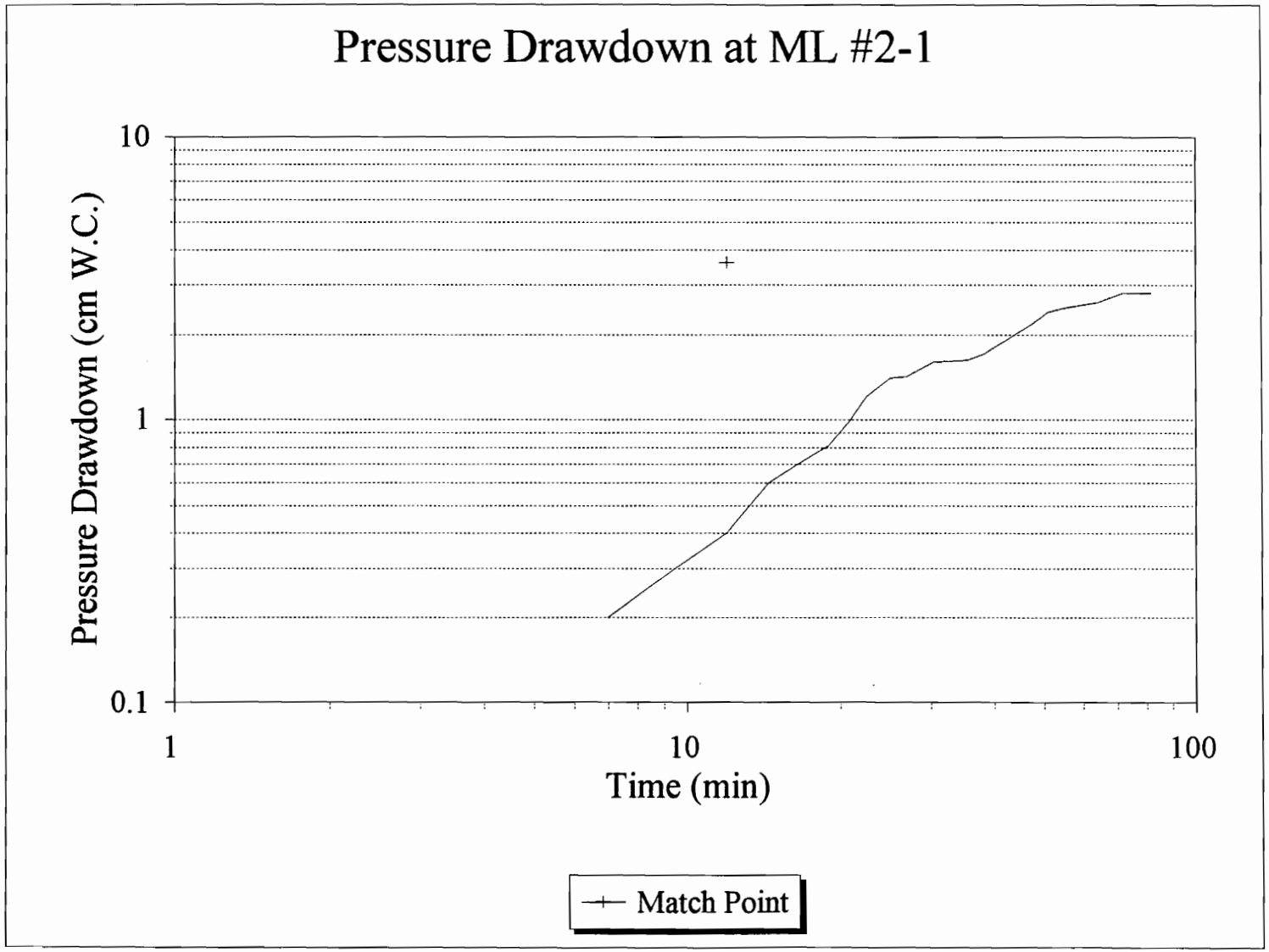

Figure 6.8: Pressure drawdown at multi-level well #2-1

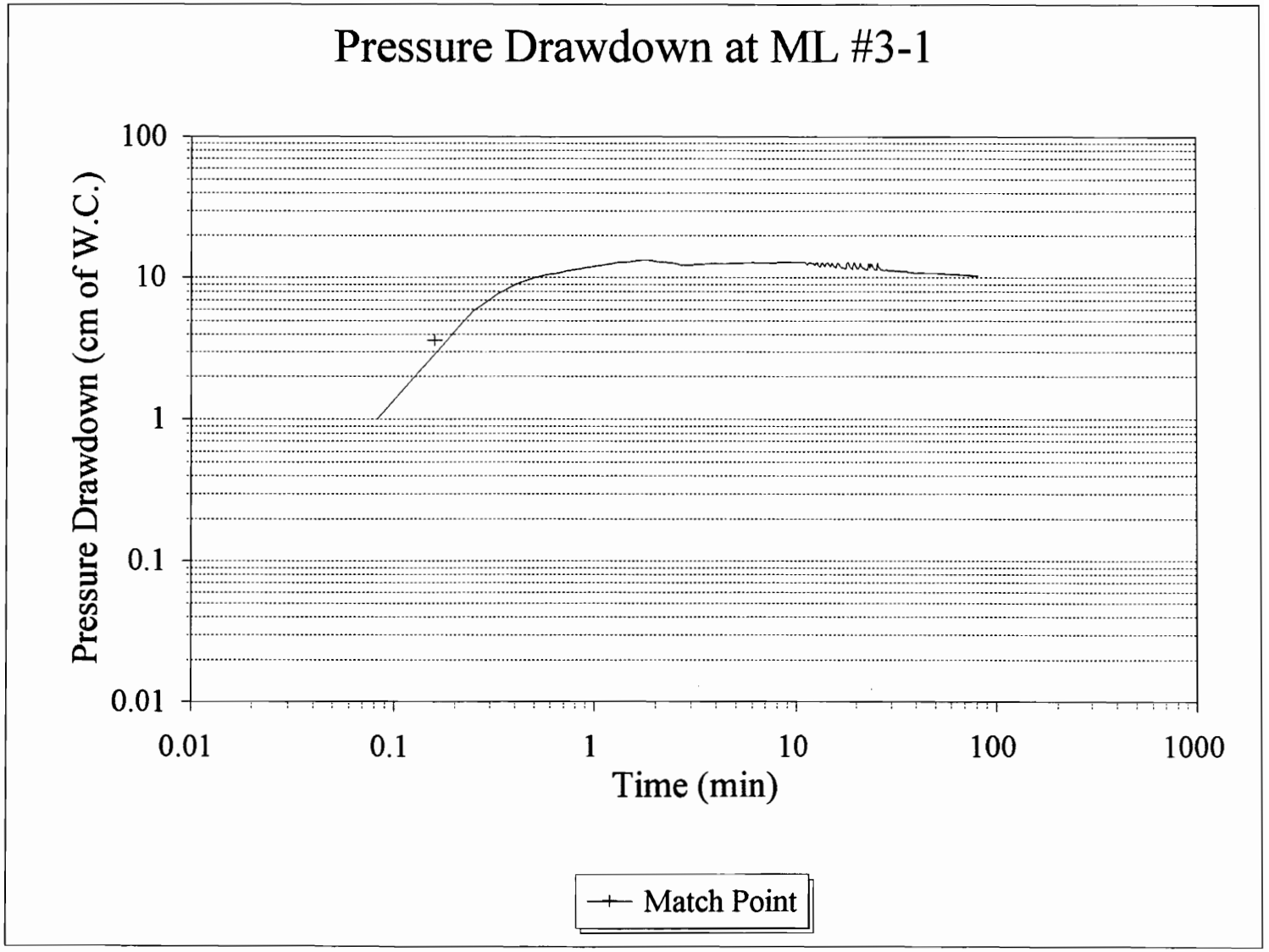

Figure 6.9: Pressure drawdown at multi-level well #3-1

6.3.4 AIRTEST FOR STEADY, TWO DIMENSIONAL, AXISYMMETRIC AIR FLOW

Ambient and extraction well temperature, flow rate, pressure drawdown data, prevailing atmospheric pressure, and well dimensions were input into AIRTEST to predict air permeabilities. Also, estimated air permeabilities were input to the program to facilitate performance of a least squares analysis. Sample model input as well as output data are also summarized in the Appendix.

As previously mentioned, the clay region (0 to 457-cm) was determined to be the region over which the leakage occurred. Because the screen interval did not extend over the entire region between 457 to 767 cm below the subsurface, the well was modeled as partially penetrating in AIRTEST. The following air permeabilities were generated using Hantush's method of solution in AIRTEST: k_r = 2.63 X 10^{-8} cm^2, k_z = 5.80 X 10^{-9} cm^2, and k' = 7.61 X 10^{-8} cm^2. In addition the rigorous method of solution option was chosen and provided the following air permeabilities: k_r = 2.51 X 10^{-8} cm^2, k_z = 1.39 X 10^{-8} cm^2, and k' = 3.01 X 10^{-7} cm^2.

CHAPTER 7

DISCUSSION OF RESULTS

The primary goal of conducting pneumatic tests was to determine air permeabilities in sequential soil layers. However, other critical parameters directly related to the permeability are important. Vapor and hydrocarbon extraction rates are parameters indicating whether conditions are favorable to SVE (Johnson et al., 1990a). Pressure at the extraction well is another parameter because it is indicative of formation and well-losses associated with air transport and assists in the selection of a blower for a full-scale SVE remediation system.

7.1 EXTRACTION WELL PRESSURE AND WELL LOSSES

Results from pneumatic tests at Port Oil Station #288 suggest significant pressure losses in the vicinity of the extraction well. Previous studies have considered losses within the vacuum system, but fail to address well and formation losses. For example, Massmann (1989) determined a head loss of 5.0 cm of water column between the top and bottom of an extraction well, which represented only 5% of the total drawdown at the well (100 cm or 0.097 atm). Similarly, head losses due to the packer system were not significant. Because their is no definitive study of SVE well losses, energy loss

energy loss theory from the groundwater literature was adopted.

In Section 6.1, pressure and flow rate at the extraction well were evaluated to take into consideration energy losses associated with the vacuum system, formation, and well. A pressure of 0.92 atm at the well screen was determined by extrapolation of drawdown data measured at ML pressure monitoring wells from pneumatic tests (see Figure 6.1). However, the extraction well pressure measured in the field was 0.53 atm. Taking into consideration the energy losses, the pressure at the well head was calculated as 0.86 atm.

A possible explanation for this phenomenon is skin damage of the *in-situ* formation during the drilling of the bore hole associated with well losses. This theory would explain the increase in pressure differentials monitored at the extraction well if the formation was actually hardened or condensed during drilling. If the media were hardened, then pressure must increase to cause the air to flow through a less permeable region. This theory is supported by analysis of energy losses at the extraction well in which well losses accounted for 82% of the total drawdown at the well while formation losses only accounted for 18% of the energy losses. Vacuum system losses were basically insignificant (1%). Therefore, the pressure differential measured at the well head would be mostly attributed to the well loss.

7.2 AIR PERMEABILITY IN SEQUENTIAL SOIL LAYERS

Air permeabilities were generated for both pressures of 0.53 and 0.92 atm at the extraction well (Tables 7.1 and 7.2). Air permeabilities derived from transient solutions, for P_w = 0.92 atmospheres, at ML #1 for soil layer #1 were 3.69 X 10^{-7} and 2.17 X 10^{-7} cm^2 for the Copper-Jacob (1946) and Hantush (1956) method of solution, respectively. Air permeabilities, derived as ML #3 were consistently less than ML #1 by a factor of two: 2.74 X 10^{-7} and 1.02 X 10^{-7} cm^2 for the former and latter solution technique. Air permeabilities derived from the transient solutions were within the same order of magnitude, but variations between k_{air} values using the same solution technique were significant but typical of field tests. Conditions unique to each axis may explain the inconsistency in air permeabilities at ML #1 and ML #3. Multi-level wells were constructed along two axes as discussed in Chapter 4 and shown in Figure 4.1. Multi-level wells on one axis were positioned so the pavement could act as a barrier of low permeability preventing "short circuiting". However, on the other axis the wells were laid out along the radial extending to the pavement boundary. This may also explain the different responses measured at ML #2 and ML #4.

Air permeabilities for soil layer #1 at ML #2 were 1.56 X 10^{-6} and 4.82 X 10^{-7} cm^2 for the Cooper-Jacob and Hantush methods of solution. These values of k_{air} are considerably

Table 7.1 Air permeabilities obtained from data analyses (P_w = 0.53 atm)

	Johnson's solution for radial flow (steady-state)	Cooper-Jacob method of solution (transient)	Hantush's leaky aquifer solution (transient)	Baehr & Hult solutions (steady-state)	
				Hantush	Rigorous
Ml #1					
k_a (cm^2)	2.02×10^{-8}	3.64×10^{-7}	2.14×10^{-7}	2.63×10^{-8}	2.51×10^{-8}
k_a' (cm^2)			7.25×10^{-8}	7.61×10^{-8}	3.01×10^{-7}
k_{az} (cm^2)				5.80×10^{-9}	1.39×10^{-8}
ML #2					
k_a (cm^2)		1.24×10^{-6}	4.75×10^{-7}		
k_a' (cm^2)			1.11×10^{-7}		
ML #2					
k_a (cm^2)		2.71×10^{-7}	1.01×10^{-7}		
k_a' (cm^2)			2.14×10^{-7}		

Table 7.2 Air permeabilities obtained from data analyses (P_w = 0.92 atm)

	Johnson's solution for radial flow (steady-state)	Cooper-Jacob method of solution (transient)	Hantush's leaky aquifer solution (transient)	Baehr & Hult solutions (steady-state)	
				Hantush	Rigorous
Ml #1					
k_a (cm^2)	3.99×10^{-7}	3.69×10^{-7}	2.17×10^{-7}	4.26×10^{-8}	-----
k_a' (cm^2)			7.35×10^{-8}	1.29×10^{-7}	-----
k_{az} (cm^2)				1.05×10^{-8}	-----
ML #2					
k_a (cm^2)		1.26×10^{-6}	4.82×10^{-7}		
k_a' (cm^2)			1.13×10^{-7}		
ML #3					
k_a (cm^2)		2.74×10^{-7}	1.02×10^{-7}		
k_a' (cm^2)			2.16×10^{-7}		

different from those values predicted for ML #2. A possible explanation for this deviation is the proximity of ML #2 to the pavement boundary. A second hypothesis is that screened layer #1 may not be consistent in layered media across the span of the axis. Existence of quartz veins which are region-specific characteristics of the Carolina Slate Belt can act as "short circuits" for air transport (Johnson, 1972). Additionally, ML #2 drawdown data was taken manually and was not easy to interpret. Therefore, ML #1 and ML # 3 are more representative of actual filed-site air-phase permeabilities.

At all three wells Cooper-Jacob solutions were consistently higher than the Hantush-derived values of k_{air}. This difference can be attributed to the difference in the technique of interpretation. A built in assumption in the Cooper-Jacob solution is that the infinite well series is estimated for $u < 0.01$. Analysis of transient data can be left open to interpretation depending on the air-filled porosity, ϵ, utilized to calculate the value of u. For pneumatic tests, the value of u varies depending on estimated values of the air-filled porosity. Therefore, application of the Cooper-Jacob method solution may not be appropriate if assumptions are violated.

Air permeabilities derived from steady-state solution techniques were comparably different according to the pressure at the extraction well. For ML #1-1 and P_w = 0.53 atm, k_{air}

values were 2.02 X 10^{-8} and 2.51 X 10^{-8} cm^2 for both the Johnson et al. (1990b) steady-state solution and AIRTEST (Hantush method of solution), respectively. However, with a P_w = 0.92 atm, k_{air} values were 3.99 X 10^{-7} and 4.26 X 10^{-8} cm^2 for the former and latter solution techniques. A hypothesis is that deviations are attributed to boundary condition at r = r_w only affects a small porion of the domain in AIRTEST; whereas, in the Johnson et al. (1990b) steady-state solution the entire domain is affected. As noticed, k_{air} derived values are within the same order of magnitude for P_w = 0.53 atm and differ by an order of magnitude for P_w = 0.92 atm.

A comparison between transient and steady-state derived air permeabilities at ML #1-1 shows that all values are within the same order of magnitude, except for those generated with AIRTEST. Values of permeability, as derived by AIRTEST, for both pressures of 0.53 and 0.92 atm are indicative of a less permeable medium with an order-of-magnitude difference. Explanations for these deviations include:

(1) AIRTEST method of solution (algorithm),

(2) Boundary conditions for partially-penetrating well.

AIRTEST utilizes an estimated value of the permeability and predicts permeabilities through a least squares analysis. Because two data points both at the same elevation could possibly vary, there may be non-unique solutions for k_{air}.

Also, AIRTEST modeled the extraction well as a partially-penetrating well with vertical flow. At the site there is likely preferential pathways for air flow (horizontal).

A comparison of k'_{air} values from AIRTEST and Hantush method solution differ by an order of magnitude in some instances. This can be attributed to the fact that AIRTEST models a partially-penetrating well; however, the Hantush solution modeled the domain as a fully-penetrating well. Substitution of a thinner region over which leakage occurs in the Hantush method of solution will generate a smaller air permeability. For example, $k'_{air} = 7.25 \times 10^{-8}$ and 3.01×10^{-7} cm^2 for the Hantush (1956) fully-penetrating well method of solution and AIRTEST rigorous method of solution, respectively.

7.3 COMPARISON WITH LABORATORY RESULTS

In Chapter 3 strata were identified in terms of lithologic description and physical properties. Intrinsic permeabilities for stratum number three (6.71 - 10.67 m below subsurface) presented in Table 3.1 ranged from 3.67×10^{-10} to 3.67×10^{-9} cm^2 for this particular stratum (Widdowson et al., 1993). Intrinsic air permeabilities of 2.47×10^{-9} to 3.23×10^{-9} cm^2 were determined from a core sample taken at bore hole (B-4) near the extraction well at approximately 6.10 m below the subsurface (Widdowson et al., 1993). Air

permeabilities determined from pneumatic tests for screened interval number one in the extraction well (6.34 - 6.57 m below the subsurface) ranged from 1.24 X 10^{-6} to 2.63 X 10^{-8} cm^2 (see Tables 7.1 and 7.2). Permeabilities obtained from pneumatic tests are consistently one to three orders of magnitude greater than laboratory results depending on the method of solution.

Two possible theories are offered to explain differences in field and laboratory results. One supporting theory is the possible deviation in permeabilities obtained from radial and vertical flow. Laboratory tests were conducted on core samples using the constant-head permeameter where the direction of flow is vertical or perpendicular to the depositional layers (Widdowson et al., 1993). However, analyses of data from pneumatic tests determine the permeability modeling flow parallel to the depositional layers. The second theory predicts that fractures in the domain caused by interaction between VOCs and clayey soils increase the air permeability.

In order to determine an average permeability the spatial variability of permeability is treated in two approaches: a law of harmonic composition, if the blocks are in series, and the law of arithmetic composition, if blocks are in parallel (de Marsily, 1986). The following equations predict average permeabilities for both a harmonic and arithmetic composition,

$$\frac{\sum L_i}{K_{mean}} = \sum \frac{L_i}{K_i} \qquad (7.1)$$

where,

L_i = length of a block in series

K_i = hydraulic conductivity of a block in series

$$k_{mean} \sum e_i = \sum e_i K_i \qquad (7.2)$$

where,

e_i = length of a block in parallel arrangement

K_i = hydraulic conductivity of a block in parallel arrangement

For the case of radial flow the arithmetic composition would be used as a means of determining the average permeability; where as, vertical permeability would be determined by a harmonic composition. If sequential layers of a soil matrix were analyzed, the arithmetic composition would produce a higher permeability due to the difference in the mathematical expressions.

Air permeabilities obtained from AIRTEST also provide a basis of comparison between vertical and radial permeabilities to support the above hypothesis. Transient methods of

basis of comparison between vertical and radial permeabilities to support the above hypothesis. Transient methods of solution modeled screened interval #1 as a fully-penetrating well. Therefore, the Hantush method of solution generated a radial permeability for the local layer and a vertical permeability for the confining zone of leakage. However, the permeabilities obtained from AIRTEST for the leaky aquifer solution for a partially penetrating well identify a vertical permeability of 10^{-9} cm^2. This on the same order of magnitude as the air permeabilities obtained from laboratory test.

Soil stratification of evenly laminated phyllite, as discussed in Chapter 3, results in interbedded zones of locally high and low permeability. These characteristics are a result of presence of clay layers which act as impermeable boundaries, and sand and quartz veins that act as local zones of high permeability (Johnson, 1972). Layers above screened interval number one from 5.16 - 5.38 m and 5.73 - 5.95 m failed to respond to pneumatic tests. Possibly these layers contained the previously mentioned clay layers acting as impermeable boundaries. The measured responses at these layers could possibly be indicative of the low permeabilities determined in the laboratory.

Existence of fractures within the parent rock or as a result of interaction between VOCs and clayey soils may also explain the higher than expected permeabilities at Port Oil

concluded that the effective permeability is greatly increased. Gibson et al. (1993) identified the existence of fractures in a field pilot test study of vapor extraction from glacial clay soil contaminated by paint thinner, resulting in increased effective porosity and permeability of the clay medium. It is unclear whether the components of gasoline would produce the same result in clay-rich Piedmont soils.

7.4 PUMP AND SYSTEM CURVES

An analysis was conducted to evaluate pump and system curves and determine the operating conditions for an actual full-scale soil vapor extraction system. Pneumatic-test results described in this thesis provided the pertinent design parameters and extraction well characteristics for design of a pilot-scale SVE system at the field site. For a single screen extraction well with a screen length of 1.52 m (5.0 ft.), the expected volumetric extraction rate would theoretically increase by a factor of five for a constant pressure at the extraction well. As previously discussed, the system curve was generated by varying the pressure and flow rate by means of an adjustable valve at the well head (see Figure 5.1). Four vacuum pump performance curves were plotted along with a modified system curve for a 1.52-m screen length to best determine an operating point (Figure 7.1). Pump curves were obtained for a model #3204 pneumatic pump supplied

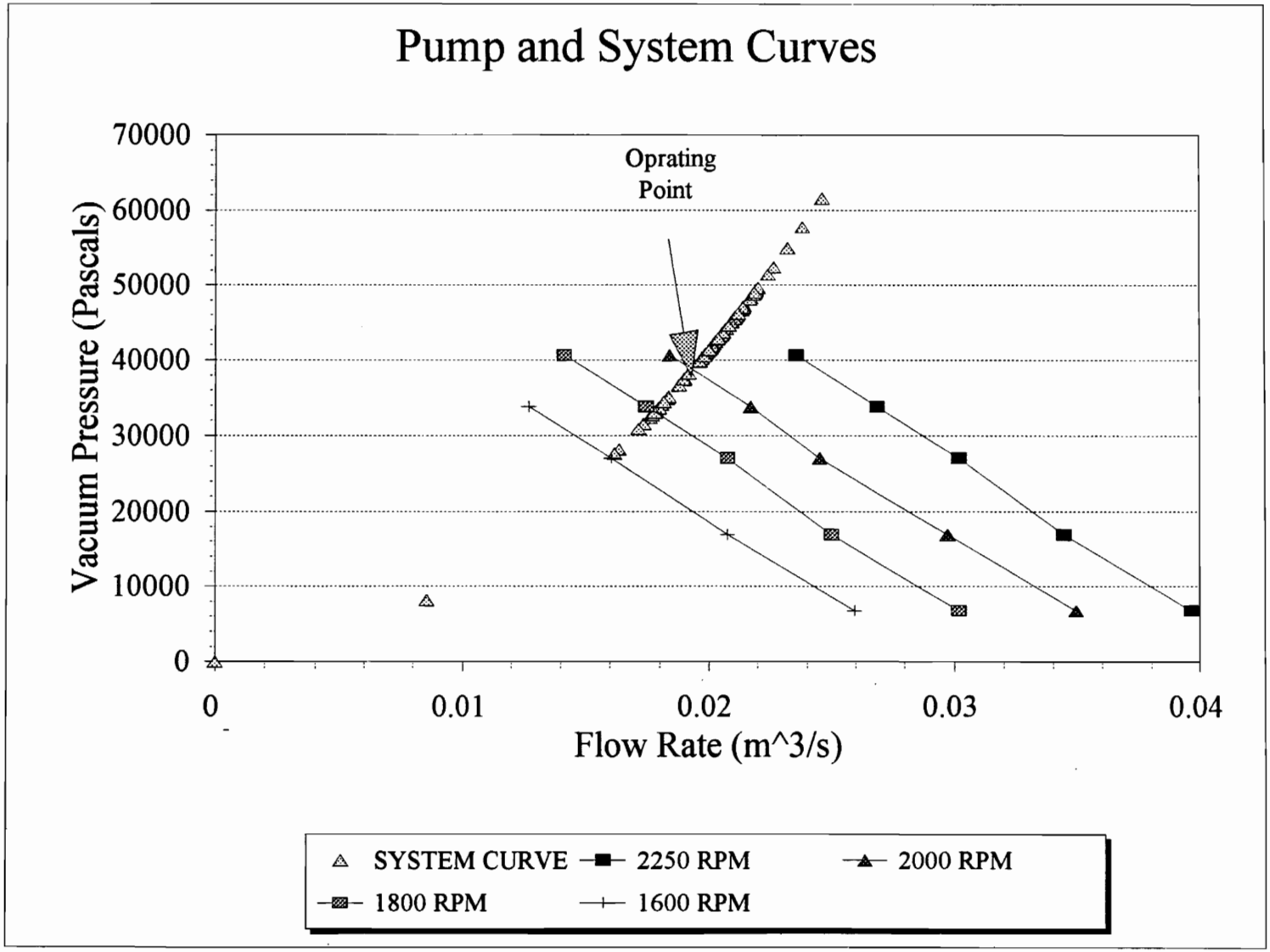

Figure 7.1: Illustration depicting operation point for a pneumatic pump

by Tuthill Corporation. For a pump speed of 2000 RPM the optimal operating condition would be a flow rate of 0.019 m^3/s and a vacuum pressure of 38200 pascals (0.62 atm). As shown other operating conditions are apparent, but these points will not provide maximum flow rates for a 1.52-m single screened extraction well in the layer where pneumatic tests were conducted.

7.5 VAPOR EXTRACTION RATE

The rate of vapor extraction is an essential parameter determined from pneumatic tests. Johnson et al. (1990a) list vapor flow rate, contaminant vapor concentration, and vapor flow path relative to the contaminant location as governing factors in SVE. The conditions favorable to a productive vapor flow path were addressed in Chapter 3. Since the extraction rate needs to be at an optimum, field techniques need to insure a best performance system is implemented. Pump and system curves for a full-scale SVE system were plotted to identify an operating point for a pneumatic test. During pneumatic tests extraction rates were approximately 3552 cm^3/s. These rates as previously mentioned do not satisfy ideal conditions. These are all site-specific characteristics and must be determined during the initial site assessment.

Ideal vapor flow conditions (i.e., 47200 - 472000-cm^3/s) was a parameter considered in the design of the full-scale

remediation system (Johnson et al., 1990a; Widdowson et al., 1993). Results from multi-level air permeability tests indicated an average flow rate of 3552-cm^3/s for screened layer #1. As described in Chapter 4, this layer of concentration was 30.48-cm thick. Pneumatic tests were important in the determination of the layers most permeable to air transport. Regional-specific geology of the area consists of layers of laminated phyllite which coarsens upward with increasing sand portions until there is a change to a flaser bedded phyllite producing alternating layers of clay and fine sand (Johnson, 1972). The location of the more permeable or coarser material was determined from pneumatic tests. Therefore, for a 152.40-cm (5.0-ft) screened interval in the zone of coarser material would at least provide a vapor extraction rate of 17760-cm^3/s. During implementation of the full-scale system 12 wells were installed having the 152.40-cm screened intervals (Widdowson et al., 1993). This would theoretically provide a vapor extraction rate of 213120-cm^3/s, a condition recognized as an ideal situation.

CHAPTER 8

SUMMARY AND CONCLUSIONS

8.1 SUMMARY

In this thesis, the design, performance, and analysis of a multi-level SVE test was presented to determine permeable zones within sequential soil layers. Pneumatic test setup consisted of one multi-level extraction well and five multi-level pressure monitoring wells. The screen locations were based on initial field-site characterization. Gas was extracted at one screen while soil gas pressure was monitored at ML pressure monitoring wells. Parameters monitored during the tests included: air velocity, pressure at the well head, pressure at ML pressure monitoring wells, and temperature. A fully automated data collection system included a programable datalogger to collect data at specified time intervals. Several tests were conducted which included: identifying vacuum pump or blower specifications, determining operating conditions, and obtaining data to quantify air permeability.

Data was examined to determine air permeabilities with applicable steady-state and transient solution techniques which included solutions by: Johnson et al. (1990a), Baehr and Hult (1991), Cooper and Jacob (1946), and Hantush (1956). Air permeabilities obtained from transient solutions were consistent for the same ML pressure monitoring wells; however,

k_{air} for wells at different radii varied. These differences were attributed to the well's location to the proximity to the surface seal boundary.

8.2 CONCLUSIONS

Since air permeability is an essential parameters in SVE systems, pneumatic tests must focus on the most permeable zones. Ordinary designs make use of a single screen extraction well which is not applicable in regions where the subsurface is highly heterogenous and has unique properties due to the interaction between contaminants and the media. Because of region-specific characteristics at the field site, consisting of alternating layers of silt and clay, a multi-level extraction well was a necessity. The multi-level approach allowed identification and characterization of the layers most conductive to air flow. Therefore, the full-scale SVE system could be centrally located to concentrate on the layers where the passage of vapors were most significant.

Head losses associated with the pneumatic test system were essential in determining pressures at the extraction well. Previous systems have focused on identifying losses due to the vacuum system, but have not addressed the losses associated with the well and formation. For pneumatic tests conducted in this thesis, energy losses due to the well and formation caused a considerable deviation from the pressure

extrapolated at the extraction well. The pressure was extrapolated using pressure drawdown at ML pressure monitoring wells.

Solution techniques utilized from the literature were all derived assuming that the basic equations which govern groundwater flow (i.e., Darcy's Law, the continuity equation, and incompressibility of the fluid provide good approximations of gas transport). Results indicate that these methods of solution provide good approximations of conditions associated with gas transport if the pressure at the extraction well is properly evaluated to determine possible energy losses. This thesis compliments pervious studies by demonstrating the application of both steady-state and transient methods of solution for soil vapor transport.

8.3 FUTURE RECOMMENDATIONS

Multi-level pneumatic tests were conducted to identify the most permeable layers in the subsurface; however, only one of the five layers under investigation permitted passage of air. The test was a success in terms of identifying the boundary between the less permeable clay and coarser sandy material. It would be interesting if the multi-level approach were implemented in a region where there is a gradual transition in air permeability. A pneumatic test of this kind would demonstrate the advantages of utilizing the multi-level

approach to quantify k_{air} in this type stratigraphy. Additionally, a multi-level pneumatic test would be advantageous when the subsurface has unique properties due the interaction between the contaminants and the soil medium. As previously described, contaminants can enhance fracturing of the soil medium and increase permeability, creating conditions sufficient for the implementation of a SVE system (Gibson et al., 1993). The multi-level approach would locate layers where this chemical interaction takes place between the contaminant and soil medium.

REFERENCES

Abdul, A. S., Gibson, T. L., and Rai, D. N., "Laboratory Studies of the Flow of Some Organic Solvents and Their Aqueous Solutions Through Bentonite and Kaolin Clays," *Ground Water*, Vol. 28, No. 4, pp. 524-533, 1990.

Baehr, Arthur L., and Hult, Marc F., "Determination of the Air-Phase Permeability Tensor of an Unsaturated Zone at the Bemidji, Minnesota, Research Site," U.S. Geological Survey, Water-Resources Investigations Report 88-4220, Reston, Virginia, pp. 55-62, 1988.

Baehr, Arthur L., and Hult, Marc F., "Evaluation of Unsaturated Zone Air Permeability Through Pneumatic Tests," *Water Resources Research*, Vol. 27, No. 10, pp. 2605-2617, October 1991.

Bear, J., Hydraulics of Groundwater, McGraw-Hill, New York, N.Y., pp. 569, 1979.

Cooper, H. H., Jr., and Jacob, C. E., "A Generalized Graphical Method for Evaluating Formation Constants and Summarizing Well Field History," *Transactions. American Geophysical Union*, Vol. 27, pp. 526-534, 1946.

Driscoll, Fletcher G., Groundwater and Wells, 2nd Edition, Johnson Division, St. Paul, Minnesota 55112, pp. 1089, 1986.

Dullian, F. A. L., Porous Media: Fluid Transport and Pore Structure, Academic Press, New York, N.Y., pp. 396, 1979.

Gibson, Thomas L., Abdul, Abdul S., Glasson, William Glasson A., Ang, Carolina C., and Gatlin Dallas W., "Vapor Extraction of Volatile Organic Compounds from Clay Soil: A Long-Term Field Pilot Study," *Ground Water*, Vol. 31, No. 4, pp. 616-626, 1993.

Hantush, M. S., and Jacob, C. E., "Nonsteady Radial Flow in an Infinite Leaky Aquifer," *Transactions. American Geophysical Union*, Vol. 36, pp. 95-100, 1955.

Hantush, M. S., "Analysis of Data from Pumping Tests in Leaky Aquifers," *Journal Geophysical Research*, Vol. 69, pp. 4221-4235, 1956.

Hantush, M. S., "Hydraulics of Wells," *Advanced Hydroscience*, Vol. 1, pp. 281-432, 1964.

Hinchee, Robert E., Downey, Douglas C., Dupont, Ryan R., Aggarwal, Pradeep K., and Miller, Ross N., "Enhancing Biodegradation of Petroleum Hydrocarbons Through Soil Venting," *Journal of Hazardous Materials*, 27, pp. 315-325, 1991.

Johnson, Thomas F., "Paleoenvironmental Analysis and Structural Petrogenesis of The Carolina Slate Belt Near Columbia, South Carolina," Master of Science Thesis, University of South Carolina, 1972.

Johnson, P. C., Kemblowski, M. W., and Colthart, J. D., "Practical Screening Models for Soil Venting Applications," *Proceedings of NWWA/API Conference on Petroleum Hydrocarbons and Organic Chemicals in Ground Water*, Houston, Texas, pp. 521-546, 1988.

Johnson, Paul C., Stanley, C. C., Kemblowski, M. W., Byers, D. L., and Colhart, J. D., "A Practical Approach to The Design, Operation, and Monitoring of In Situ Soil-Venting Systems," *Ground Water Monitoring Review*, Vol. 10, No. 2, pp. 159-178, 1990a.

Johnson, Paul C., Kemblowski, Marian W., and Colthart, James D., "Quantitative Analysis for the Cleanup of Hydrocarbon-Contaminated Soils by In-Situ Soil Venting," *Ground Water*, Vol. 28, No. 3, pp. 413-429, 1990b.

Joss, C. J., and Baehr, A. L., "AIRTEST - A Computer Code to Simulate Two Dimensional Axisymetric Flow in The Unsaturated Zone", U.S. Geological Survey Open File Report, Under Review, 1993.

Klinkenberg, L. J., "The Permeability of Porous Media to Liquids and Gases, *Drilling and Production Practice*, American Petroleum Institute, New York, pp. 200-213, 1941.

Krishnayya, A. V., O'Connor, M. J., Agar, J. G., and King, R. D., "Vapour Extraction Systems Factors Affecting Their Design and Performance," *Proceedings of NWWA/API Conference on Petroleum Hydrocarbons and Organic Chemicals in Ground Water*, Houston, Texas, pp. 547-569, 1988.

Law Environmental, Inc., "Report of Phase II Assessment," Report 41-0604-01, Law Environmental, Inc., Kennesaw, GA, 1991.

De Marsily, Ghislain, Quantitative Hydrogeology, Academic Press, Inc., San Diego, California, pp. 440, 1986.

Massmann, J.W., "Applying Groundwater Flow Models in Vapor Extraction System Design," *Journal of Environmental Engineering*, Vol. 115, No. 1, pp. 129-149, February 1989.

Munson, Bruce R., Young, Donald F., Okliishi, Theodore H., Fundamentals of Fluid Mechanics, John Wiley & Sons, Inc., New York, pp. 843, 1990.

Nanjunjeswar, B. V., Truitt, Duane J., and Krabbe, John L., *Vacuum Extraction Pilot Test Standard Operating Procedures*, Delta Technical Review, Vol. 2, No. 4, pp. 8-11, December 1990.

Noggle, J., Physical Chemistry on a Microcomputer, Little Brown, Boston, Mass., pp. 239, 1985.

Sabersky, Rolf H., Acosta, Allan J., and Hauptmann, Edward G., Fluid Flow, 3rd Edition, Macmillan Publishing Company, New York, pp. 537, 1989.

Theis, C. V., "The Relation Between the Lowering of the Piezometric Surface and the Rate and Duration of Discharge of a Well Using Ground-Water Storage," *Transactions. American Geophysical Union*, Vol. 16, pp. 519-524, 1935.

Todd, David K., Groundwater Hydrology, Second Edition, John Wiley & Sons, Inc., New York, pp. 535, 1980.

Walton, W. C., *Leaky Artesian Aquifer Conditions in Illinois*, Illinois State Water Survey Rept. Invest. 39, Urbana, Illinois.

Widdowson, Mark A., Ray, Richard P., Reeves, Howard W., Aelion, Marjorie C., and Holbrooks, Kenneth D., "Investigation of Soil Venting-Based Remediation at a UST Site in The Appalachian Piedmont," Bioremediation of Pollutants in Soil and Water, ASTM STP 1235, In press.

Yu, L. L., "Study of Air Flow Through Porous Media," Master of Science Thesis, University of Conn., 1985.

APPENDIX A

Sample input and output files from AIRTEST

PROJECT : PORT OIL STATION #288
=======

SCOPE : RESULTS OF FULL-SCALE PERMEABILITY TESTS
TEST DATE : 11/29/93
WELL NUMBER : VW-1

1. MODEL INPUT SUMMARY
----- ----- -------

MODEL DOMAIN	: THICKNESS = 280.400 cm
	: ESTIMATED HORIZONTAL PERMEABILITY =.100E-07 cm^2
	: ESTIMATED ANISOTROPY RATIO = 2.00
UPPER CONFINING UNIT	: THICKNESS = 481.520 cm
	: ESTIMATED PERMEABILITY =.100E-08 cm^2
WELL DEPTH (HANTUSH d)	: TOP OF SCREEN = 152.46 cm
WELL DEPTH (HANTUSH l)	: BOTTOM OF SCREEN = 182.94 cm
WELL RADIUS	: EFFECTIVE RADIUS = 5.71 cm
AIR FLOW DIRECTION	: VAPOR EXTRACTION

2. MODEL OUTPUT SUMMARY
----- ------ -------

AIR TEMP degC	SOIL TEMP degC	ATMOS. PRESS. atm	SYSTEM PRESS. atm	FLOW METER TYPE	SCALE READING --	PREVAIL. FLOW cm^3/sec	ACTUAL FLOW cm^3/sec
30.00	26.50	1.000	.530	NONE	--	--	4524.000

MASS FLOW g/sec	HORIZON. PERM. cm^2	VERTICAL PERM. cm^2	LEAKAGE RATIO(k/b) cm^2/cm	ANISOTPY RATIO (kr/kz)	MEAN OF ERROR IN PRESS.	STD DEV OF ERROR IN PRESS.
2.792	.263E-07	.580E-08	.158E-09	4.526	.159E-03	.328E-05

PROJECT : PORT OIL STATION #288
=======

SCOPE : RESULTS OF FULL-SCALE PERMEABILITY TESTS
TEST DATE : 11/29/93
WELL NUMBER : VW-1

1. MODEL INPUT SUMMARY
----- ----- -------

MODEL DOMAIN	: THICKNESS = 280.400 cm
	: ESTIMATED HORIZONTAL PERMEABILITY =.200E-07 cm^2
	: ESTIMATED ANISOTROPY RATIO = 2.00
UPPER CONFINING UNIT	: THICKNESS = 481.520 cm
	: ESTIMATED PERMEABILITY =.100E-06 cm^2
WELL DEPTH (HANTUSH d)	: TOP OF SCREEN = 152.46 cm
WELL DEPTH (HANTUSH 1)	: BOTTOM OF SCREEN = 182.94 cm
WELL RADIUS	: EFFECTIVE RADIUS = 5.71 cm
AIR FLOW DIRECTION	: VAPOR EXTRACTION

2. MODEL OUTPUT SUMMARY
----- ------ -------

AIR TEMP degC	SOIL TEMP degC	ATMOS. PRESS. atm	SYSTEM PRESS. atm	FLOW METER TYPE	SCALE READING --	PREVAIL. FLOW cm^3/sec	ACTUAL FLOW cm^3/sec
30.00	26.50	1.000	.530	NONE	--	--	4524.000

MASS FLOW g/sec	HORIZON. PERM. cm^2	VERTICAL PERM. cm^2	LEAKAGE RATIO(k/b) cm^2/cm	ANISOTPY RATIO (kr/kz)	MEAN OF ERROR IN PRESS.	STD DEV OF ERROR IN PRESS.
2.792	.251E-07	.139E-07	.627E-09	1.811	-.257E-02	.332E-03

APPENDIX B

Sample program for the CR10 datalogger

```
Program:
  Flag Usage:
  Input Channel Usage:
  Excitation Channel Usage:
  Control Port Usage:
  Pulse Input Channel Usage:
  Output Array Definitions:


  *      1          Table 1 Programs
    01: .5          Sec. Execution Interval

  01:  P17          Module Temperature
    01: 1           Loc :

  02:  P14          Thermocouple Temp (DIFF)
    01: 1           Rep
    02: 1           2.5 mV slow Range
    03: 5           IN Chan
    04: 1           Type T (Copper-Constantan)
    05: 1           Ref Temp Loc
    06: 2           Loc :
    07: 1.8         Mult
    08: 32          Offset

  03:  P11          Temp 107 Probe
    01: 1           Rep
    02: 3           IN Chan
    03: 2           Excite all reps w/EXchan 2
    04: 3           Loc :
    05: 1.8         Mult
    06: 32          Offset

  04:  P6           Full Bridge
    01: 1           Rep
    02: 23          25 mV 60 Hz rejection Range
    03: 1           IN Chan
    04: 1           Excite all reps w/EXchan 1
    05: 2500        mV Excitation
    06: 4           Loc :
    07: 71.979      Mult
    08: -12.366     Offset

  05:  P6           Full Bridge
    01: 1           Rep
    02: 23          25 mV 60 Hz rejection Range
    03: 4           IN Chan
    04: 3           Excite all reps w/EXchan 3
    05: 2500        mV Excitation
```

```
  06: 5        Loc :
  07: 67.912   Mult
  08: -7.5722  Offset


Page 2   Table 1

06:  P2        Volt (DIFF)
  01: 1        Rep
  02: 5        2500 mV slow Range
  03: 3        IN Chan
  04: 6        Loc :
  05: .5       Mult
  06: -250     Offset

07:  P2        Volt (DIFF)
  01: 1        Rep
  02: 5        2500 mV slow Range
  03: 6        IN Chan
  04: 7        Loc :
  05: -.0074   Mult
  06: 3.9143   Offset

08:  P10       Battery Voltage
  01: 8        Loc :

09:  P86       Do
  01: 10       Set high Flag 0 (output)

10:  P77       Real Time
  01: 110      Day,Hour-Minute

11:  P70       Sample
  01: 1        Reps
  02: 1        Loc

12:  P70       Sample
  01: 1        Reps
  02: 2        Loc

13:  P70       Sample
  01: 1        Reps
  02: 3        Loc

14:  P70       Sample
  01: 1        Reps
  02: 4        Loc

15:  P70       Sample
```

```
  01: 1         Reps
  02: 5         Loc

16:  P70        Sample
  01: 1         Reps
  02: 6         Loc

17:  P70        Sample
  01: 1         Reps
  02: 7         Loc

Page 3   Table 1

18:  P          End Table 1


*      2        Table 2 Programs
  01: 0         Sec. Execution Interval

01:  P          End Table 2


*      3        Table 3 Subroutines

01:  P          End Table 3


*      A        Mode 10 Memory Allocation
  01: 28        Input Locations
  02: 64        Intermediate Locations
  03: 0         Final Storage Area 2


*      C        Mode 12 Security
  01: 0         LOCK 1
  02: 0         LOCK 2
  03: 0         LOCK 3


Page 4    Input Location Assignments (with comments):


 Key:
 T=Table Number
 E=Entry Number
 L=Location Number

 T:  E:  L:
```

```
1:  1:  1:  Loc :Module Temperature
1:  2:  2:  Loc :Thermocouple (Copper-Constantan)
1:  3:  3:  Loc :Thermistor 107 Probe
1:  4:  4:  Loc :Pressure Tansducer Omega#PX236-005G V
1:  5:  5:  Loc :Pressure Tansducer Omega#PX236-005G V
1:  6:  6:  Loc :Velocity Transmitter (640 Series)
1:  7:  7:  Loc :Pressure Transducer
                 Omega #PX6303-30VAC5V
1:  8:  8:  Loc :Battery Voltage
```

APPENDIX C

Pneumatic test apparatus and procedure

APPARATUS AND PROCEDURE FOR PNEUMATIC TESTS

1. Equipment required to conduct a vapor extraction pilot test

   - Magnehelic gauges of various ranges at ML (multi-level) wells
   - 40 feet of 1/4" polyethylene tubing
   - Swage lock fittings for 1/4" O.D. tubing and 1/8" male NPT threads
   - Two pneumatic packers with proper connections, 3/16" inflation tubing, and 1/2" X 10′ perforated tubing; male threaded on both sides for 3/8" NPT threads
   - Supply of compressed nitrogen gas
   - Two Omega pressure transducers rated at 5 psi
   - Two 1-1/4" X 2.5′ Trilock PVC pipe sections
   - One 1-1/4" tee and cap with 1/4" O.D. air tight port
   - Three 1-1/4" X 5.0′ Trilock PVC pipe sections
   - One thermistor
   - Air velocity transmitter
   - One 2.0" X 5.0′ PVC pipe section with 5/16" O.D. port
   - Portable vacuum pump
   - CR10 datalogger and lap top computer for data acquisition

- 3/16" steel cable to attach to packer assembly
- Multi-meter to monitor voltage output

2. Test Procedure

A. Data acquisition assembly

- Setup data acquisition station and calibrate pressure transducers for site conditions
- Connect pressure transducer to desired ML well locations by means of 1/4" polyethylene tubing
- Set air velocity transmitter for desired range, send heat sensor probe through port in 2" O.D. PVC, and link up with the CR10 datalogger
- Connect thermistor to air tight 1/4" O.D. port in 1-1/4" tee and link up with datalogger

B. Vacuum system

1). System integrity

- Install regulator with quick disconnect fitting to the nitrogen tank
- Connect the 3/16" steel cable and nylon inflation tubing to pneumatic packers
- Assembly pneumatic packers and insure connections are air tight by supplying pressure
- Deflate the packer assembly

2). System installation

- Determine designed depth of extraction
- Assemble packers for either single or straddle packer operation
- Connect the 1/2" O.D. male threaded expansion joint to top packer to increase pipe size to 1-1/4" O.D. Trilock PVC
- According to length needed, determine the number of 1-1/4" Trilock PVC sections to reach desired screen in the extraction well from the well head
- Lower the packer assembly into the venting well by connecting 5 ft. pipe sections
- After reaching the desired depth with the packer assembly inflate the packers to specified pressure
- Connect the 1-1/4" tee to the 1-1/4" tee to the 1-1/4" PVC section at the well head
- Connect expansion joint to tee to increase pipe size to tee to 2.0"
- Link 2.0" X 5' PVC section to expansion joint at the well-head 1-1/4" tee
- Join vacuum pump with the 2" vacuum line

C. Vacuum extraction pilot test

- Program the CR10 to collect data at a desirable interval and initiate program
- Monitor ML wells locations, not linked up with the CR10 datalogger, with magnehelic gauges to determine necessary intervals to collect readings in pressure drawdown
- In addition to the above parameters monitored, the exhaust should be monitored using a GC-PID/FID or organic vapor analyzer and/or explosimeter
- The test should remain at constant vacuum at the well head and continue until the vacuum readings level off at the ML wells
- Test is completed by disconnecting all monitoring points, vacuum line assembly, and electrical connections

APPENDIX D

Pneumatic-test data on September 9, 1993

SEPTEMBER 9, 1993
File C:\PC208\SCRN1a.DAT

VAPOR EXTRACTION AT WELL SCREEN # 1						
Time (min)	Pressure at Extraction Well (Pascals)	Air Velocity (cm/s)	Volumetric Flow (cm^3/s)	Density of Air (g/cm^3)	S.G. of air	Mass Flow (g/s)
0.08	-48883.83	215.49	4790.13	0.000597	0.000600	2.86
0.17	-48883.83	215.49	4790.13	0.000597	0.000600	2.86
0.25	-48883.83	215.49	4790.13	0.000597	0.000600	2.86
0.33	-48883.83	215.49	4790.13	0.000597	0.000600	2.86
0.42	-48883.83	215.49	4790.13	0.000597	0.000600	2.86
0.50	-48883.83	215.49	4790.13	0.000597	0.000600	2.86
0.58	-48883.83	215.49	4790.13	0.000597	0.000600	2.86
0.67	-48401.20	215.49	4790.13	0.000603	0.000605	2.89
0.75	-48152.98	217.42	4833.04	0.000605	0.000608	2.93
0.83	-48745.93	215.49	4790.13	0.000599	0.000601	2.87
0.92	-48745.93	227.48	5056.63	0.000599	0.000601	3.03
1.00	-48001.30	221.49	4923.38	0.000607	0.000610	2.99
1.08	-48401.20	227.48	5056.63	0.000603	0.000606	3.05
1.17	-48745.93	229.41	5099.54	0.000599	0.000602	3.05
1.25	-48332.25	228.60	5081.47	0.000604	0.000606	3.07
1.33	-47966.83	221.49	4923.38	0.000608	0.000611	2.99
1.42	-48608.04	227.48	5056.63	0.000601	0.000603	3.04
1.50	-48608.04	233.17	5183.10	0.000601	0.000603	3.11
1.58	-47835.83	233.48	5189.87	0.000610	0.000612	3.16
1.67	-48332.25	229.41	5099.54	0.000604	0.000607	3.08
1.75	-48676.99	233.48	5189.87	0.000600	0.000603	3.11
1.83	-47884.09	233.48	5189.87	0.000609	0.000612	3.16
1.92	-48152.98	233.48	5189.87	0.000606	0.000609	3.15
2.00	-48676.99	233.48	5189.87	0.000600	0.000603	3.11
2.08	-48242.62	230.68	5127.77	0.000605	0.000608	3.10
2.17	-47918.56	239.67	5327.64	0.000609	0.000612	3.24
2.25	-48539.09	235.41	5232.78	0.000602	0.000605	3.15
2.33	-48608.04	233.48	5189.87	0.000601	0.000604	3.12
2.42	-47863.41	239.67	5327.64	0.000610	0.000612	3.25
2.50	-48608.04	229.41	5099.54	0.000601	0.000604	3.07
2.58	-48608.04	235.41	5232.78	0.000601	0.000604	3.15
2.67	-48139.20	235.41	5232.78	0.000607	0.000609	3.17
2.75	-47863.41	233.48	5189.87	0.000610	0.000613	3.17
2.83	-48539.09	235.41	5232.78	0.000602	0.000605	3.15

2.92	-48263.30	239.67	5327.64	0.000605	0.000608	3.23
3.00	-47711.72	243.64	5415.72	0.000612	0.000614	3.31
3.08	-48401.20	229.36	5098.41	0.000604	0.000607	3.08
3.17	-48152.98	233.48	5189.87	0.000607	0.000610	3.15
3.25	-47932.35	233.38	5187.62	0.000609	0.000612	3.16
3.33	-47884.09	239.73	5328.77	0.000610	0.000613	3.25
3.42	-48539.09	233.48	5189.87	0.000603	0.000605	3.13
3.50	-48332.25	239.67	5327.64	0.000605	0.000608	3.22
3.58	-47711.72	233.38	5187.62	0.000612	0.000615	3.18
3.67	-48187.46	235.41	5232.78	0.000607	0.000610	3.18
3.75	-48539.09	233.48	5189.87	0.000603	0.000605	3.13
3.83	-47780.67	235.41	5232.78	0.000612	0.000614	3.20
3.92	-47780.67	233.48	5189.87	0.000612	0.000614	3.17
4.00	-48470.14	235.41	5232.78	0.000604	0.000606	3.16
4.08	-48401.20	233.38	5187.62	0.000605	0.000607	3.14
4.17	-47628.98	233.38	5187.62	0.000614	0.000616	3.18
4.25	-48070.25	239.67	5327.64	0.000609	0.000611	3.24
4.33	-48470.14	233.48	5189.87	0.000604	0.000607	3.13
4.42	-47863.41	233.48	5189.87	0.000611	0.000614	3.17
4.50	-47966.83	239.67	5327.64	0.000610	0.000613	3.25
4.58	-48401.20	229.36	5098.41	0.000605	0.000608	3.08
4.67	-48332.25	236.52	5257.63	0.000606	0.000609	3.19
4.75	-47608.30	233.48	5189.87	0.000614	0.000617	3.19
4.83	-47953.04	235.41	5232.78	0.000610	0.000613	3.19
4.92	-48470.14	233.48	5189.87	0.000604	0.000607	3.14
5.00	-47966.83	233.48	5189.87	0.000610	0.000613	3.17
5.08	-47732.40	233.48	5189.87	0.000613	0.000616	3.18
5.17	-48021.98	235.41	5232.78	0.000610	0.000612	3.19
5.25	-48263.30	235.41	5232.78	0.000607	0.000610	3.18
5.33	-47580.72	239.62	5326.51	0.000615	0.000618	3.28
5.42	-48139.20	229.36	5098.41	0.000609	0.000611	3.10
5.50	-48401.20	233.48	5189.87	0.000606	0.000608	3.14
5.58	-47801.35	233.48	5189.87	0.000612	0.000615	3.18
5.67	-47863.41	239.62	5326.51	0.000612	0.000615	3.26
5.75	-48332.25	233.48	5189.87	0.000607	0.000609	3.15
5.83	-47608.30	235.41	5232.78	0.000615	0.000618	3.22
5.92	-47546.25	235.41	5232.78	0.000616	0.000618	3.22
6.00	-47987.51	227.48	5056.63	0.000611	0.000613	3.09
6.08	-48401.20	233.48	5189.87	0.000606	0.000609	3.14
6.17	-47801.35	235.41	5232.78	0.000613	0.000616	3.21
6.25	-47697.93	235.41	5232.78	0.000614	0.000617	3.21

6.33	-48332.25	233.48	5189.87	0.000607	0.000610	3.15
6.42	-48173.67	235.41	5232.78	0.000609	0.000611	3.19
6.50	-47594.51	229.41	5099.54	0.000615	0.000618	3.14
6.58	-47987.51	229.41	5099.54	0.000611	0.000614	3.12
6.67	-48332.25	233.48	5189.87	0.000607	0.000610	3.15
6.75	-47746.19	233.48	5189.87	0.000614	0.000617	3.19
6.83	-47642.77	229.41	5099.54	0.000615	0.000618	3.14
6.92	-48263.30	229.36	5098.41	0.000608	0.000611	3.10
7.00	-48070.25	233.48	5189.87	0.000611	0.000613	3.17
7.08	-47456.61	227.48	5056.63	0.000618	0.000620	3.12
7.17	-48152.98	229.41	5099.54	0.000610	0.000612	3.11
7.25	-48332.25	229.36	5098.41	0.000608	0.000610	3.10
7.33	-47780.67	233.38	5187.62	0.000614	0.000617	3.18
7.42	-47456.61	231.85	5153.74	0.000618	0.000621	3.18
7.50	-48084.04	233.48	5189.87	0.000611	0.000613	3.17
7.58	-48263.30	235.41	5232.78	0.000609	0.000611	3.18
7.67	-47477.30	239.62	5326.51	0.000618	0.000621	3.29
7.75	-47491.09	229.41	5099.54	0.000618	0.000620	3.15
7.83	-48256.41	233.48	5189.87	0.000609	0.000612	3.16
7.92	-48187.46	229.31	5097.28	0.000610	0.000612	3.11
8.00	-47491.09	233.48	5189.87	0.000618	0.000620	3.21
8.08	-47546.25	235.41	5232.78	0.000617	0.000620	3.23
8.17	-48118.51	229.41	5099.54	0.000611	0.000613	3.11
8.25	-48035.77	235.41	5232.78	0.000612	0.000614	3.20
8.33	-47422.14	235.41	5232.78	0.000619	0.000622	3.24
8.42	-47794.46	229.41	5099.54	0.000615	0.000617	3.13
8.50	-47663.46	227.48	5056.63	0.000616	0.000619	3.12
8.58	-48104.72	233.48	5189.87	0.000611	0.000614	3.17
8.67	-47353.19	235.41	5232.78	0.000620	0.000623	3.24
8.75	-47511.77	233.48	5189.87	0.000618	0.000621	3.21
8.83	-48152.98	234.75	5218.11	0.000611	0.000614	3.19
8.92	-48139.20	229.31	5097.28	0.000611	0.000614	3.11
9.00	-47442.82	229.31	5097.28	0.000619	0.000622	3.16
9.08	-47491.09	233.48	5189.87	0.000619	0.000621	3.21
9.17	-48139.20	233.48	5189.87	0.000611	0.000614	3.17
9.25	-48118.51	233.48	5189.87	0.000611	0.000614	3.17
9.33	-47387.67	229.31	5097.28	0.000620	0.000623	3.16
9.42	-47456.61	227.48	5056.63	0.000619	0.000622	3.13
9.50	-48152.98	227.48	5056.63	0.000611	0.000614	3.09
9.58	-48118.51	227.48	5056.63	0.000612	0.000614	3.09
9.67	-47387.67	229.31	5097.28	0.000620	0.000623	3.16

9.75	-47511.77	227.48	5056.63	0.000619	0.000621	3.13
9.83	-47766.88	223.67	4971.94	0.000616	0.000618	3.06
9.92	-48049.56	229.41	5099.54	0.000612	0.000615	3.12
10.00	-47408.35	229.31	5097.28	0.000620	0.000623	3.16
10.08	-47511.77	227.48	5056.63	0.000619	0.000621	3.13
10.17	-48118.51	223.67	4971.94	0.000612	0.000614	3.04
10.25	-48084.04	223.67	4971.94	0.000612	0.000615	3.04
10.33	-47235.98	221.49	4923.38	0.000622	0.000625	3.06
10.42	-47628.98	229.31	5097.28	0.000618	0.000620	3.15
10.50	-48159.88	227.48	5056.63	0.000611	0.000614	3.09
10.58	-48021.98	229.46	5100.67	0.000613	0.000616	3.13
10.67	-47311.82	228.09	5070.18	0.000621	0.000624	3.15
10.75	-47546.25	229.46	5100.67	0.000618	0.000621	3.15
10.83	-48159.88	233.48	5189.87	0.000611	0.000614	3.17
10.92	-47870.30	221.49	4923.38	0.000615	0.000617	3.03
11.00	-47222.19	227.48	5056.63	0.000622	0.000625	3.15
11.08	-47766.88	227.48	5056.63	0.000616	0.000619	3.12
11.17	-47497.98	229.36	5098.41	0.000619	0.000622	3.16
11.25	-47649.67	227.48	5056.63	0.000617	0.000620	3.12
11.33	-47222.19	221.49	4923.38	0.000622	0.000625	3.06
11.42	-47849.62	221.49	4923.38	0.000615	0.000618	3.03
11.50	-48070.25	221.49	4923.38	0.000613	0.000615	3.02
11.58	-47566.93	217.42	4833.04	0.000618	0.000621	2.99
11.67	-47187.72	223.77	4974.19	0.000623	0.000625	3.10
11.75	-47663.46	229.36	5098.41	0.000617	0.000620	3.15
11.83	-48008.20	223.67	4971.94	0.000613	0.000616	3.05
11.92	-47801.35	233.43	5188.75	0.000616	0.000618	3.20
12.00	-47208.40	224.79	4996.78	0.000623	0.000625	3.11
12.08	-47566.93	229.36	5098.41	0.000618	0.000621	3.15
12.17	-47822.04	227.48	5056.63	0.000616	0.000618	3.11
12.25	-47918.56	223.67	4971.94	0.000614	0.000617	3.05
12.33	-47291.14	227.48	5056.63	0.000622	0.000624	3.14
12.42	-47346.30	229.36	5098.41	0.000621	0.000624	3.17
12.50	-48042.67	223.67	4971.94	0.000613	0.000616	3.05
12.58	-48021.98	229.36	5098.41	0.000613	0.000616	3.13
12.67	-47566.93	228.96	5089.37	0.000619	0.000621	3.15
12.75	-47187.72	227.48	5056.63	0.000623	0.000626	3.15
12.83	-47649.67	227.48	5056.63	0.000618	0.000620	3.12
12.92	-47884.09	229.36	5098.41	0.000615	0.000618	3.14
13.00	-47801.35	223.77	4974.19	0.000616	0.000619	3.06
13.08	-47208.40	227.48	5056.63	0.000623	0.000626	3.15

13.17	-47649.67	233.48	5189.87	0.000618	0.000620	3.21
13.25	-48008.20	229.46	5100.67	0.000614	0.000616	3.13
13.33	-47987.51	233.48	5189.87	0.000614	0.000617	3.19
13.42	-47360.09	229.36	5098.41	0.000621	0.000624	3.17
13.50	-47208.40	228.45	5078.08	0.000623	0.000626	3.16
13.58	-47766.88	229.41	5099.54	0.000616	0.000619	3.14
13.67	-48021.98	227.48	5056.63	0.000614	0.000616	3.10
13.75	-47732.40	235.46	5233.91	0.000617	0.000620	3.23
13.83	-47918.56	229.36	5098.41	0.000615	0.000618	3.13
13.92	-47463.51	229.41	5099.54	0.000620	0.000623	3.16
14.00	-47884.09	223.67	4971.94	0.000615	0.000618	3.06
14.08	-47973.72	229.36	5098.41	0.000614	0.000617	3.13
14.17	-47546.25	235.46	5233.91	0.000619	0.000622	3.24
14.25	-47187.72	229.41	5099.54	0.000623	0.000626	3.18
14.33	-47532.46	233.48	5189.87	0.000619	0.000622	3.21
14.42	-47904.77	223.67	4971.94	0.000615	0.000618	3.06
14.50	-47104.98	227.48	5056.63	0.000624	0.000627	3.16
14.58	-47222.19	229.36	5098.41	0.000623	0.000626	3.18
14.67	-47242.88	227.48	5056.63	0.000623	0.000626	3.15
14.75	-47753.09	229.36	5098.41	0.000617	0.000620	3.15
14.83	-47918.56	233.48	5189.87	0.000615	0.000618	3.19
14.92	-47442.82	229.36	5098.41	0.000620	0.000623	3.16
15.00	-47118.77	230.43	5122.12	0.000624	0.000627	3.20
15.08	-47477.30	229.41	5099.54	0.000620	0.000623	3.16
15.17	-47560.04	227.48	5056.63	0.000619	0.000622	3.13
15.25	-47732.40	233.48	5189.87	0.000617	0.000620	3.20
15.33	-47001.56	229.36	5098.41	0.000626	0.000628	3.19
15.42	-47256.67	229.36	5098.41	0.000623	0.000625	3.17
15.50	-47870.30	223.67	4971.94	0.000616	0.000618	3.06
15.58	-47884.09	229.36	5098.41	0.000615	0.000618	3.14
15.67	-47153.25	233.48	5189.87	0.000624	0.000627	3.24
15.75	-47104.98	227.48	5056.63	0.000624	0.000627	3.16
15.83	-47939.25	229.36	5098.41	0.000615	0.000618	3.13
15.92	-47939.25	229.36	5098.41	0.000615	0.000618	3.13
16.00	-47394.56	235.46	5233.91	0.000621	0.000624	3.25
16.08	-47091.19	229.36	5098.41	0.000625	0.000627	3.18
16.17	-47511.77	229.36	5098.41	0.000620	0.000623	3.16
16.25	-47904.77	233.43	5188.75	0.000615	0.000618	3.19
16.33	-47801.35	233.43	5188.75	0.000616	0.000619	3.20
16.42	-47256.67	235.41	5232.78	0.000623	0.000625	3.26
16.50	-47649.67	229.36	5098.41	0.000618	0.000621	3.15

16.58	-47732.40	229.36	5098.41	0.000617	0.000620	3.15
16.67	-47884.09	229.36	5098.41	0.000616	0.000618	3.14
16.75	-47463.51	234.44	5211.33	0.000620	0.000623	3.23
16.83	-47022.24	233.48	5189.87	0.000626	0.000628	3.25
16.92	-47525.56	227.48	5056.63	0.000620	0.000622	3.13
17.00	-47884.09	229.36	5098.41	0.000616	0.000618	3.14
17.08	-47663.46	232.82	5175.19	0.000618	0.000621	3.20
17.17	-47070.51	229.41	5099.54	0.000625	0.000628	3.19
17.25	-47139.46	229.36	5098.41	0.000624	0.000627	3.18
17.33	-47711.72	229.41	5099.54	0.000618	0.000620	3.15
17.42	-47918.56	233.48	5189.87	0.000615	0.000618	3.19
17.50	-47525.56	233.48	5189.87	0.000620	0.000623	3.22
17.58	-47070.51	233.48	5189.87	0.000625	0.000628	3.24
17.67	-47242.88	229.36	5098.41	0.000623	0.000626	3.18
17.75	-47870.30	227.48	5056.63	0.000616	0.000619	3.11
17.83	-47360.09	233.48	5189.87	0.000622	0.000625	3.23
17.92	-47256.67	235.41	5232.78	0.000623	0.000626	3.26
18.00	-47049.82	233.43	5188.75	0.000625	0.000628	3.25
18.08	-47628.98	229.36	5098.41	0.000619	0.000622	3.15
18.17	-47870.30	239.67	5327.64	0.000616	0.000619	3.28
18.25	-47780.67	229.36	5098.41	0.000617	0.000620	3.15
18.33	-47222.19	229.41	5099.54	0.000624	0.000626	3.18
18.42	-47084.30	235.41	5232.78	0.000625	0.000628	3.27
18.50	-47849.62	233.48	5189.87	0.000616	0.000619	3.20
18.58	-47870.30	233.48	5189.87	0.000616	0.000619	3.20
18.67	-47580.72	235.41	5232.78	0.000620	0.000622	3.24
18.75	-47022.24	233.48	5189.87	0.000626	0.000629	3.25
18.83	-47325.61	239.67	5327.64	0.000622	0.000625	3.32
18.92	-47628.98	233.48	5189.87	0.000619	0.000622	3.21
19.00	-47884.09	233.48	5189.87	0.000616	0.000619	3.20
19.08	-47560.04	229.36	5098.41	0.000620	0.000623	3.16
19.17	-47022.24	235.41	5232.78	0.000626	0.000629	3.28
19.25	-47173.93	233.48	5189.87	0.000624	0.000627	3.24
19.33	-47677.25	233.38	5187.62	0.000619	0.000622	3.21
19.42	-47828.93	233.48	5189.87	0.000617	0.000620	3.20
19.50	-47318.72	231.34	5142.45	0.000623	0.000626	3.20
19.58	-46932.61	229.31	5097.28	0.000627	0.000630	3.20
19.67	-47201.51	233.48	5189.87	0.000624	0.000627	3.24
19.75	-47711.72	227.53	5057.76	0.000619	0.000621	3.13
19.83	-46946.40	233.48	5189.87	0.000627	0.000630	3.26
19.92	-47304.93	233.48	5189.87	0.000623	0.000626	3.23

20.00	-47029.14	227.48	5056.63	0.000626	0.000629	3.17
20.08	-47304.93	233.48	5189.87	0.000623	0.000626	3.23
20.17	-47815.14	233.48	5189.87	0.000618	0.000620	3.20
20.25	-47759.98	229.41	5099.54	0.000618	0.000621	3.15
20.33	-47249.77	233.48	5189.87	0.000624	0.000627	3.24
20.42	-46932.61	227.53	5057.76	0.000628	0.000631	3.18
20.50	-47828.93	227.53	5057.76	0.000617	0.000620	3.12
20.58	-47691.04	227.53	5057.76	0.000619	0.000622	3.13
20.67	-47849.62	233.48	5189.87	0.000617	0.000620	3.20
20.75	-47560.04	229.31	5097.28	0.000621	0.000623	3.16
20.83	-47001.56	229.31	5097.28	0.000627	0.000630	3.20
20.92	-47118.77	233.48	5189.87	0.000626	0.000629	3.25
21.00	-47560.04	227.48	5056.63	0.000621	0.000623	3.14
21.08	-47828.93	227.48	5056.63	0.000618	0.000620	3.12
21.17	-47201.51	233.48	5189.87	0.000625	0.000628	3.24
21.25	-46980.88	227.48	5056.63	0.000628	0.000630	3.17
21.33	-47049.82	229.31	5097.28	0.000627	0.000630	3.20
21.42	-47594.51	229.41	5099.54	0.000621	0.000623	3.16
21.50	-47815.14	229.31	5097.28	0.000618	0.000621	3.15
21.58	-47746.19	233.48	5189.87	0.000619	0.000622	3.21
21.67	-47270.46	229.31	5097.28	0.000624	0.000627	3.18
21.75	-46967.09	233.48	5189.87	0.000628	0.000631	3.26
21.83	-47387.67	229.41	5099.54	0.000623	0.000626	3.18
21.92	-47759.98	221.49	4923.38	0.000619	0.000621	3.05
22.00	-47780.67	227.48	5056.63	0.000619	0.000621	3.13
22.08	-47304.93	231.04	5135.67	0.000624	0.000627	3.20
22.17	-47249.77	229.31	5097.28	0.000625	0.000628	3.18
22.25	-46760.24	227.53	5057.76	0.000630	0.000633	3.19
22.33	-47201.51	221.44	4922.25	0.000625	0.000628	3.08
22.42	-47622.09	227.53	5057.76	0.000620	0.000623	3.14
22.50	-47015.35	229.41	5099.54	0.000628	0.000630	3.20
22.58	-46925.72	228.40	5076.95	0.000629	0.000631	3.19
22.67	-46994.67	229.31	5097.28	0.000628	0.000631	3.20
22.75	-47332.51	221.44	4922.25	0.000624	0.000627	3.07
22.83	-47794.46	223.67	4971.94	0.000619	0.000621	3.08
22.92	-47725.51	225.60	5014.85	0.000619	0.000622	3.11
23.00	-47098.09	223.67	4971.94	0.000627	0.000630	3.12
23.08	-46877.45	221.44	4922.25	0.000629	0.000632	3.10
23.17	-47622.09	223.67	4971.94	0.000621	0.000623	3.09
23.25	-47656.56	221.44	4922.25	0.000620	0.000623	3.05
23.33	-47759.98	219.35	4875.95	0.000619	0.000622	3.02

23.42	-47435.93	221.44	4922.25	0.000623	0.000626	3.07
23.50	-46877.45	223.67	4971.94	0.000629	0.000632	3.13
23.58	-47180.82	223.67	4971.94	0.000626	0.000629	3.11
23.67	-47504.88	223.67	4971.94	0.000622	0.000625	3.09
23.75	-47759.98	221.44	4922.25	0.000619	0.000622	3.05
23.83	-46960.19	227.53	5057.76	0.000629	0.000631	3.18
23.92	-47077.40	223.72	4973.07	0.000627	0.000630	3.12
24.00	-46960.19	223.67	4971.94	0.000629	0.000631	3.13
24.08	-47366.98	223.72	4973.07	0.000624	0.000627	3.10
24.17	-47739.30	221.44	4922.25	0.000620	0.000622	3.05
24.25	-47759.98	217.32	4830.78	0.000619	0.000622	2.99
24.33	-47422.14	221.44	4922.25	0.000623	0.000626	3.07
24.42	-46960.19	227.53	5057.76	0.000629	0.000631	3.18
24.50	-47842.72	217.32	4830.78	0.000618	0.000621	2.99
24.58	-47608.30	217.42	4833.04	0.000621	0.000624	3.00
24.67	-47842.72	223.67	4971.94	0.000618	0.000621	3.08
24.75	-47587.61	221.44	4922.25	0.000621	0.000624	3.06
24.83	-47284.25	223.67	4971.94	0.000625	0.000628	3.11
24.92	-46946.40	223.06	4958.39	0.000629	0.000632	3.12
25.00	-47201.51	222.66	4949.35	0.000626	0.000629	3.10
25.08	-47677.25	221.44	4922.25	0.000620	0.000623	3.05
25.17	-47822.04	227.53	5057.76	0.000619	0.000622	3.13
25.25	-47656.56	221.44	4922.25	0.000621	0.000623	3.06
25.33	-47263.56	226.52	5035.17	0.000625	0.000628	3.15
25.42	-47042.93	223.62	4970.81	0.000628	0.000631	3.12
25.50	-47098.09	217.32	4830.78	0.000627	0.000630	3.03
25.58	-47656.56	223.62	4970.81	0.000621	0.000623	3.09
25.67	-47856.51	217.32	4830.78	0.000618	0.000621	2.99
25.75	-47794.46	221.44	4922.25	0.000619	0.000622	3.05
25.83	-47353.19	221.39	4921.12	0.000624	0.000627	3.07
25.92	-46960.19	221.44	4922.25	0.000629	0.000632	3.10
26.00	-47249.77	217.37	4831.91	0.000626	0.000628	3.02
26.08	-47573.83	217.32	4830.78	0.000622	0.000625	3.00
26.17	-47890.98	217.37	4831.91	0.000618	0.000621	2.99
26.25	-47773.77	217.32	4830.78	0.000620	0.000622	2.99
26.33	-47366.98	223.62	4970.81	0.000624	0.000627	3.10
26.42	-47077.40	221.44	4922.25	0.000628	0.000630	3.09
26.50	-47704.83	221.44	4922.25	0.000620	0.000623	3.05
26.58	-47808.25	221.44	4922.25	0.000619	0.000622	3.05
26.67	-47842.72	218.34	4853.37	0.000619	0.000621	3.00
26.75	-47518.67	217.37	4831.91	0.000622	0.000625	3.01

26.83	-47132.56	217.37	4831.91	0.000627	0.000630	3.03
26.92	-47132.56	221.44	4922.25	0.000627	0.000630	3.09
27.00	-47622.09	221.44	4922.25	0.000621	0.000624	3.06
27.08	-47925.46	217.32	4830.78	0.000618	0.000621	2.98
27.17	-47180.82	223.62	4970.81	0.000626	0.000629	3.11
27.25	-47298.04	221.44	4922.25	0.000625	0.000628	3.08
27.33	-46960.19	211.38	4698.67	0.000629	0.000632	2.96
27.42	-47229.09	221.44	4922.25	0.000626	0.000629	3.08
27.50	-47842.72	223.62	4970.81	0.000619	0.000622	3.08
27.58	-47911.67	217.37	4831.91	0.000618	0.000621	2.99
27.67	-47794.46	211.38	4698.67	0.000619	0.000622	2.91
27.75	-47249.77	221.44	4922.25	0.000626	0.000629	3.08
27.83	-47180.82	221.44	4922.25	0.000627	0.000629	3.08
27.92	-47504.88	221.44	4922.25	0.000623	0.000625	3.07
28.00	-47739.30	221.44	4922.25	0.000620	0.000623	3.05
28.08	-47911.67	223.62	4970.81	0.000618	0.000621	3.07
28.17	-47739.30	219.10	4870.31	0.000620	0.000623	3.02
28.25	-47098.09	217.37	4831.91	0.000628	0.000630	3.03
28.33	-47063.61	217.32	4830.78	0.000628	0.000631	3.03
28.42	-47553.14	220.01	4890.63	0.000622	0.000625	3.04
28.50	-47573.83	221.44	4922.25	0.000622	0.000625	3.06
28.58	-47946.14	221.44	4922.25	0.000618	0.000620	3.04
28.67	-47670.35	221.44	4922.25	0.000621	0.000624	3.06
28.75	-47318.72	215.54	4791.26	0.000625	0.000628	2.99
28.83	-47167.03	221.44	4922.25	0.000627	0.000630	3.09
28.92	-47353.19	221.44	4922.25	0.000625	0.000627	3.08
29.00	-47863.41	214.78	4774.32	0.000619	0.000621	2.95
29.08	-47959.93	217.37	4831.91	0.000618	0.000620	2.98
29.17	-47215.30	221.44	4922.25	0.000626	0.000629	3.08
29.25	-47249.77	221.44	4922.25	0.000626	0.000629	3.08
29.33	-47063.61	221.44	4922.25	0.000628	0.000631	3.09
29.42	-47484.19	217.32	4830.78	0.000623	0.000626	3.01
29.50	-47759.98	217.32	4830.78	0.000620	0.000623	2.99
29.58	-47959.93	217.37	4831.91	0.000618	0.000620	2.98
29.67	-47890.98	217.47	4834.17	0.000618	0.000621	2.99
29.75	-47401.46	221.44	4922.25	0.000624	0.000627	3.07
29.83	-47504.88	221.44	4922.25	0.000623	0.000626	3.07
29.92	-47249.77	221.44	4922.25	0.000626	0.000629	3.08
30.00	-47656.56	223.67	4971.94	0.000621	0.000624	3.09
30.08	-47925.46	211.38	4698.67	0.000618	0.000621	2.90
30.17	-48015.09	221.44	4922.25	0.000617	0.000620	3.04

30.25	-47725.51	221.44	4922.25	0.000620	0.000623	3.05
30.33	-47422.14	217.32	4830.78	0.000624	0.000626	3.01
30.42	-47180.82	221.44	4922.25	0.000626	0.000629	3.08
30.50	-47656.56	223.67	4971.94	0.000621	0.000624	3.09
30.58	-47773.77	217.37	4831.91	0.000620	0.000622	2.99
30.67	-47994.41	221.44	4922.25	0.000617	0.000620	3.04
30.75	-47911.67	221.44	4922.25	0.000618	0.000621	3.04
30.83	-47622.09	217.37	4831.91	0.000621	0.000624	3.00
30.92	-47111.88	217.37	4831.91	0.000627	0.000630	3.03
31.00	-47263.56	215.80	4796.91	0.000626	0.000628	3.00
31.08	-47773.77	219.41	4877.08	0.000620	0.000622	3.02
31.17	-47959.93	217.32	4830.78	0.000617	0.000620	2.98
31.25	-47994.41	221.44	4922.25	0.000617	0.000620	3.04
31.33	-47725.51	223.37	4965.16	0.000620	0.000623	3.08
31.42	-47284.25	217.32	4830.78	0.000625	0.000628	3.02
31.50	-47180.82	221.44	4922.25	0.000626	0.000629	3.08
31.58	-47725.51	223.72	4973.07	0.000620	0.000623	3.08
31.67	-47911.67	217.37	4831.91	0.000618	0.000621	2.99
31.75	-48008.20	221.44	4922.25	0.000617	0.000619	3.04
31.83	-47415.25	217.37	4831.91	0.000624	0.000626	3.01
31.92	-47449.72	221.44	4922.25	0.000623	0.000626	3.07
32.00	-47229.09	221.44	4922.25	0.000626	0.000628	3.08
32.08	-47380.77	223.62	4970.81	0.000624	0.000627	3.10
32.17	-47946.14	223.62	4970.81	0.000617	0.000620	3.07
32.25	-48008.20	221.44	4922.25	0.000617	0.000619	3.03
32.33	-47856.51	221.44	4922.25	0.000618	0.000621	3.04
32.42	-47504.88	211.38	4698.67	0.000622	0.000625	2.92
32.50	-47739.30	221.44	4922.25	0.000620	0.000623	3.05
32.58	-47311.82	223.62	4970.81	0.000625	0.000627	3.10
32.67	-47753.09	217.37	4831.91	0.000620	0.000622	2.99
32.75	-48008.20	221.44	4922.25	0.000617	0.000619	3.03
32.83	-48008.20	223.47	4967.42	0.000617	0.000619	3.06
32.92	-47553.14	221.44	4922.25	0.000622	0.000625	3.06
33.00	-47215.30	221.44	4922.25	0.000626	0.000628	3.08
33.08	-47194.61	223.62	4970.81	0.000626	0.000629	3.11
33.17	-48028.88	217.37	4831.91	0.000616	0.000619	2.98
33.25	-47856.51	223.62	4970.81	0.000618	0.000621	3.07
33.33	-48042.67	223.72	4973.07	0.000616	0.000619	3.06
33.42	-47911.67	221.44	4922.25	0.000618	0.000620	3.04
33.50	-47553.14	227.53	5057.76	0.000622	0.000625	3.15
33.58	-47194.61	215.70	4794.65	0.000626	0.000629	3.00

33.67	-47215.30	221.44	4922.25	0.000626	0.000628	3.08
33.75	-47532.46	227.43	5055.50	0.000622	0.000625	3.14
33.83	-48063.35	221.44	4922.25	0.000616	0.000619	3.03
33.92	-48042.67	217.37	4831.91	0.000616	0.000619	2.98
34.00	-47939.25	223.72	4973.07	0.000617	0.000620	3.07
34.08	-47622.09	223.72	4973.07	0.000621	0.000624	3.09
34.17	-47180.82	223.72	4973.07	0.000626	0.000629	3.11
34.25	-47215.30	221.44	4922.25	0.000626	0.000628	3.08
34.33	-47449.72	215.44	4789.00	0.000623	0.000626	2.98
34.42	-47787.56	227.43	5055.50	0.000619	0.000622	3.13
34.50	-47601.40	223.62	4970.81	0.000621	0.000624	3.09
34.58	-48042.67	221.44	4922.25	0.000616	0.000619	3.03
34.67	-47856.51	223.72	4973.07	0.000618	0.000621	3.07
34.75	-47587.61	221.44	4922.25	0.000621	0.000624	3.06
34.83	-47160.14	227.53	5057.76	0.000626	0.000629	3.17
34.92	-47298.04	215.54	4791.26	0.000625	0.000627	2.99
35.00	-47194.61	225.40	5010.33	0.000626	0.000629	3.14
35.08	-47925.46	226.31	5030.66	0.000617	0.000620	3.11
35.17	-47215.30	223.72	4973.07	0.000626	0.000628	3.11
35.25	-47890.98	223.72	4973.07	0.000618	0.000620	3.07
35.33	-47622.09	227.43	5055.50	0.000621	0.000624	3.14
35.42	-47160.14	223.72	4973.07	0.000626	0.000629	3.11
35.50	-47298.04	223.72	4973.07	0.000625	0.000627	3.11
35.58	-47670.35	227.43	5055.50	0.000620	0.000623	3.14
35.67	-47890.98	227.43	5055.50	0.000618	0.000620	3.12
35.75	-48063.35	215.44	4789.00	0.000616	0.000618	2.95
35.83	-47553.14	229.36	5098.41	0.000622	0.000624	3.17
35.92	-47566.93	223.72	4973.07	0.000621	0.000624	3.09
36.00	-47160.14	227.53	5057.76	0.000626	0.000629	3.17
36.08	-47229.09	223.72	4973.07	0.000625	0.000628	3.11
36.17	-47484.19	227.43	5055.50	0.000622	0.000625	3.15
36.25	-47856.51	227.43	5055.50	0.000618	0.000621	3.12
36.33	-47994.41	223.72	4973.07	0.000616	0.000619	3.07
36.42	-47904.77	223.98	4978.71	0.000618	0.000620	3.07
36.50	-47380.77	223.62	4970.81	0.000623	0.000626	3.10
36.58	-47091.19	227.53	5057.76	0.000627	0.000630	3.17
36.67	-47180.82	227.43	5055.50	0.000626	0.000629	3.16
36.75	-47463.51	223.62	4970.81	0.000623	0.000625	3.09
36.83	-47856.51	221.44	4922.25	0.000618	0.000621	3.04
36.92	-47973.72	223.11	4959.51	0.000617	0.000619	3.06
37.00	-47925.46	221.44	4922.25	0.000617	0.000620	3.04

37.08	-47566.93	227.53	5057.76	0.000621	0.000624	3.14
37.17	-47125.67	221.44	4922.25	0.000627	0.000629	3.08
37.25	-47173.93	223.62	4970.81	0.000626	0.000629	3.11
37.33	-47449.72	227.53	5057.76	0.000623	0.000626	3.15
37.42	-47939.25	227.43	5055.50	0.000617	0.000620	3.12
37.50	-47973.72	229.36	5098.41	0.000617	0.000619	3.14
37.58	-47904.77	232.00	5157.13	0.000618	0.000620	3.18
37.67	-47649.67	223.72	4973.07	0.000620	0.000623	3.09
37.75	-47208.40	227.53	5057.76	0.000626	0.000628	3.16
37.83	-47925.46	227.43	5055.50	0.000617	0.000620	3.12
37.92	-47194.61	229.36	5098.41	0.000626	0.000629	3.19
38.00	-47801.35	223.62	4970.81	0.000619	0.000622	3.08
38.08	-47870.30	223.72	4973.07	0.000618	0.000621	3.07
38.17	-47939.25	223.62	4970.81	0.000617	0.000620	3.07
38.25	-47739.30	228.09	5070.18	0.000620	0.000622	3.14
38.33	-47463.51	228.45	5078.08	0.000623	0.000626	3.16
38.42	-47125.67	227.43	5055.50	0.000627	0.000630	3.17
38.50	-47753.09	227.53	5057.76	0.000620	0.000622	3.13
38.58	-47580.72	227.43	5055.50	0.000622	0.000624	3.14
38.67	-47773.77	229.36	5098.41	0.000619	0.000622	3.16
38.75	-47959.93	232.66	5171.81	0.000617	0.000620	3.19
38.83	-47890.98	223.62	4970.81	0.000618	0.000621	3.07
38.92	-47463.51	227.43	5055.50	0.000623	0.000626	3.15
39.00	-47139.46	229.36	5098.41	0.000627	0.000629	3.20
39.08	-47139.46	229.21	5095.02	0.000627	0.000629	3.19
39.17	-47959.93	223.62	4970.81	0.000617	0.000620	3.07
39.25	-47704.83	221.69	4927.90	0.000620	0.000623	3.06
39.33	-47904.77	221.44	4922.25	0.000618	0.000621	3.04
39.42	-47870.30	223.62	4970.81	0.000618	0.000621	3.07
39.50	-47615.19	223.62	4970.81	0.000621	0.000624	3.09
39.58	-47173.93	227.43	5055.50	0.000627	0.000629	3.17
39.67	-47056.72	227.53	5057.76	0.000628	0.000631	3.18
39.75	-47332.51	223.62	4970.81	0.000625	0.000627	3.11
39.83	-47856.51	227.53	5057.76	0.000619	0.000622	3.13
39.92	-47925.46	221.44	4922.25	0.000618	0.000621	3.04
40.00	-47890.98	227.53	5057.76	0.000618	0.000621	3.13
40.08	-47497.98	223.62	4970.81	0.000623	0.000626	3.10
40.17	-47173.93	223.72	4973.07	0.000627	0.000629	3.12
40.25	-47173.93	224.64	4993.39	0.000627	0.000630	3.13
40.33	-47429.04	223.62	4970.81	0.000624	0.000627	3.10
40.42	-47870.30	223.62	4970.81	0.000619	0.000621	3.08

40.50	-47208.40	223.62	4970.81	0.000626	0.000629	3.11
40.58	-47801.35	229.36	5098.41	0.000620	0.000622	3.16
40.67	-47325.61	223.62	4970.81	0.000625	0.000628	3.11
40.75	-47173.93	223.62	4970.81	0.000627	0.000630	3.12
40.83	-47298.04	223.72	4973.07	0.000625	0.000628	3.11
40.92	-47718.62	227.43	5055.50	0.000620	0.000623	3.14
41.00	-47973.72	223.62	4970.81	0.000618	0.000620	3.07
41.08	-47925.46	223.62	4970.81	0.000618	0.000621	3.07
41.17	-47091.19	215.44	4789.00	0.000628	0.000631	3.01
41.25	-47139.46	217.37	4831.91	0.000627	0.000630	3.03
41.33	-47173.93	227.43	5055.50	0.000627	0.000630	3.17
41.42	-47346.30	223.62	4970.81	0.000625	0.000628	3.11
41.50	-47801.35	221.44	4922.25	0.000620	0.000622	3.05
41.58	-47890.98	223.62	4970.81	0.000619	0.000621	3.07
41.67	-47704.83	217.47	4834.17	0.000621	0.000624	3.00
41.75	-47449.72	223.62	4970.81	0.000624	0.000627	3.10
41.83	-47415.25	217.37	4831.91	0.000624	0.000627	3.02
41.92	-47139.46	223.62	4970.81	0.000627	0.000630	3.12
42.00	-47463.51	217.37	4831.91	0.000624	0.000626	3.01
42.08	-47787.56	217.37	4831.91	0.000620	0.000623	2.99
42.17	-47904.77	217.37	4831.91	0.000619	0.000621	2.99
42.25	-47704.83	221.44	4922.25	0.000621	0.000624	3.06
42.33	-47415.25	217.37	4831.91	0.000624	0.000627	3.02
42.42	-47008.46	221.44	4922.25	0.000629	0.000632	3.10
42.50	-47580.72	223.62	4970.81	0.000622	0.000625	3.09
42.58	-47518.67	217.37	4831.91	0.000623	0.000626	3.01
42.67	-47890.98	223.62	4970.81	0.000619	0.000621	3.08
42.75	-47904.77	221.44	4922.25	0.000619	0.000621	3.04
42.83	-47697.93	221.44	4922.25	0.000621	0.000624	3.06
42.92	-47449.72	223.62	4970.81	0.000624	0.000627	3.10
43.00	-47036.03	221.44	4922.25	0.000629	0.000631	3.09
43.08	-47091.19	215.49	4790.13	0.000628	0.000631	3.01
43.17	-47856.51	217.37	4831.91	0.000619	0.000622	2.99
43.25	-47732.40	211.28	4696.41	0.000621	0.000623	2.91
43.33	-47856.51	215.49	4790.13	0.000619	0.000622	2.97
43.42	-47835.83	222.00	4934.67	0.000619	0.000622	3.06
43.50	-47684.14	221.44	4922.25	0.000621	0.000624	3.06
43.58	-47091.19	215.44	4789.00	0.000628	0.000631	3.01
43.67	-47056.72	215.44	4789.00	0.000628	0.000631	3.01
43.75	-47125.67	221.44	4922.25	0.000628	0.000630	3.09
43.83	-47801.35	221.44	4922.25	0.000620	0.000623	3.05

43.92	-47787.56	221.44	4922.25	0.000620	0.000623	3.05
44.00	-47835.83	215.49	4790.13	0.000619	0.000622	2.97
44.08	-47732.40	217.47	4834.17	0.000621	0.000623	3.00
44.17	-47194.61	217.47	4834.17	0.000627	0.000630	3.03
44.25	-47070.51	217.47	4834.17	0.000628	0.000631	3.04
44.33	-47104.98	215.49	4790.13	0.000628	0.000631	3.01
44.42	-47311.82	215.44	4789.00	0.000626	0.000628	3.00
44.50	-47904.77	217.37	4831.91	0.000619	0.000622	2.99
44.58	-47856.51	217.37	4831.91	0.000619	0.000622	2.99
44.67	-47904.77	217.37	4831.91	0.000619	0.000622	2.99
44.75	-47835.83	221.44	4922.25	0.000620	0.000622	3.05
44.83	-47566.93	217.47	4834.17	0.000623	0.000625	3.01
44.92	-47091.19	217.47	4834.17	0.000628	0.000631	3.04
45.00	-47056.72	217.37	4831.91	0.000629	0.000631	3.04
45.08	-47139.46	221.44	4922.25	0.000628	0.000631	3.09
45.17	-47753.09	217.47	4834.17	0.000621	0.000623	3.00
45.25	-47801.35	221.84	4931.28	0.000620	0.000623	3.06
45.33	-47904.77	215.49	4790.13	0.000619	0.000622	2.96
45.42	-47856.51	223.72	4973.07	0.000619	0.000622	3.08
45.50	-47670.35	216.71	4817.23	0.000622	0.000624	2.99
45.58	-47277.35	217.47	4834.17	0.000626	0.000629	3.03
45.67	-47022.24	217.37	4831.91	0.000629	0.000632	3.04
45.75	-47070.51	217.37	4831.91	0.000629	0.000631	3.04
45.83	-47718.62	207.67	4616.23	0.000621	0.000624	2.87
45.92	-47649.67	211.43	4699.80	0.000622	0.000625	2.92
46.00	-47766.88	209.45	4655.76	0.000621	0.000623	2.89
46.08	-47870.30	219.41	4877.08	0.000619	0.000622	3.02
46.17	-47835.83	214.43	4766.42	0.000620	0.000622	2.95
46.25	-47635.88	221.44	4922.25	0.000622	0.000625	3.06
46.33	-47346.30	221.44	4922.25	0.000625	0.000628	3.08
46.42	-47022.24	215.49	4790.13	0.000629	0.000632	3.01
46.50	-47380.77	217.37	4831.91	0.000625	0.000628	3.02
46.58	-47160.14	217.47	4834.17	0.000628	0.000630	3.03
46.67	-47477.30	215.49	4790.13	0.000624	0.000627	2.99
46.75	-47732.40	217.47	4834.17	0.000621	0.000624	3.00
46.83	-47835.83	209.45	4655.76	0.000620	0.000623	2.89
46.92	-47732.40	215.49	4790.13	0.000621	0.000624	2.97
47.00	-47546.25	221.44	4922.25	0.000623	0.000626	3.07
47.08	-47056.72	217.47	4834.17	0.000629	0.000632	3.04
47.17	-47394.56	215.44	4789.00	0.000625	0.000628	2.99
47.25	-47125.67	211.43	4699.80	0.000628	0.000631	2.95

47.33	-47429.04	215.44	4789.00	0.000625	0.000627	2.99
47.42	-47663.46	217.37	4831.91	0.000622	0.000625	3.01
47.50	-47856.51	217.47	4834.17	0.000620	0.000622	3.00
47.58	-47870.30	215.44	4789.00	0.000620	0.000622	2.97
47.67	-47649.67	217.37	4831.91	0.000622	0.000625	3.01
47.75	-47415.25	215.44	4789.00	0.000625	0.000628	2.99
47.83	-47394.56	209.45	4655.76	0.000625	0.000628	2.91
47.92	-46973.98	209.45	4655.76	0.000630	0.000633	2.93
48.00	-47070.51	211.38	4698.67	0.000629	0.000632	2.95
48.08	-47277.35	215.44	4789.00	0.000626	0.000629	3.00
48.17	-47497.98	215.49	4790.13	0.000624	0.000627	2.99
48.25	-47718.62	215.44	4789.00	0.000621	0.000624	2.98
48.33	-47856.51	211.38	4698.67	0.000620	0.000622	2.91
48.42	-47856.51	215.44	4789.00	0.000620	0.000622	2.97
48.50	-47615.19	215.44	4789.00	0.000622	0.000625	2.98
48.58	-47835.83	217.37	4831.91	0.000620	0.000623	3.00
48.67	-47649.67	217.42	4833.04	0.000622	0.000625	3.01
48.75	-47546.25	217.42	4833.04	0.000623	0.000626	3.01
48.83	-47208.40	215.44	4789.00	0.000627	0.000630	3.00
48.92	-47125.67	217.42	4833.04	0.000628	0.000631	3.04
49.00	-46987.77	215.44	4789.00	0.000630	0.000633	3.02
49.08	-47070.51	217.42	4833.04	0.000629	0.000632	3.04
49.17	-47870.30	211.38	4698.67	0.000620	0.000622	2.91
49.25	-47325.61	215.49	4790.13	0.000626	0.000629	3.00
49.33	-47511.77	215.44	4789.00	0.000624	0.000626	2.99
49.42	-47718.62	209.40	4654.63	0.000621	0.000624	2.89
49.50	-47787.56	215.44	4789.00	0.000621	0.000623	2.97
49.58	-47870.30	215.44	4789.00	0.000620	0.000622	2.97
49.67	-47870.30	217.42	4833.04	0.000620	0.000622	2.99
49.75	-47753.09	217.42	4833.04	0.000621	0.000624	3.00
49.83	-47056.72	217.37	4831.91	0.000629	0.000632	3.04
49.92	-47346.30	211.38	4698.67	0.000626	0.000628	2.94
50.00	-47277.35	211.38	4698.67	0.000626	0.000629	2.94
50.08	-47022.24	213.97	4756.26	0.000629	0.000632	2.99
50.17	-47022.24	217.42	4833.04	0.000629	0.000632	3.04
50.25	-47036.03	211.43	4699.80	0.000629	0.000632	2.96
50.33	-47187.72	211.38	4698.67	0.000627	0.000630	2.95
50.42	-47463.51	215.44	4789.00	0.000624	0.000627	2.99
50.50	-47835.83	215.44	4789.00	0.000620	0.000623	2.97
50.58	-47801.35	215.44	4789.00	0.000620	0.000623	2.97
50.67	-47870.30	215.49	4790.13	0.000620	0.000622	2.97

50.75	-47849.62	211.38	4698.67	0.000620	0.000623	2.91
50.83	-47649.67	215.44	4789.00	0.000622	0.000625	2.98
50.92	-47580.72	215.44	4789.00	0.000623	0.000626	2.98
51.00	-47346.30	215.44	4789.00	0.000626	0.000628	3.00
51.08	-47242.88	217.37	4831.91	0.000627	0.000630	3.03
51.17	-46987.77	215.44	4789.00	0.000630	0.000632	3.02
51.25	-47022.24	217.42	4833.04	0.000629	0.000632	3.04
51.33	-46967.09	215.49	4790.13	0.000630	0.000633	3.02
51.42	-47056.72	211.38	4698.67	0.000629	0.000632	2.95
51.50	-47001.56	208.33	4630.91	0.000630	0.000632	2.92
51.58	-47070.51	211.38	4698.67	0.000629	0.000632	2.95
51.67	-47091.19	212.55	4724.64	0.000628	0.000631	2.97
51.75	-47153.25	215.44	4789.00	0.000628	0.000631	3.01
51.83	-47497.98	213.21	4739.32	0.000624	0.000626	2.96
51.92	-47187.72	216.87	4820.62	0.000627	0.000630	3.02
52.00	-47070.51	211.38	4698.67	0.000629	0.000632	2.95
52.08	-47173.93	215.44	4789.00	0.000627	0.000630	3.01
52.17	-47036.03	215.44	4789.00	0.000629	0.000632	3.01
52.25	-47056.72	217.37	4831.91	0.000629	0.000632	3.04
52.33	-47056.72	220.42	4899.67	0.000629	0.000632	3.08
52.42	-47208.40	217.37	4831.91	0.000627	0.000630	3.03
52.50	-47580.72	215.44	4789.00	0.000623	0.000626	2.98
52.58	-47463.51	211.38	4698.67	0.000624	0.000627	2.93
52.67	-47497.98	215.49	4790.13	0.000624	0.000626	2.99
52.75	-47815.14	217.37	4831.91	0.000620	0.000623	3.00
52.83	-47884.09	217.37	4831.91	0.000619	0.000622	2.99
52.92	-47939.25	217.37	4831.91	0.000619	0.000621	2.99
53.00	-47904.77	221.44	4922.25	0.000619	0.000622	3.05
53.08	-47628.98	209.40	4654.63	0.000622	0.000625	2.90
53.17	-47939.25	215.49	4790.13	0.000619	0.000621	2.96
53.25	-47139.46	213.46	4744.96	0.000628	0.000631	2.98
53.33	-47091.19	221.49	4923.38	0.000628	0.000631	3.09
53.42	-47139.46	217.27	4829.65	0.000628	0.000631	3.03
53.50	-47408.35	221.44	4922.25	0.000625	0.000627	3.07
53.58	-47442.82	217.37	4831.91	0.000624	0.000627	3.02
53.67	-47663.46	217.37	4831.91	0.000622	0.000624	3.00
53.75	-47684.14	217.93	4844.33	0.000621	0.000624	3.01
53.83	-47091.19	221.44	4922.25	0.000628	0.000631	3.09
53.92	-47870.30	217.37	4831.91	0.000619	0.000622	2.99
54.00	-47884.09	215.44	4789.00	0.000619	0.000622	2.96
54.08	-47835.83	217.37	4831.91	0.000620	0.000622	2.99

54.17	-47815.14	221.44	4922.25	0.000620	0.000623	3.05
54.25	-47787.56	221.44	4922.25	0.000620	0.000623	3.05
54.33	-47904.77	221.44	4922.25	0.000619	0.000622	3.05
54.42	-47870.30	221.44	4922.25	0.000619	0.000622	3.05
54.50	-47849.62	223.62	4970.81	0.000619	0.000622	3.08
54.58	-47904.77	217.42	4833.04	0.000619	0.000622	2.99
54.67	-47870.30	220.73	4906.44	0.000619	0.000622	3.04
54.75	-47849.62	217.42	4833.04	0.000619	0.000622	2.99
54.83	-47870.30	217.42	4833.04	0.000619	0.000622	2.99
54.92	-47835.83	217.42	4833.04	0.000619	0.000622	2.99
55.00	-47835.83	211.38	4698.67	0.000619	0.000622	2.91
55.08	-47815.14	217.37	4831.91	0.000620	0.000622	2.99
55.17	-47001.56	211.38	4698.67	0.000629	0.000632	2.96
55.25	-47718.62	221.44	4922.25	0.000621	0.000624	3.06
55.33	-47511.77	223.67	4971.94	0.000623	0.000626	3.10
55.42	-47477.30	223.67	4971.94	0.000624	0.000626	3.10
55.50	-47277.35	221.44	4922.25	0.000626	0.000629	3.08
55.58	-46932.61	215.49	4790.13	0.000630	0.000633	3.02
55.67	-46918.82	223.67	4971.94	0.000630	0.000633	3.13
55.75	-47036.03	215.44	4789.00	0.000629	0.000632	3.01
55.83	-47532.46	221.44	4922.25	0.000623	0.000626	3.07
55.92	-47463.51	221.44	4922.25	0.000624	0.000627	3.07
56.00	-47615.19	215.44	4789.00	0.000622	0.000625	2.98
56.08	-47732.40	223.67	4971.94	0.000621	0.000623	3.09
56.17	-47732.40	211.38	4698.67	0.000621	0.000623	2.92
56.25	-47697.93	223.47	4967.42	0.000621	0.000624	3.09
56.33	-47408.35	222.86	4953.87	0.000625	0.000627	3.09
56.42	-47187.72	223.67	4971.94	0.000627	0.000630	3.12
56.50	-47091.19	211.38	4698.67	0.000628	0.000631	2.95
56.58	-46932.61	221.44	4922.25	0.000630	0.000633	3.10
56.67	-47187.72	221.44	4922.25	0.000627	0.000630	3.09
56.75	-47373.88	217.42	4833.04	0.000625	0.000628	3.02
56.83	-47684.14	217.37	4831.91	0.000621	0.000624	3.00
56.92	-47649.67	221.44	4922.25	0.000622	0.000624	3.06
57.00	-47546.25	221.44	4922.25	0.000623	0.000626	3.07
57.08	-47325.61	223.62	4970.81	0.000625	0.000628	3.11
57.17	-46836.09	227.43	5055.50	0.000631	0.000634	3.19
57.25	-46767.14	221.44	4922.25	0.000632	0.000635	3.11
57.33	-46905.03	227.48	5056.63	0.000630	0.000633	3.19
57.42	-47394.56	221.44	4922.25	0.000625	0.000627	3.07
57.50	-47546.25	223.62	4970.81	0.000623	0.000626	3.10

57.58	-47684.14	221.44	4922.25	0.000621	0.000624	3.06
57.67	-47649.67	223.62	4970.81	0.000622	0.000625	3.09
57.75	-47291.14	223.67	4971.94	0.000626	0.000629	3.11
57.83	-47187.72	223.27	4962.90	0.000627	0.000630	3.11
57.92	-46849.88	221.44	4922.25	0.000631	0.000634	3.11
58.00	-46849.88	223.62	4970.81	0.000631	0.000634	3.14
58.08	-46953.30	221.44	4922.25	0.000630	0.000633	3.10
58.17	-47408.35	211.38	4698.67	0.000625	0.000627	2.94
58.25	-47511.77	227.48	5056.63	0.000623	0.000626	3.15
58.33	-47649.67	215.49	4790.13	0.000622	0.000625	2.98
58.42	-47594.51	227.48	5056.63	0.000623	0.000625	3.15
58.50	-46836.09	217.37	4831.91	0.000631	0.000634	3.05
58.58	-47118.77	217.42	4833.04	0.000628	0.000631	3.04
58.67	-47022.24	217.37	4831.91	0.000629	0.000632	3.04
58.75	-46746.45	221.44	4922.25	0.000632	0.000635	3.11
58.83	-46767.14	223.62	4970.81	0.000632	0.000635	3.14
58.92	-46801.61	217.37	4831.91	0.000632	0.000635	3.05
59.00	-46987.77	221.44	4922.25	0.000630	0.000632	3.10
59.08	-47187.72	215.39	4787.87	0.000627	0.000630	3.00
59.17	-47580.72	217.42	4833.04	0.000623	0.000626	3.01
59.25	-47497.98	215.49	4790.13	0.000624	0.000626	2.99
59.33	-47615.19	223.62	4970.81	0.000622	0.000625	3.09
59.42	-47594.51	211.38	4698.67	0.000623	0.000625	2.93
59.50	-47463.51	217.37	4831.91	0.000624	0.000627	3.02
59.58	-47532.46	221.44	4922.25	0.000623	0.000626	3.07
59.67	-47187.72	217.42	4833.04	0.000627	0.000630	3.03
59.75	-47139.46	221.44	4922.25	0.000628	0.000631	3.09
59.83	-46780.93	223.67	4971.94	0.000632	0.000635	3.14
59.92	-46801.61	221.44	4922.25	0.000632	0.000635	3.11
60.00	-46746.45	217.42	4833.04	0.000633	0.000635	3.06
60.08	-46870.56	215.39	4787.87	0.000631	0.000634	3.02
60.17	-46987.77	221.44	4922.25	0.000630	0.000633	3.10
60.25	-47256.67	217.37	4831.91	0.000627	0.000629	3.03
60.33	-47532.46	221.44	4922.25	0.000623	0.000626	3.07
60.42	-47594.51	221.44	4922.25	0.000623	0.000625	3.07
60.50	-47408.35	215.39	4787.87	0.000625	0.000628	2.99
60.58	-47615.19	217.42	4833.04	0.000622	0.000625	3.01
60.67	-47442.82	223.62	4970.81	0.000624	0.000627	3.10
60.75	-47256.67	215.39	4787.87	0.000627	0.000630	3.00
60.83	-46987.77	215.90	4799.17	0.000630	0.000633	3.02
60.92	-46767.14	221.44	4922.25	0.000632	0.000635	3.11

61.00	-46884.35	216.15	4804.81	0.000631	0.000634	3.03
61.08	-47036.03	215.49	4790.13	0.000629	0.000632	3.01
61.17	-47615.19	217.42	4833.04	0.000622	0.000625	3.01
61.25	-47546.25	211.38	4698.67	0.000623	0.000626	2.93
61.33	-47594.51	213.46	4744.96	0.000623	0.000625	2.95
61.42	-47532.46	221.44	4922.25	0.000623	0.000626	3.07
61.50	-47153.25	215.49	4790.13	0.000628	0.000631	3.01
61.58	-46849.88	217.37	4831.91	0.000631	0.000634	3.05
61.67	-46767.14	217.37	4831.91	0.000632	0.000635	3.06
61.75	-46801.61	215.39	4787.87	0.000632	0.000635	3.03
61.83	-47580.72	221.44	4922.25	0.000623	0.000626	3.07
61.92	-47442.82	223.77	4974.19	0.000625	0.000627	3.11
62.00	-47580.72	217.37	4831.91	0.000623	0.000626	3.01
62.08	-47546.25	215.49	4790.13	0.000623	0.000626	2.99
62.17	-47408.35	214.43	4766.42	0.000625	0.000628	2.98
62.25	-47001.56	217.37	4831.91	0.000630	0.000632	3.04
62.33	-46801.61	213.97	4756.26	0.000632	0.000635	3.01
62.42	-46767.14	215.39	4787.87	0.000632	0.000635	3.03
62.50	-47532.46	217.42	4833.04	0.000623	0.000626	3.01
62.58	-47339.40	215.49	4790.13	0.000626	0.000628	3.00
62.67	-47511.77	211.43	4699.80	0.000624	0.000626	2.93
62.75	-47560.04	215.49	4790.13	0.000623	0.000626	2.98
62.83	-47408.35	217.37	4831.91	0.000625	0.000628	3.02
62.92	-46898.14	217.37	4831.91	0.000631	0.000633	3.05
63.00	-46649.93	215.49	4790.13	0.000633	0.000636	3.03
63.08	-46732.66	217.37	4831.91	0.000632	0.000635	3.06
63.17	-47325.61	215.39	4787.87	0.000626	0.000628	3.00
63.25	-47339.40	209.40	4654.63	0.000625	0.000628	2.91
63.33	-47532.46	215.49	4790.13	0.000623	0.000626	2.99
63.42	-47497.98	211.38	4698.67	0.000624	0.000626	2.93
63.50	-47242.88	217.42	4833.04	0.000626	0.000629	3.03
63.58	-46711.98	217.37	4831.91	0.000633	0.000636	3.06
63.67	-46677.51	220.83	4908.70	0.000633	0.000636	3.11
63.75	-46918.82	215.39	4787.87	0.000630	0.000633	3.02
63.83	-47442.82	215.39	4787.87	0.000624	0.000627	2.99
63.92	-47463.51	215.39	4787.87	0.000624	0.000627	2.99
64.00	-47532.46	215.75	4795.78	0.000623	0.000626	2.99
64.08	-47339.40	215.49	4790.13	0.000625	0.000628	3.00
64.17	-47139.46	221.44	4922.25	0.000628	0.000630	3.09
64.25	-46732.66	209.40	4654.63	0.000632	0.000635	2.94
64.33	-46649.93	215.39	4787.87	0.000633	0.000636	3.03

64.42	-46780.93	216.10	4803.68	0.000632	0.000635	3.03
64.50	-47373.88	221.44	4922.25	0.000625	0.000628	3.08
64.58	-47373.88	220.32	4897.41	0.000625	0.000628	3.06
64.67	-47532.46	217.37	4831.91	0.000623	0.000626	3.01
64.75	-47477.30	221.44	4922.25	0.000624	0.000626	3.07
64.83	-47291.14	217.42	4833.04	0.000626	0.000629	3.03
64.92	-46836.09	221.44	4922.25	0.000631	0.000634	3.11
65.00	-46649.93	221.44	4922.25	0.000633	0.000636	3.12
65.08	-46698.19	221.44	4922.25	0.000633	0.000636	3.11
65.17	-47360.09	221.44	4922.25	0.000625	0.000628	3.08
65.25	-47429.04	221.44	4922.25	0.000624	0.000627	3.07
65.33	-47497.98	217.37	4831.91	0.000624	0.000626	3.01
65.42	-47463.51	221.44	4922.25	0.000624	0.000627	3.07
65.50	-47056.72	223.62	4970.81	0.000629	0.000632	3.13
65.58	-46732.66	223.62	4970.81	0.000632	0.000635	3.14
65.67	-46649.93	221.44	4922.25	0.000633	0.000636	3.12
65.75	-46711.98	221.44	4922.25	0.000633	0.000636	3.11
65.83	-47311.82	221.44	4922.25	0.000626	0.000629	3.08
65.92	-47311.82	221.44	4922.25	0.000626	0.000629	3.08
66.00	-47477.30	217.37	4831.91	0.000624	0.000627	3.01
66.08	-47429.04	211.38	4698.67	0.000624	0.000627	2.93
66.17	-47208.40	221.44	4922.25	0.000627	0.000630	3.09
66.25	-46932.61	221.44	4922.25	0.000630	0.000633	3.10
66.33	-46643.03	217.42	4833.04	0.000634	0.000636	3.06
66.42	-46615.45	221.44	4922.25	0.000634	0.000637	3.12
66.50	-47256.67	221.44	4922.25	0.000626	0.000629	3.08
66.58	-47153.25	223.67	4971.94	0.000628	0.000630	3.12
66.67	-47442.82	215.39	4787.87	0.000624	0.000627	2.99
66.75	-47497.98	217.42	4833.04	0.000624	0.000626	3.01
66.83	-47304.93	223.67	4971.94	0.000626	0.000629	3.11
66.92	-47173.93	223.62	4970.81	0.000627	0.000630	3.12
67.00	-46643.03	223.67	4971.94	0.000634	0.000636	3.15
67.08	-46594.77	223.62	4970.81	0.000634	0.000637	3.15
67.17	-47463.51	221.44	4922.25	0.000624	0.000627	3.07
67.25	-46898.14	221.44	4922.25	0.000631	0.000633	3.10
67.33	-47070.51	221.44	4922.25	0.000629	0.000631	3.09
67.42	-47429.04	223.62	4970.81	0.000625	0.000627	3.10
67.50	-47429.04	217.37	4831.91	0.000625	0.000627	3.02
67.58	-47242.88	223.62	4970.81	0.000627	0.000629	3.12
67.67	-47084.30	221.44	4922.25	0.000629	0.000631	3.09
67.75	-46732.66	221.44	4922.25	0.000633	0.000635	3.11

67.83	-47036.03	217.42	4833.04	0.000629	0.000632	3.04
67.92	-46663.72	211.38	4698.67	0.000634	0.000636	2.98
68.00	-47139.46	223.62	4970.81	0.000628	0.000631	3.12
68.08	-47291.14	217.37	4831.91	0.000626	0.000629	3.03
68.17	-47394.56	217.37	4831.91	0.000625	0.000628	3.02
68.25	-47360.09	220.42	4899.67	0.000625	0.000628	3.06
68.33	-46884.35	217.42	4833.04	0.000631	0.000634	3.05
68.42	-46580.98	223.67	4971.94	0.000634	0.000637	3.15
68.50	-47325.61	215.39	4787.87	0.000626	0.000629	3.00
68.58	-46836.09	215.39	4787.87	0.000632	0.000634	3.02
68.67	-47208.40	217.42	4833.04	0.000627	0.000630	3.03
68.75	-47394.56	215.39	4787.87	0.000625	0.000628	2.99
68.83	-47291.14	215.49	4790.13	0.000626	0.000629	3.00
68.92	-47001.56	217.42	4833.04	0.000630	0.000632	3.04
69.00	-46546.51	217.37	4831.91	0.000635	0.000638	3.07
69.08	-46477.56	221.44	4922.25	0.000636	0.000638	3.13
69.17	-46698.19	221.44	4922.25	0.000633	0.000636	3.12
69.25	-47118.77	221.44	4922.25	0.000628	0.000631	3.09
69.33	-47360.09	215.39	4787.87	0.000625	0.000628	2.99
69.42	-47408.35	217.37	4831.91	0.000625	0.000628	3.02
69.50	-47173.93	215.39	4787.87	0.000628	0.000630	3.00
69.58	-46863.67	217.42	4833.04	0.000631	0.000634	3.05
69.67	-46456.87	221.44	4922.25	0.000636	0.000639	3.13
69.75	-46594.77	217.42	4833.04	0.000634	0.000637	3.07
69.83	-47304.93	211.38	4698.67	0.000626	0.000629	2.94
69.92	-47187.72	217.42	4833.04	0.000627	0.000630	3.03
70.00	-47373.88	215.49	4790.13	0.000625	0.000628	2.99
70.08	-47339.40	211.43	4699.80	0.000626	0.000628	2.94
70.17	-47242.88	215.39	4787.87	0.000627	0.000629	3.00
70.25	-46836.09	211.38	4698.67	0.000631	0.000634	2.97
70.33	-46615.45	217.42	4833.04	0.000634	0.000637	3.06
70.42	-46512.03	215.49	4790.13	0.000635	0.000638	3.04
70.50	-47001.56	219.46	4878.21	0.000629	0.000632	3.07
70.58	-47070.51	215.49	4790.13	0.000629	0.000631	3.01
70.67	-47187.72	217.37	4831.91	0.000627	0.000630	3.03
70.75	-47325.61	215.39	4787.87	0.000626	0.000628	3.00
70.83	-47325.61	215.49	4790.13	0.000626	0.000628	3.00
70.92	-47104.98	217.37	4831.91	0.000628	0.000631	3.04
71.00	-46767.14	215.39	4787.87	0.000632	0.000635	3.03
71.08	-46477.56	216.51	4812.72	0.000635	0.000638	3.06
71.17	-47022.24	217.37	4831.91	0.000629	0.000632	3.04

71.25	-46898.14	211.38	4698.67	0.000631	0.000633	2.96
71.33	-46967.09	215.39	4787.87	0.000630	0.000632	3.01
71.42	-47304.93	217.37	4831.91	0.000626	0.000629	3.02
71.50	-47360.09	215.39	4787.87	0.000625	0.000628	2.99
71.58	-47153.25	221.44	4922.25	0.000627	0.000630	3.09
71.67	-47070.51	211.38	4698.67	0.000628	0.000631	2.95
71.75	-46546.51	217.37	4831.91	0.000635	0.000637	3.07
71.83	-46525.82	221.44	4922.25	0.000635	0.000638	3.12
71.92	-46643.03	217.37	4831.91	0.000633	0.000636	3.06
72.00	-46932.61	223.62	4970.81	0.000630	0.000633	3.13
72.08	-47222.19	217.37	4831.91	0.000627	0.000629	3.03
72.17	-47304.93	215.49	4790.13	0.000626	0.000628	3.00
72.25	-47104.98	221.44	4922.25	0.000628	0.000631	3.09
72.33	-46594.77	217.42	4833.04	0.000634	0.000637	3.06
72.42	-46422.40	217.37	4831.91	0.000636	0.000639	3.07
72.50	-47256.67	215.39	4787.87	0.000626	0.000629	3.00
72.58	-46918.82	215.39	4787.87	0.000630	0.000633	3.02
72.67	-47153.25	223.62	4970.81	0.000627	0.000630	3.12
72.75	-47304.93	221.44	4922.25	0.000626	0.000628	3.08
72.83	-47187.72	221.44	4922.25	0.000627	0.000630	3.09
72.92	-46746.45	215.49	4790.13	0.000632	0.000635	3.03
73.00	-46512.03	221.44	4922.25	0.000635	0.000637	3.12
73.08	-46360.35	223.62	4970.81	0.000636	0.000639	3.16
73.17	-47291.14	217.37	4831.91	0.000626	0.000628	3.02
73.25	-46863.67	217.37	4831.91	0.000630	0.000633	3.05
73.33	-47208.40	221.44	4922.25	0.000627	0.000629	3.08
73.42	-47277.35	221.44	4922.25	0.000626	0.000628	3.08
73.50	-47104.98	217.42	4833.04	0.000628	0.000630	3.03
73.58	-46849.88	227.43	5055.50	0.000631	0.000633	3.19
73.67	-46422.40	223.67	4971.94	0.000635	0.000638	3.16
73.75	-46394.82	215.39	4787.87	0.000636	0.000639	3.04
73.83	-47139.46	221.44	4922.25	0.000627	0.000630	3.09
73.92	-46884.35	223.67	4971.94	0.000630	0.000633	3.13
74.00	-47070.51	221.44	4922.25	0.000628	0.000631	3.09
74.08	-47242.88	221.44	4922.25	0.000626	0.000629	3.08
74.17	-47153.25	217.37	4831.91	0.000627	0.000630	3.03
74.25	-46711.98	223.62	4970.81	0.000632	0.000635	3.14
74.33	-46456.87	223.67	4971.94	0.000635	0.000638	3.16
74.42	-46422.40	221.44	4922.25	0.000635	0.000638	3.13
74.50	-46918.82	223.67	4971.94	0.000630	0.000632	3.13
74.58	-46953.30	223.62	4970.81	0.000629	0.000632	3.13

74.67	-47104.98	223.62	4970.81	0.000627	0.000630	3.12
74.75	-47173.93	223.67	4971.94	0.000627	0.000629	3.12
74.83	-47118.77	223.67	4971.94	0.000627	0.000630	3.12
74.92	-46767.14	223.67	4971.94	0.000631	0.000634	3.14
75.00	-46512.03	223.67	4971.94	0.000634	0.000637	3.15
75.08	-46360.35	226.06	5025.01	0.000636	0.000639	3.20
75.17	-47070.51	223.67	4971.94	0.000628	0.000631	3.12
75.25	-46767.14	222.61	4948.22	0.000631	0.000634	3.12
75.33	-47001.56	227.48	5056.63	0.000628	0.000631	3.18
75.42	-47173.93	223.67	4971.94	0.000627	0.000629	3.12
75.50	-47187.72	223.62	4970.81	0.000626	0.000629	3.11
75.58	-46918.82	223.62	4970.81	0.000630	0.000632	3.13
75.67	-46594.77	227.43	5055.50	0.000633	0.000636	3.20
75.75	-46256.93	221.39	4921.12	0.000637	0.000640	3.14
75.83	-46711.98	215.39	4787.87	0.000632	0.000635	3.03
75.92	-46732.66	221.39	4921.12	0.000632	0.000634	3.11
76.00	-46967.09	223.62	4970.81	0.000629	0.000632	3.13
76.08	-47118.77	223.67	4971.94	0.000627	0.000630	3.12
76.17	-47084.30	227.43	5055.50	0.000628	0.000630	3.17
76.25	-46987.77	221.39	4921.12	0.000629	0.000631	3.09
76.33	-46456.87	227.48	5056.63	0.000635	0.000638	3.21
76.42	-46291.40	223.67	4971.94	0.000637	0.000640	3.17
76.50	-46898.14	221.39	4921.12	0.000630	0.000633	3.10
76.58	-46394.82	218.29	4852.24	0.000636	0.000638	3.08
76.67	-46698.19	229.36	5098.41	0.000632	0.000635	3.22
76.75	-46967.09	227.43	5055.50	0.000629	0.000632	3.18
76.83	-47118.77	217.42	4833.04	0.000627	0.000630	3.03
76.92	-47070.51	227.43	5055.50	0.000628	0.000631	3.17
77.00	-46987.77	229.36	5098.41	0.000629	0.000631	3.21
77.08	-46546.51	223.62	4970.81	0.000634	0.000636	3.15
77.17	-46525.82	221.39	4921.12	0.000634	0.000637	3.12
77.25	-46291.40	223.67	4971.94	0.000637	0.000640	3.17
77.33	-46443.09	227.43	5055.50	0.000635	0.000638	3.21
77.42	-46863.67	227.48	5056.63	0.000630	0.000633	3.19
77.50	-47036.03	227.43	5055.50	0.000628	0.000631	3.18
77.58	-47118.77	227.48	5056.63	0.000627	0.000630	3.17
77.67	-46918.82	227.48	5056.63	0.000629	0.000632	3.18
77.75	-46836.09	223.62	4970.81	0.000630	0.000633	3.13
77.83	-46222.45	229.36	5098.41	0.000638	0.000640	3.25
77.92	-46222.45	227.43	5055.50	0.000638	0.000640	3.22
78.00	-46374.14	227.43	5055.50	0.000636	0.000639	3.21

78.08	-46594.77	227.48	5056.63	0.000633	0.000636	3.20
78.17	-46987.77	217.37	4831.91	0.000629	0.000631	3.04
78.25	-47056.72	223.62	4970.81	0.000628	0.000631	3.12
78.33	-47036.03	229.36	5098.41	0.000628	0.000631	3.20
78.42	-46849.88	223.62	4970.81	0.000630	0.000633	3.13
78.50	-46360.35	227.43	5055.50	0.000636	0.000639	3.21
78.58	-46291.40	223.62	4970.81	0.000637	0.000640	3.17
78.67	-46174.19	223.67	4971.94	0.000638	0.000641	3.17
78.75	-46408.61	227.48	5056.63	0.000635	0.000638	3.21
78.83	-46643.03	229.36	5098.41	0.000633	0.000635	3.23
78.92	-46801.61	221.39	4921.12	0.000631	0.000634	3.10
79.00	-47022.24	223.67	4971.94	0.000628	0.000631	3.12
79.08	-47036.03	227.94	5066.79	0.000628	0.000631	3.18
79.17	-46139.72	217.37	4831.91	0.000638	0.000641	3.08
79.25	-46663.72	229.41	5099.54	0.000632	0.000635	3.22
79.33	-46374.14	229.36	5098.41	0.000636	0.000638	3.24
79.42	-46187.98	225.81	5019.36	0.000638	0.000641	3.20
79.50	-46270.72	227.48	5056.63	0.000637	0.000640	3.22
79.58	-46374.14	229.36	5098.41	0.000636	0.000638	3.24
79.67	-46801.61	227.48	5056.63	0.000631	0.000633	3.19
79.75	-46884.35	227.48	5056.63	0.000630	0.000632	3.18
79.83	-46849.88	227.43	5055.50	0.000630	0.000633	3.19
79.92	-47022.24	223.62	4970.81	0.000628	0.000631	3.12
80.00	-46898.14	223.62	4970.81	0.000629	0.000632	3.13
80.08	-46643.03	227.48	5056.63	0.000632	0.000635	3.20
80.17	-46394.82	227.48	5056.63	0.000635	0.000638	3.21
80.25	-46105.24	223.62	4970.81	0.000639	0.000641	3.17
80.33	-46201.77	227.48	5056.63	0.000637	0.000640	3.22
80.42	-46491.35	229.36	5098.41	0.000634	0.000637	3.23
80.50	-46898.14	223.67	4971.94	0.000629	0.000632	3.13
80.58	-46918.82	227.48	5056.63	0.000629	0.000632	3.18
80.67	-46932.61	227.48	5056.63	0.000629	0.000632	3.18
80.75	-46849.88	225.55	5013.72	0.000629	0.000632	3.16
80.83	-46394.82	227.94	5066.79	0.000634	0.000637	3.21
80.92	-46201.77	223.62	4970.81	0.000636	0.000639	3.16
81.00	-46050.08	227.48	5056.63	0.000638	0.000640	3.22
81.08	-46153.51	229.41	5099.54	0.000636	0.000639	3.25
81.17	-46898.14	233.43	5188.75	0.000739	0.000742	3.83
81.25	-46698.19	229.41	5099.54	0.000741	0.000745	3.78
81.33	-46898.14	227.48	5056.63	0.000739	0.000742	3.74
81.42	-46884.35	229.41	5099.54	0.000739	0.000742	3.77

81.50	-46698.19	229.41	5099.54	0.000741	0.000745	3.78
81.58	-46201.77	233.43	5188.75	0.000748	0.000751	3.88
81.67	-46084.56	227.43	5055.50	0.000750	0.000753	3.79
81.75	-46015.61	227.48	5056.63	0.000751	0.000754	3.80
81.83	-46849.88	229.36	5098.41	0.000739	0.000743	3.77
81.92	-46594.77	232.05	5158.26	0.000743	0.000746	3.83
82.00	-46884.35	227.48	5056.63	0.000739	0.000742	3.74
82.08	-46884.35	229.36	5098.41	0.000739	0.000742	3.77
82.17	-46767.14	235.36	5231.66	0.000740	0.000744	3.87
82.25	-46629.24	227.58	5058.89	0.000742	0.000746	3.76
82.33	-46174.19	233.43	5188.75	0.000748	0.000752	3.88
82.42	-46070.77	228.70	5083.73	0.000750	0.000753	3.81
82.50	-46663.72	227.48	5056.63	0.000742	0.000745	3.75
82.58	-46236.24	229.36	5098.41	0.000748	0.000751	3.81
82.67	-46580.98	229.01	5090.50	0.000743	0.000746	3.78

SEPTEMBER 9, 1993
File C:\PC208\SCRN1a.DAT

VAPOR EXTRACTION AT WELL SCREEN #1					
Time (min)	Ambient Temperature (Celsius)	Temperature at Extraction Well (Celsius)	Pressure Drawdown ML Well #1 (cm W.C.)	Pressure Drawdown ML Well #3 (cm W.C.)	Pressure Drawdown ML Well #2 (cm W.C.)
0.08	31.06	31.28	0.964	1.009	
0.17	30.28	31.33	3.079	3.019	
0.25	29.94	31.28	5.617	5.777	
0.33	29.67	31.28	7.330	7.740	
0.42	29.83	31.28	8.410	9.140	
0.50	29.89	31.28	9.190	10.010	
0.58	30.22	31.28	9.800	10.500	
0.67	30.11	31.22	10.180	10.900	
0.75	30.17	31.22	10.550	11.320	
0.83	29.94	31.22	10.860	11.570	
0.92	29.22	31.17	11.160	11.850	
1.00	28.33	31.17	11.400	12.130	
1.08	28.06	31.11	11.730	12.300	
1.17	27.94	31.11	11.890	12.480	
1.25	27.89	31.11	12.080	12.700	
1.33	28.00	31.06	12.270	12.910	
1.42	28.06	31.06	12.460	12.950	
1.50	28.28	31.06	12.600	13.020	
1.58	29.00	31.00	12.710	13.140	
1.67	29.17	31.00	12.860	13.260	
1.75	28.78	30.94	13.000	13.330	
1.83	28.78	30.94	13.160	13.330	
1.92	28.67	30.89	13.250	13.300	

2.00	28.61	30.89	13.400	13.160
2.08	28.39	30.83	13.470	13.070
2.17	28.67	30.83	13.580	13.000
2.25	28.83	30.78	13.750	12.910
2.33	29.28	30.78	13.820	12.880
2.42	29.61	30.78	13.960	12.860
2.50	29.83	30.72	14.010	12.770
2.58	30.17	30.72	14.100	12.560
2.67	30.33	30.67	14.120	12.410
2.75	30.17	30.67	14.170	12.410
2.83	30.22	30.61	14.220	12.390
2.92	29.89	30.61	14.310	12.320
3.00	29.17	30.61	14.360	12.410
3.08	28.44	30.50	14.430	12.410
3.17	27.67	30.50	14.450	12.480
3.25	27.39	30.50	14.520	12.480
3.33	27.11	30.44	14.590	12.480
3.42	27.39	30.39	14.710	12.480
3.50	27.83	30.39	14.760	12.510
3.58	28.33	30.33	14.760	12.560
3.67	28.61	30.33	14.830	12.600
3.75	28.78	30.33	14.920	12.600
3.83	28.89	30.28	14.950	12.630
3.92	28.89	30.28	14.970	12.600
4.00	29.50	30.28	15.020	12.630
4.08	29.89	30.22	15.090	12.600
4.17	29.89	30.17	15.110	12.600
4.25	29.94	30.11	15.180	12.560
4.33	30.11	30.11	15.230	12.580
4.42	29.72	30.11	15.280	12.560

4.50	29.11	30.06	15.320	12.600
4.58	28.50	30.06	15.390	12.650
4.67	28.00	30.00	15.390	12.630
4.75	27.72	30.00	15.420	12.630
4.83	27.56	29.94	15.490	12.630
4.92	27.39	29.94	15.510	12.670
5.00	27.28	29.89	15.560	12.670
5.08	27.61	29.89	15.580	12.700
5.17	27.78	29.83	15.600	12.770
5.25	27.89	29.83	15.600	12.810
5.33	28.33	29.78	15.680	12.770
5.42	28.83	29.78	15.680	12.790
5.50	28.94	29.72	15.680	12.810
5.58	29.00	29.72	15.700	12.840
5.67	28.94	29.67	15.770	12.880
5.75	28.44	29.61	15.770	12.880
5.83	27.78	29.61	15.820	12.880
5.92	27.72	29.61	15.820	12.880
6.00	27.33	29.56	15.820	12.880
6.08	27.22	29.56	15.890	12.910
6.17	27.22	29.50	15.930	12.910
6.25	27.06	29.50	15.960	12.880
6.33	27.00	29.44	16.000	12.880
6.42	27.22	29.44	16.030	12.860
6.50	27.28	29.44	16.070	12.860
6.58	27.28	29.39	16.070	12.860
6.67	27.33	29.33	16.100	12.860
6.75	27.50	29.33	16.150	12.840
6.83	27.61	29.28	16.150	12.880
6.92	27.67	29.22	16.170	12.880

7.00	27.78	29.17	16.190	12.880	0.20
7.08	27.67	29.17	16.220	12.880	
7.17	27.67	29.17	16.220	12.880	
7.25	27.67	29.17	16.240	12.880	
7.33	27.50	29.11	16.260	12.880	
7.42	27.50	29.06	16.290	12.880	
7.50	27.44	29.00	16.290	12.880	
7.58	27.50	29.00	16.330	12.880	
7.67	27.61	28.94	16.310	12.860	
7.75	27.72	28.94	16.400	12.860	
7.83	28.00	28.89	16.400	12.840	
7.92	28.22	28.89	16.500	12.840	
8.00	28.00	28.89	16.470	12.860	
8.08	27.94	28.83	16.500	12.880	
8.17	28.11	28.78	16.540	12.910	
8.25	28.17	28.78	16.570	12.930	
8.33	28.39	28.72	16.540	12.910	
8.42	28.33	28.72	16.540	12.910	
8.50	28.56	28.67	16.620	12.910	
8.58	28.78	28.67	16.660	12.910	
8.67	28.83	28.61	16.660	12.950	
8.75	28.89	28.61	16.690	12.980	
8.83	29.44	28.56	16.690	12.930	
8.92	30.22	28.56	16.710	12.950	
9.00	30.89	28.56	16.730	12.930	
9.08	31.28	28.50	16.760	12.930	
9.17	31.44	28.50	16.780	12.910	
9.25	31.72	28.50	16.780	12.930	
9.33	32.11	28.44	16.760	12.910	
9.42	32.72	28.44	16.800	12.930	

9.50	32.83	28.39	16.900	12.950	0.30
9.58	32.72	28.39	16.870	12.950	
9.67	32.28	28.39	16.940	12.980	
9.75	32.06	28.33	16.900	12.950	
9.83	32.00	28.33	16.900	12.950	
9.92	32.06	28.33	16.940	12.980	
10.00	32.11	28.28	16.940	12.980	
10.08	32.50	28.28	16.990	13.000	
10.17	32.67	28.28	16.970	13.000	
10.25	32.94	28.22	16.970	13.000	
10.33	33.11	28.22	16.990	13.000	
10.42	32.89	28.22	16.970	13.000	
10.50	32.67	28.22	16.990	12.950	
10.58	32.67	28.22	16.990	12.950	
10.67	32.33	28.22	17.040	12.980	
10.75	31.83	28.22	17.060	12.980	
10.83	31.56	28.22	17.040	12.980	
10.92	31.67	28.22	17.090	13.000	
11.00	31.83	28.17	17.110	13.000	
11.08	31.94	28.17	17.110	13.000	
11.17	31.72	28.17	17.110	13.000	
11.25	31.11	28.17	17.130	13.000	
11.33	30.72	28.17	17.160	12.790	
11.42	30.89	28.11	17.160	12.480	
11.50	31.00	28.11	17.160	12.390	
11.58	31.00	28.11	17.160	12.580	
11.67	31.22	28.17	17.180	12.700	
11.75	31.39	28.11	17.180	12.790	
11.83	31.00	28.11	17.200	12.810	
11.92	30.50	28.11	17.160	12.860	

12.00	30.50	28.11	17.180	12.860	0.40
12.08	30.83	28.11	17.180	12.770	
12.17	30.61	28.11	17.230	12.580	
12.25	30.61	28.11	17.250	12.770	
12.33	30.83	28.11	17.270	12.790	
12.42	31.17	28.06	17.270	12.580	
12.50	31.39	28.06	17.300	12.320	
12.58	31.22	28.06	17.320	12.480	
12.67	31.78	28.06	17.320	12.630	
12.75	32.11	28.06	17.320	12.790	
12.83	32.22	28.00	17.340	12.810	
12.92	32.39	28.06	17.340	12.810	
13.00	32.44	28.00	17.440	12.510	
13.08	32.56	28.00	17.370	12.300	
13.17	32.39	28.00	17.390	12.160	
13.25	31.61	28.00	17.460	12.040	
13.33	31.06	28.00	17.440	11.900	
13.42	31.00	27.94	17.480	12.300	
13.50	31.61	27.94	17.480	12.630	
13.58	31.00	27.94	17.480	12.770	
13.67	30.44	27.94	17.510	12.860	
13.75	29.94	27.94	17.510	12.810	
13.83	29.94	27.89	17.560	12.530	
13.92	29.67	27.89	17.560	12.300	
14.00	29.56	27.89	17.560	12.180	
14.08	29.83	27.89	17.600	12.040	
14.17	29.67	27.89	17.630	12.090	
14.25	29.61	27.89	17.600	12.530	
14.33	29.28	27.83	17.600	12.770	
14.42	29.33	27.89	17.600	12.840	

					0.60
14.50	29.28	27.89	17.630	12.840	
14.58	29.94	27.89	17.650	12.840	
14.67	30.06	27.83	17.650	12.600	
14.75	29.94	27.83	17.650	12.440	
14.83	30.06	27.83	17.650	12.230	
14.92	30.00	27.83	17.650	12.130	
15.00	30.33	27.83	17.650	12.200	
15.08	30.33	27.78	17.650	12.460	
15.17	30.28	27.83	17.670	12.650	
15.25	30.39	27.83	17.670	12.790	
15.33	30.00	27.78	17.770	12.700	
15.42	29.67	27.78	17.740	12.460	
15.50	29.22	27.83	17.720	12.270	
15.58	29.06	27.78	17.740	12.160	
15.67	29.06	27.78	17.740	12.090	
15.75	28.72	27.78	17.740	12.020	
15.83	28.72	27.78	17.770	11.850	
15.92	28.89	27.78	17.740	11.830	
16.00	29.33	27.78	17.790	11.920	
16.08	29.17	27.78	17.790	12.390	
16.17	29.28	27.78	17.810	12.650	
16.25	29.39	27.72	17.840	12.790	
16.33	28.89	27.78	17.860	12.840	
16.42	28.89	27.78	17.810	12.770	
16.50	29.39	27.72	17.840	12.480	
16.58	29.50	27.72	17.840	12.300	
16.67	30.06	27.72	17.880	12.180	
16.75	29.89	27.72	17.860	12.060	
16.83	29.67	27.72	17.810	12.020	
16.92	29.00	27.72	17.860	11.950	

17.00	29.11	27.67	17.860	11.850	0.72
17.08	29.33	27.67	17.880	11.850	
17.17	29.06	27.72	17.880	11.810	
17.25	29.06	27.67	17.930	11.780	
17.33	29.22	27.67	17.930	11.740	
17.42	29.06	27.67	17.930	11.710	
17.50	28.39	27.67	17.930	11.710	
17.58	27.83	27.67	17.930	11.690	
17.67	28.00	27.67	17.930	11.670	
17.75	27.44	27.67	17.930	11.670	
17.83	27.28	27.61	17.930	11.620	
17.92	27.28	27.61	17.980	11.640	
18.00	27.22	27.61	17.930	11.970	
18.08	27.11	27.61	17.980	12.530	
18.17	26.83	27.56	17.950	12.880	
18.25	26.89	27.56	18.030	12.930	
18.33	26.78	27.56	18.030	12.930	
18.42	26.39	27.56	18.000	12.670	
18.50	26.56	27.50	18.000	12.460	
18.58	26.67	27.50	18.030	12.270	
18.67	26.61	27.50	17.980	12.160	
18.75	26.83	27.50	18.050	12.020	
18.83	26.78	27.50	18.050	11.920	
18.92	26.83	27.44	18.030	11.830	
19.00	27.06	27.39	18.030	11.740	0.81
19.08	27.17	27.39	18.070	11.670	
19.17	27.28	27.39	18.100	11.640	
19.25	27.33	27.39	18.100	11.600	
19.33	27.56	27.33	18.030	11.570	
19.42	27.94	27.33	18.100	11.990	

19.50	27.67	27.33	18.050	12.460		
19.58	27.78	27.28	18.050	12.790		
19.67	27.78	27.28	18.070	12.840		
19.75	27.61	27.28	18.070	12.860		
19.83	27.61	27.28	18.070	12.650		
19.92	27.67	27.22	18.050	12.370		
20.00	27.78	27.22	18.100	12.180		
20.08	28.22	27.22	18.100	12.110		
20.17	28.50	27.17	18.070	11.970		
20.25	28.83	27.17	18.100	11.830		
20.33	29.00	27.11	18.120	11.810		
20.42	29.11	27.11	18.100	11.670		
20.50	28.78	27.11	18.120	11.640		
20.58	28.72	27.11	18.100	11.620		
20.67	28.72	27.06	18.100	11.620		
20.75	28.72	27.06	18.120	11.620		
20.83	28.67	27.06	18.120	11.670		
20.92	28.56	27.06	18.120	12.180		
21.00	28.61	27.06	18.170	12.530	1.00	
21.08	28.61	27.00	18.210	12.530		
21.17	28.78	27.00	18.170	12.670		
21.25	28.89	27.00	18.190	12.600		
21.33	28.89	26.94	18.140	12.320		
21.42	29.00	26.94	18.140	12.200		
21.50	28.94	26.94	18.210	12.040		
21.58	28.94	26.94	18.190	11.970		
21.67	28.94	26.94	18.240	11.830		
21.75	29.06	26.89	18.240	11.830		
21.83	29.33	26.89	18.240	11.830		
21.92	29.22	26.89	18.210	11.740		

22.00	28.94	26.89	18.240	11.690	
22.08	29.22	26.89	18.210	11.600	
22.17	29.22	26.83	18.240	11.640	
22.25	29.28	26.83	18.190	11.620	
22.33	29.39	26.83	18.240	11.570	
22.42	29.44	26.83	18.240	11.550	
22.50	29.56	26.78	18.240	11.530	1.20
22.58	29.50	26.78	18.240	11.500	
22.67	29.61	26.78	18.240	11.480	
22.75	29.28	26.78	18.240	11.500	
22.83	29.17	26.78	18.240	11.500	
22.92	29.17	26.72	18.240	11.480	
23.00	29.28	26.72	18.260	11.430	
23.08	29.22	26.67	18.240	11.600	
23.17	29.33	26.72	18.240	12.250	
23.25	29.44	26.67	18.240	12.560	
23.33	29.72	26.67	18.260	12.580	
23.42	29.83	26.67	18.240	12.300	
23.50	30.06	26.67	18.260	12.160	
23.58	30.06	26.61	18.260	12.040	
23.67	30.22	26.61	18.240	11.850	
23.75	30.28	26.61	18.240	12.040	
23.83	30.50	26.61	18.240	12.410	
23.92	30.33	26.61	18.240	12.580	
24.00	30.11	26.56	18.310	12.440	
24.08	30.44	26.56	18.260	12.270	
24.17	31.17	26.56	18.260	12.460	
24.25	31.83	26.56	18.310	12.300	
24.33	32.28	26.56	18.280	12.180	
24.42	32.89	26.56	18.330	12.060	

24.50	33.06	26.56	18.310	11.920	
24.58	32.44	26.56	18.310	11.830	
24.67	32.00	26.56	18.280	11.740	
24.75	31.44	26.56	18.310	11.670	
24.83	31.33	26.56	18.310	11.620	
24.92	31.06	26.50	18.310	11.600	
25.00	31.06	26.56	18.310	11.530	1.40
25.08	30.78	26.56	18.330	11.500	
25.17	30.44	26.50	18.310	11.500	
25.25	30.28	26.50	18.310	11.480	
25.33	30.06	26.50	18.280	11.460	
25.42	29.89	26.50	18.310	11.430	
25.50	30.17	26.50	18.310	11.410	
25.58	30.28	26.50	18.310	11.460	
25.67	30.17	26.50	18.310	12.130	
25.75	30.00	26.44	18.310	12.530	
25.83	30.11	26.44	18.310	12.700	
25.92	30.17	26.44	18.280	12.790	
26.00	30.28	26.44	18.280	12.460	
26.08	30.33	26.44	18.280	12.250	
26.17	30.28	26.44	18.280	12.130	
26.25	30.33	26.44	18.310	12.040	
26.33	30.33	26.44	18.260	11.830	
26.42	30.28	26.44	18.280	11.780	
26.50	30.22	26.44	18.310	11.690	
26.58	30.72	26.44	18.260	11.670	
26.67	30.72	26.44	18.280	11.530	
26.75	30.39	26.44	18.260	11.500	
26.83	30.17	26.39	18.260	11.480	
26.92	30.22	26.44	18.280	11.480	

27.00	30.11	26.39	18.310	11.430	1.42
27.08	30.33	26.39	18.260	11.410	
27.17	30.61	26.39	18.280	11.390	
27.25	30.61	26.39	18.310	11.360	
27.33	30.61	26.39	18.330	11.360	
27.42	30.39	26.39	18.310	11.340	
27.50	30.06	26.39	18.310	11.320	
27.58	30.11	26.39	18.310	11.340	
27.67	30.17	26.39	18.310	11.320	
27.75	30.22	26.33	18.310	11.320	
27.83	30.39	26.33	18.260	11.290	
27.92	30.44	26.39	18.280	11.270	
28.00	30.17	26.33	18.260	11.290	
28.08	30.22	26.33	18.280	11.270	
28.17	30.22	26.33	18.310	11.250	
28.25	30.56	26.33	18.280	11.290	
28.33	31.00	26.33	18.280	11.250	
28.42	31.28	26.33	18.260	11.320	
28.50	31.28	26.33	18.310	11.360	
28.58	31.33	26.33	18.280	11.410	
28.67	31.89	26.33	18.310	11.430	
28.75	32.06	26.33	18.310	11.360	
28.83	32.50	26.33	18.310	11.360	
28.92	32.83	26.28	18.280	11.360	
29.00	33.06	26.33	18.310	11.320	
29.08	33.28	26.33	18.310	11.320	
29.17	33.39	26.33	18.310	11.290	
29.25	33.11	26.33	18.260	11.290	
29.33	33.06	26.33	18.310	11.270	
29.42	33.39	26.33	18.260	11.250	

29.50	33.28	26.33	18.260	11.290	
29.58	33.06	26.33	18.280	11.270	
29.67	33.28	26.33	18.280	11.290	
29.75	33.22	26.33	18.280	11.250	
29.83	33.00	26.33	18.260	11.270	
29.92	33.00	26.33	18.280	11.250	
30.00	32.94	26.39	18.240	11.220	
30.08	32.44	26.33	18.260	11.250	
30.17	32.50	26.33	18.310	11.220	
30.25	32.50	26.33	18.280	11.220	
30.33	32.89	26.39	18.260	11.270	
30.42	32.94	26.39	18.310	11.250	
30.50	32.89	26.39	18.280	11.250	1.60
30.58	33.00	26.39	18.260	11.250	
30.67	33.11	26.39	18.280	11.220	
30.75	32.56	26.44	18.260	11.250	
30.83	32.67	26.44	18.260	11.250	
30.92	32.44	26.44	18.240	11.220	
31.00	31.33	26.39	18.260	11.220	
31.08	30.78	26.44	18.260	11.250	
31.17	30.44	26.44	18.280	11.250	
31.25	30.83	26.44	18.260	11.200	
31.33	30.83	26.44	18.240	11.200	
31.42	31.06	26.44	18.280	11.180	
31.50	31.72	26.44	18.240	11.200	
31.58	32.17	26.44	18.260	11.180	
31.67	32.44	26.44	18.240	11.220	
31.75	32.33	26.50	18.260	11.180	
31.83	32.33	26.50	18.260	11.200	
31.92	32.56	26.50	18.260	11.150	

32.00	31.67	26.50	18.260	11.200	
32.08	31.28	26.50	18.260	11.200	
32.17	30.61	26.50	18.240	11.220	
32.25	30.56	26.56	18.260	11.220	
32.33	30.67	26.50	18.260	11.220	
32.42	30.94	26.56	18.260	11.200	
32.50	30.83	26.50	18.240	11.200	
32.58	30.94	26.56	18.280	11.200	
32.67	31.33	26.56	18.260	11.180	
32.75	31.50	26.56	18.280	11.200	
32.83	32.11	26.56	18.280	11.220	
32.92	32.06	26.56	18.280	11.220	
33.00	32.11	26.56	18.350	11.130	1.61
33.08	32.56	26.50	18.350	11.150	
33.17	32.83	26.56	18.350	11.200	
33.25	32.67	26.56	18.310	11.200	
33.33	32.50	26.56	18.280	11.220	
33.42	32.28	26.56	18.330	11.180	
33.50	32.56	26.56	18.280	11.200	
33.58	32.39	26.56	18.310	11.180	
33.67	32.33	26.56	18.310	11.150	
33.75	32.17	26.56	18.310	11.180	
33.83	32.00	26.56	18.280	11.150	
33.92	32.17	26.56	18.280	11.130	
34.00	32.33	26.56	18.260	11.110	
34.08	32.50	26.61	18.310	11.110	
34.17	32.72	26.61	18.280	11.110	
34.25	32.89	26.56	18.260	11.110	
34.33	32.89	26.61	18.240	11.080	
34.42	33.06	26.61	18.240	11.110	

34.50	32.83	26.61	18.240	11.060	
34.58	33.06	26.61	18.260	11.110	
34.67	32.11	26.61	18.240	11.080	
34.75	31.39	26.61	18.260	11.110	
34.83	31.22	26.61	18.240	11.110	
34.92	31.28	26.61	18.240	11.130	
35.00	31.83	26.61	18.260	11.110	
35.08	31.67	26.61	18.210	11.110	
35.17	30.44	26.61	18.240	11.110	
35.25	30.28	26.67	18.240	11.110	
35.33	30.17	26.67	18.240	11.110	
35.42	29.61	26.67	18.240	11.110	
35.50	29.00	26.67	18.240	11.080	1.62
35.58	29.17	26.67	18.210	11.080	
35.67	28.78	26.72	18.240	11.080	
35.75	28.44	26.67	18.240	11.080	
35.83	27.94	26.67	18.240	11.130	
35.92	27.22	26.72	18.210	11.080	
36.00	26.17	26.67	18.210	11.110	
36.08	25.94	26.67	18.210	11.080	
36.17	25.94	26.67	18.210	11.080	
36.25	26.11	26.67	18.210	11.080	
36.33	25.83	26.72	18.210	11.110	
36.42	26.00	26.67	18.240	11.080	
36.50	26.22	26.72	18.240	11.110	
36.58	26.83	26.67	18.260	11.110	
36.67	26.72	26.72	18.260	11.060	
36.75	27.50	26.67	18.260	11.010	
36.83	27.89	26.67	18.260	11.040	
36.92	28.83	26.67	18.210	10.970	

37.00	28.50	26.67	18.240	11.010	
37.08	28.61	26.67	18.240	10.940	
37.17	28.22	26.67	18.240	10.970	
37.25	27.33	26.67	18.280	10.940	
37.33	26.89	26.67	18.260	10.920	
37.42	26.78	26.61	18.260	10.940	
37.50	26.83	26.67	18.310	10.940	
37.58	27.06	26.67	18.280	10.940	
37.67	27.72	26.67	18.310	10.970	
37.75	27.89	26.67	18.280	10.940	
37.83	28.11	26.61	18.280	10.970	
37.92	27.83	26.61	18.350	10.940	
38.00	27.72	26.61	18.310	10.940	1.70
38.08	27.94	26.61	18.330	10.940	
38.17	28.00	26.56	18.350	10.940	
38.25	28.44	26.56	18.310	10.940	
38.33	28.78	26.56	18.350	10.940	
38.42	28.94	26.56	18.350	10.940	
38.50	29.11	26.56	18.330	10.970	
38.58	28.67	26.56	18.330	10.990	
38.67	29.00	26.56	18.350	10.970	
38.75	29.11	26.50	18.350	10.940	
38.83	29.06	26.44	18.380	10.970	
38.92	28.94	26.50	18.380	10.940	
39.00	29.28	26.50	18.350	10.970	
39.08	29.44	26.50	18.380	10.970	
39.17	29.61	26.44	18.350	10.940	
39.25	29.56	26.44	18.310	10.940	
39.33	29.33	26.44	18.330	10.940	
39.42	29.17	26.44	18.350	10.940	

39.50	29.61	26.39	18.350	10.920	
39.58	29.83	26.39	18.350	10.920	
39.67	29.61	26.39	18.330	10.970	
39.75	29.33	26.39	18.310	10.940	
39.83	29.17	26.33	18.310	10.940	
39.92	29.17	26.33	18.280	10.900	
40.00	29.06	26.33	18.260	10.900	1.80
40.08	29.28	26.28	18.240	10.900	
40.17	28.83	26.33	18.260	10.900	
40.25	28.61	26.28	18.260	10.900	
40.33	28.44	26.28	18.260	10.870	
40.42	28.83	26.33	18.240	10.900	
40.50	28.61	26.28	18.240	10.850	
40.58	28.44	26.28	18.260	10.900	
40.67	28.50	26.22	18.240	10.900	
40.75	28.78	26.28	18.240	10.870	
40.83	29.06	26.28	18.210	10.870	
40.92	29.11	26.28	18.240	10.870	
41.00	28.94	26.22	18.240	10.870	
41.08	28.89	26.22	18.210	10.900	
41.17	28.78	26.22	18.240	10.900	
41.25	29.00	26.22	18.240	10.870	
41.33	28.78	26.22	18.240	10.900	
41.42	28.61	26.22	18.240	10.900	
41.50	29.00	26.22	18.260	10.900	
41.58	29.06	26.22	18.260	10.900	
41.67	29.22	26.22	18.260	10.900	
41.75	29.17	26.17	18.240	10.900	
41.83	29.17	26.17	18.260	10.920	
41.92	29.17	26.17	18.280	10.920	

42.00	29.28	26.17	18.260	10.920	1.90
42.08	29.56	26.22	18.260	10.870	
42.17	29.44	26.17	18.310	10.900	
42.25	29.33	26.17	18.310	10.920	
42.33	29.39	26.22	18.310	10.900	
42.42	29.39	26.17	18.280	10.920	
42.50	29.50	26.17	18.330	10.870	
42.58	29.72	26.17	18.310	10.900	
42.67	29.94	26.17	18.310	10.870	
42.75	29.89	26.17	18.310	10.900	
42.83	29.89	26.17	18.260	10.870	
42.92	30.00	26.17	18.310	10.920	
43.00	30.06	26.17	18.280	10.870	
43.08	30.06	26.17	18.310	10.900	
43.17	29.83	26.17	18.310	10.870	
43.25	29.72	26.11	18.330	10.900	
43.33	29.44	26.11	18.350	10.900	
43.42	29.61	26.11	18.350	10.900	
43.50	29.50	26.11	18.350	10.900	
43.58	29.50	26.11	18.380	10.900	
43.67	29.39	26.11	18.400	10.900	
43.75	29.22	26.11	18.350	10.900	
43.83	29.11	26.11	18.380	10.870	
43.92	29.11	26.11	18.380	10.850	
44.00	29.06	26.11	18.350	10.900	2.00
44.08	29.28	26.11	18.350	10.870	
44.17	29.33	26.11	18.380	10.900	
44.25	29.39	26.11	18.350	10.850	
44.33	29.67	26.11	18.310	10.900	
44.42	29.89	26.11	18.380	10.830	

44.50	29.89	26.06	18.400	10.870
44.58	30.06	26.06	18.380	10.850
44.67	30.11	26.06	18.380	10.830
44.75	30.22	26.06	18.420	10.850
44.83	30.39	26.06	18.400	10.870
44.92	30.61	26.00	18.420	10.850
45.00	30.61	26.06	18.400	10.830
45.08	30.67	26.00	18.400	10.800
45.17	30.83	26.00	18.420	10.870
45.25	30.94	26.00	18.420	10.830
45.33	30.89	26.00	18.450	10.850
45.42	30.72	26.00	18.450	10.900
45.50	30.83	26.00	18.450	10.850
45.58	30.61	26.00	18.450	10.850
45.67	30.67	26.00	18.450	10.850
45.75	30.61	26.00	18.450	10.870
45.83	30.50	26.00	18.450	10.900
45.92	30.56	26.00	18.490	10.870
46.00	30.61	26.00	18.470	10.850
46.08	30.83	25.94	18.490	10.850
46.17	31.00	26.00	18.470	10.900
46.25	31.00	25.94	18.470	10.900
46.33	31.11	25.94	18.450	10.900
46.42	31.28	25.94	18.470	10.900
46.50	31.44	25.94	18.490	10.830
46.58	31.44	25.94	18.450	10.900
46.67	31.44	25.94	18.450	10.900
46.75	31.50	25.94	18.450	10.850
46.83	31.33	25.94	18.470	10.850
46.92	31.28	25.94	18.450	10.850

47.00	31.28	25.94	18.470	10.900	
47.08	31.28	25.94	18.450	10.830	
47.17	31.39	25.89	18.470	10.800	
47.25	31.39	25.89	18.470	10.850	
47.33	31.39	25.94	18.470	10.870	
47.42	31.22	25.89	18.490	10.850	
47.50	31.22	25.94	18.470	10.830	
47.58	31.22	25.89	18.450	10.830	
47.67	31.39	25.89	18.490	10.850	
47.75	31.44	25.89	18.490	10.850	
47.83	31.39	25.89	18.490	10.800	
47.92	31.50	25.89	18.470	10.830	
48.00	31.61	25.89	18.490	10.830	2.20
48.08	31.78	25.89	18.490	10.850	
48.17	31.78	25.89	18.470	10.830	
48.25	31.83	25.89	18.470	10.830	
48.33	31.89	25.89	18.520	10.830	
48.42	32.00	25.89	18.470	10.830	
48.50	31.94	25.89	18.490	10.870	
48.58	32.06	25.89	18.490	10.850	
48.67	32.17	25.83	18.490	10.780	
48.75	31.83	25.89	18.490	10.850	
48.83	31.89	25.89	18.470	10.830	
48.92	32.39	25.89	18.520	10.850	
49.00	33.00	25.83	18.490	10.830	
49.08	33.33	25.89	18.520	10.830	
49.17	33.28	25.83	18.520	10.850	
49.25	33.33	25.83	18.520	10.830	
49.33	33.22	25.89	18.520	10.800	
49.42	34.00	25.89	18.490	10.830	

49.50	34.50	25.83	18.540	10.850	
49.58	34.28	25.89	18.520	10.830	
49.67	34.17	25.89	18.490	10.850	
49.75	33.78	25.83	18.520	10.850	
49.83	33.56	25.89	18.520	10.850	
49.92	33.61	25.89	18.520	10.800	
50.00	33.83	25.89	18.540	10.830	
50.08	33.89	25.89	18.520	10.800	
50.17	34.28	25.89	18.470	10.800	
50.25	33.78	25.89	18.490	10.830	
50.33	34.06	25.89	18.540	10.800	
50.42	34.17	25.89	18.540	10.800	
50.50	33.89	25.89	18.520	10.800	
50.58	32.61	25.89	18.570	10.780	
50.67	32.11	25.89	18.520	10.800	
50.75	31.72	25.89	18.540	10.780	
50.83	31.22	25.89	18.540	10.780	
50.92	30.94	25.89	18.590	10.780	
51.00	31.00	25.89	18.560	10.830	2.40
51.08	30.94	25.89	18.540	10.800	
51.17	30.89	25.94	18.490	10.760	
51.25	30.83	25.94	18.560	10.780	
51.33	30.72	25.94	18.540	10.780	
51.42	31.17	25.94	18.520	10.780	
51.50	31.94	25.89	18.520	10.800	
51.58	32.50	25.89	18.520	10.780	
51.67	32.83	25.94	18.520	10.780	
51.75	32.67	25.94	18.520	10.760	
51.83	31.78	25.94	18.590	10.780	
51.92	31.22	25.89	18.610	10.760	

52.00	30.78	25.89	18.540	10.780
52.08	30.61	25.94	18.540	10.780
52.17	30.67	25.89	18.520	10.780
52.25	30.72	25.94	18.520	10.760
52.33	30.72	25.94	18.560	10.730
52.42	30.78	25.94	18.560	10.780
52.50	32.11	25.94	18.520	10.730
52.58	32.56	25.94	18.590	10.730
52.67	33.11	25.94	18.560	10.730
52.75	33.06	25.94	18.560	10.730
52.83	33.28	25.94	18.560	10.710
52.92	33.39	26.00	18.560	10.730
53.00	33.56	25.94	18.560	10.730
53.08	33.44	26.00	18.540	10.690
53.17	33.00	26.00	18.540	10.710
53.25	32.72	26.00	18.540	10.690
53.33	32.72	26.00	18.560	10.760
53.42	32.67	26.00	18.560	10.760
53.50	33.28	26.00	18.560	10.760
53.58	33.72	26.00	18.590	10.780
53.67	33.89	26.00	18.560	10.730
53.75	34.06	26.00	18.560	10.760
53.83	33.56	26.00	18.560	10.690
53.92	32.89	26.00	18.590	10.710
54.00	32.72	26.06	18.540	10.710
54.08	32.89	26.06	18.560	10.730
54.17	32.78	26.06	18.610	10.730
54.25	32.50	26.06	18.610	10.710
54.33	32.28	26.00	18.590	10.780
54.42	32.06	26.06	18.590	10.730

54.50	32.06	26.06	18.520	10.730		
54.58	32.00	26.06	18.590	10.730		
54.67	31.00	26.06	18.590	10.780		
54.75	30.33	26.06	18.560	10.760		
54.83	30.06	26.11	18.590	10.760		
54.92	29.78	26.11	18.590	10.780		
55.00	29.83	26.11	18.610	10.730	2.48	
55.08	29.67	26.11	18.590	10.730		
55.17	29.67	26.11	18.610	10.710		
55.25	29.17	26.11	18.590	10.710		
55.33	29.50	26.11	18.590	10.780		
55.42	29.83	26.11	18.590	10.760		
55.50	29.61	26.11	18.610	10.690		
55.58	29.56	26.11	18.560	10.730		
55.67	29.78	26.11	18.590	10.710		
55.75	29.78	26.11	18.610	10.710		
55.83	29.67	26.06	18.660	10.690		
55.92	29.50	26.11	18.640	10.660		
56.00	29.61	26.11	18.590	10.660		
56.08	28.94	26.11	18.610	10.710		
56.17	28.78	26.11	18.610	10.660		
56.25	28.61	26.11	18.610	10.710		
56.33	28.67	26.06	18.610	10.690		
56.42	28.61	26.06	18.590	10.640		
56.50	28.61	26.11	18.610	10.660		
56.58	28.44	26.06	18.590	10.690		
56.67	28.28	26.11	18.590	10.640		
56.75	28.06	26.06	18.590	10.640		
56.83	28.33	26.06	18.610	10.660		
56.92	28.44	26.06	18.610	10.660		

57.00	28.61	26.06	18.560	10.640
57.08	28.78	26.06	18.590	10.640
57.17	28.94	26.06	18.590	10.620
57.25	28.83	26.06	18.590	10.620
57.33	28.89	26.06	18.590	10.640
57.42	28.89	26.06	18.590	10.640
57.50	29.00	26.06	18.610	10.620
57.58	29.11	26.06	18.560	10.640
57.67	29.28	26.00	18.590	10.640
57.75	29.44	26.00	18.590	10.620
57.83	29.61	26.00	18.590	10.640
57.92	29.56	26.00	18.610	10.640
58.00	29.50	26.00	18.680	10.640
58.08	29.72	26.00	18.680	10.640
58.17	29.89	26.00	18.640	10.590
58.25	30.00	26.00	18.640	10.640
58.33	30.11	25.94	18.640	10.640
58.42	30.06	25.94	18.640	10.640
58.50	30.22	25.94	18.610	10.660
58.58	29.94	26.00	18.640	10.640
58.67	30.00	25.94	18.660	10.640
58.75	30.11	25.94	18.640	10.570
58.83	30.00	25.94	18.660	10.590
58.92	30.06	25.94	18.660	10.620
59.00	29.78	25.94	18.660	10.590
59.08	29.78	25.94	18.640	10.570
59.17	30.00	25.94	18.640	10.620
59.25	30.00	25.94	18.680	10.590
59.33	30.28	25.94	18.680	10.620
59.42	30.44	25.89	18.680	10.590

59.50	30.72	25.89	18.680	10.620
59.58	30.67	25.89	18.640	10.570
59.67	30.72	25.89	18.660	10.620
59.75	30.72	25.89	18.660	10.590
59.83	31.11	25.89	18.640	10.590
59.92	31.22	25.89	18.680	10.620
60.00	31.17	25.89	18.610	10.590
60.08	31.39	25.89	18.660	10.590
60.17	31.50	25.89	18.640	10.590
60.25	31.56	25.89	18.660	10.570
60.33	31.33	25.89	18.640	10.590
60.42	31.33	25.89	18.680	10.590
60.50	31.50	25.89	18.640	10.620
60.58	31.56	25.89	18.640	10.620
60.67	31.67	25.89	18.640	10.620
60.75	31.78	25.83	18.640	10.620
60.83	31.94	25.89	18.660	10.590
60.92	32.22	25.89	18.640	10.620
61.00	32.72	25.83	18.660	10.620
61.08	33.39	25.83	18.680	10.620
61.17	33.67	25.89	18.660	10.640
61.25	33.94	25.89	18.680	10.620
61.33	33.78	25.89	18.660	10.620
61.42	33.06	25.89	18.660	10.640
61.50	33.06	25.89	18.680	10.590
61.58	33.11	25.83	18.680	10.620
61.67	33.78	25.83	18.680	10.590
61.75	34.61	25.89	18.680	10.590
61.83	34.78	25.89	18.680	10.620
61.92	34.94	25.83	18.660	10.620

62.00	35.44	25.89	18.660	10.590	
62.08	35.28	25.89	18.660	10.620	
62.17	35.22	25.94	18.660	10.590	
62.25	35.50	25.89	18.680	10.590	
62.33	35.06	25.89	18.680	10.590	
62.42	34.50	25.94	18.680	10.590	
62.50	34.44	25.94	18.680	10.640	
62.58	34.33	25.94	18.660	10.620	
62.67	34.56	25.94	18.660	10.590	
62.75	34.06	25.94	18.640	10.590	
62.83	33.56	25.94	18.640	10.570	
62.92	33.78	25.94	18.660	10.620	
63.00	33.67	26.00	18.660	10.620	
63.08	33.56	26.00	18.660	10.620	
63.17	33.56	26.00	18.680	10.620	
63.25	32.17	26.00	18.680	10.590	
63.33	31.06	26.00	18.640	10.590	
63.42	30.67	26.00	18.660	10.620	
63.50	30.61	26.06	18.640	10.570	
63.58	30.50	26.00	18.680	10.590	
63.67	30.44	26.00	18.640	10.620	
63.75	30.33	26.06	18.680	10.590	
63.83	30.50	26.06	18.640	10.620	
63.92	30.39	26.06	18.640	10.590	
64.00	30.17	26.06	18.660	10.590	2.60
64.08	30.17	26.06	18.640	10.590	
64.17	29.89	26.06	18.660	10.590	
64.25	29.78	26.06	18.680	10.570	
64.33	30.28	26.06	18.640	10.550	
64.42	31.06	26.06	18.660	10.570	

64.50	30.83	26.06	18.680	10.620
64.58	30.67	26.06	18.610	10.570
64.67	30.39	26.06	18.610	10.570
64.75	30.50	26.06	18.710	10.590
64.83	30.50	26.00	18.680	10.590
64.92	30.22	26.06	18.680	10.620
65.00	30.33	26.06	18.660	10.550
65.08	30.28	26.06	18.660	10.570
65.17	30.00	26.00	18.680	10.590
65.25	29.67	26.00	18.660	10.520
65.33	29.39	26.00	18.680	10.520
65.42	29.44	26.06	18.660	10.520
65.50	29.78	26.00	18.660	10.550
65.58	29.78	26.06	18.660	10.550
65.67	29.94	26.00	18.710	10.550
65.75	30.00	26.00	18.680	10.520
65.83	29.83	26.00	18.710	10.570
65.92	29.94	26.00	18.680	10.550
66.00	29.94	26.00	18.680	10.550
66.08	29.78	26.00	18.680	10.570
66.17	29.89	26.00	18.710	10.550
66.25	30.06	26.00	18.680	10.590
66.33	30.06	26.00	18.680	10.590
66.42	29.89	26.00	18.640	10.550
66.50	29.67	26.00	18.680	10.550
66.58	29.67	26.00	18.680	10.570
66.67	29.72	26.00	18.680	10.570
66.75	29.89	26.00	18.680	10.550
66.83	29.72	25.94	18.680	10.550
66.92	29.78	26.00	18.660	10.550

67.00	29.83	25.94	18.680	10.550	
67.08	30.06	25.94	18.680	10.550	
67.17	30.11	25.94	18.660	10.570	
67.25	30.17	25.94	18.660	10.520	
67.33	30.17	25.94	18.680	10.550	
67.42	30.28	25.94	18.680	10.520	
67.50	30.28	25.94	18.680	10.500	
67.58	30.33	25.94	18.710	10.520	
67.67	30.28	25.89	18.660	10.520	
67.75	30.39	25.94	18.640	10.550	
67.83	30.39	25.94	18.640	10.550	
67.92	30.56	25.89	18.680	10.550	
68.00	30.78	25.89	18.640	10.550	2.70
68.08	30.83	25.89	18.680	10.550	
68.17	30.67	25.89	18.680	10.520	
68.25	30.67	25.89	18.680	10.550	
68.33	30.67	25.89	18.680	10.520	
68.42	31.00	25.89	18.680	10.550	
68.50	31.17	25.89	18.680	10.520	
68.58	30.94	25.89	18.710	10.550	
68.67	31.17	25.89	18.710	10.550	
68.75	31.50	25.89	18.710	10.550	
68.83	32.39	25.89	18.710	10.550	
68.92	33.22	25.89	18.680	10.570	
69.00	33.39	25.89	18.680	10.590	
69.08	33.56	25.89	18.710	10.570	
69.17	33.44	25.89	18.680	10.550	
69.25	33.83	25.89	18.710	10.570	
69.33	34.00	25.89	18.680	10.550	
69.42	33.72	25.89	18.710	10.550	

69.50	33.72	25.89	18.710	10.550
69.58	33.78	25.94	18.710	10.570
69.67	33.67	25.94	18.680	10.550
69.75	33.39	25.89	18.680	10.550
69.83	33.67	25.94	18.680	10.520
69.92	33.67	25.94	18.660	10.550
70.00	33.44	25.94	18.680	10.520
70.08	33.50	25.94	18.710	10.550
70.17	33.61	25.94	18.660	10.500
70.25	33.22	25.94	18.710	10.480
70.33	33.17	26.00	18.710	10.500
70.42	33.11	26.00	18.680	10.550
70.50	33.17	26.00	18.680	10.520
70.58	33.56	25.94	18.680	10.500
70.67	34.00	26.00	18.710	10.520
70.75	34.67	26.00	18.710	10.550
70.83	34.94	26.00	18.710	10.550
70.92	35.00	26.00	18.710	10.570
71.00	33.78	26.00	18.710	10.550
71.08	32.83	26.00	18.710	10.570
71.17	32.44	26.00	18.680	10.520
71.25	32.50	26.00	18.680	10.550
71.33	32.78	26.06	18.710	10.520
71.42	32.72	26.06	18.710	10.500
71.50	32.56	26.06	18.710	10.520
71.58	32.50	26.06	18.710	10.520
71.67	32.33	26.06	18.710	10.520
71.75	31.78	26.06	18.710	10.550
71.83	31.67	26.06	18.730	10.550
71.92	31.89	26.11	18.730	10.520

72.00	32.11	26.06	18.710	10.520	2.80
72.08	33.06	26.11	18.710	10.520	
72.17	33.56	26.11	18.710	10.520	
72.25	34.00	26.11	18.780	10.520	
72.33	33.44	26.11	18.730	10.520	
72.42	32.06	26.11	18.750	10.520	
72.50	31.28	26.11	18.730	10.480	
72.58	30.50	26.17	18.710	10.500	
72.67	31.39	26.17	18.710	10.500	
72.75	32.00	26.17	18.730	10.520	
72.83	32.28	26.17	18.710	10.520	
72.92	32.83	26.17	18.680	10.500	
73.00	33.17	26.17	18.750	10.450	
73.08	32.89	26.17	18.750	10.480	
73.17	32.89	26.22	18.750	10.500	
73.25	33.17	26.22	18.730	10.500	
73.33	32.89	26.22	18.710	10.480	
73.42	32.61	26.22	18.750	10.480	
73.50	32.78	26.22	18.730	10.450	
73.58	33.06	26.22	18.730	10.450	
73.67	33.06	26.28	18.730	10.480	
73.75	33.50	26.22	18.730	10.500	
73.83	33.28	26.28	18.730	10.450	
73.92	33.61	26.28	18.730	10.430	
74.00	33.22	26.28	18.710	10.500	
74.08	33.06	26.28	18.710	10.480	
74.17	32.78	26.28	18.680	10.480	
74.25	33.11	26.33	18.710	10.450	
74.33	32.83	26.28	18.710	10.430	
74.42	31.89	26.33	18.710	10.380	

74.50	32.22	26.33	18.730	10.430
74.58	31.94	26.33	18.710	10.380
74.67	31.94	26.33	18.710	10.450
74.75	31.67	26.33	18.730	10.410
74.83	32.00	26.33	18.730	10.450
74.92	32.00	26.39	18.710	10.480
75.00	32.44	26.33	18.710	10.450
75.08	32.50	26.39	18.730	10.430
75.17	32.33	26.39	18.750	10.450
75.25	32.17	26.39	18.730	10.500
75.33	32.06	26.44	18.730	10.410
75.42	31.61	26.39	18.730	10.380
75.50	31.00	26.44	18.710	10.410
75.58	29.94	26.39	18.750	10.410
75.67	29.56	26.39	18.710	10.430
75.75	29.50	26.39	18.710	10.410
75.83	28.50	26.39	18.710	10.410
75.92	27.89	26.44	18.710	10.430
76.00	27.83	26.39	18.710	10.410
76.08	27.33	26.39	18.710	10.410
76.17	27.22	26.39	18.710	10.380
76.25	27.22	26.39	18.710	10.450
76.33	27.50	26.39	18.710	10.410
76.42	27.72	26.33	18.710	10.410
76.50	27.89	26.39	18.730	10.430
76.58	28.72	26.39	18.730	10.430
76.67	30.28	26.39	18.750	10.430
76.75	30.89	26.39	18.750	10.450
76.83	31.67	26.39	18.710	10.450
76.92	32.39	26.39	18.730	10.410

77.00	32.72	26.39	18.730	10.430
77.08	32.78	26.44	18.710	10.450
77.17	32.89	26.39	18.710	10.430
77.25	32.00	26.39	18.710	10.430
77.33	31.67	26.39	18.730	10.360
77.42	31.11	26.39	18.710	10.340
77.50	30.94	26.39	18.710	10.340
77.58	31.17	26.39	18.710	10.340
77.67	31.22	26.44	18.750	10.380
77.75	30.50	26.44	18.730	10.380
77.83	30.17	26.39	18.730	10.340
77.92	30.17	26.39	18.710	10.360
78.00	30.67	26.39	18.730	10.360
78.08	31.44	26.44	18.710	10.360
78.17	32.56	26.44	18.730	10.380
78.25	32.94	26.44	18.730	10.380
78.33	33.33	26.44	18.730	10.380
78.42	33.06	26.44	18.710	10.360
78.50	33.50	26.44	18.710	10.380
78.58	33.28	26.39	18.710	10.360
78.67	33.22	26.44	18.710	10.380
78.75	33.06	26.44	18.710	10.360
78.83	33.00	26.44	18.710	10.360
78.92	33.00	26.44	18.680	10.340
79.00	31.89	26.44	18.710	10.340
79.08	32.17	26.50	18.680	10.360
79.17	32.78	26.50	18.680	10.360
79.25	32.61	26.50	18.680	10.340
79.33	32.39	26.50	18.680	10.340
79.42	32.56	26.50	18.710	10.360

79.50	32.22	26.50	18.730	10.340
79.58	31.06	26.50	18.710	10.340
79.67	30.61	26.50	18.710	10.340
79.75	31.33	26.50	18.710	10.340
79.83	31.83	26.50	18.710	10.340
79.92	31.94	26.50	18.710	10.340
80.00	31.94	26.56	18.710	10.340
80.08	31.33	26.56	18.710	10.340
80.17	31.39	26.56	18.710	10.310
80.25	30.56	26.56	18.680	10.310
80.33	29.67	26.56	18.680	10.310
80.42	29.22	26.56	18.680	10.310
80.50	28.83	26.56	18.660	10.310
80.58	28.61	26.56	18.680	10.340
80.67	28.39	26.56	18.660	10.340
80.75	28.83	26.78	18.710	10.340
80.83	28.50	27.00	18.680	10.340
80.92	28.67	27.17	18.710	10.260
81.00	28.78	27.28	18.680	10.240
81.08	28.56	27.33	18.680	10.290
81.17	-17.78	-17.78	18.680	10.310
81.25	-17.78	-17.78	18.710	10.310
81.33	-17.78	-17.78	18.710	10.310
81.42	-17.78	-17.78	18.710	10.340
81.50	-17.78	-17.78	18.730	10.340
81.58	-17.78	-17.78	18.710	10.290
81.67	-17.78	-17.78	18.680	10.290
81.75	-17.78	-17.78	18.710	10.260
81.83	-17.78	-17.78	18.680	10.290
81.92	-17.78	-17.78	18.660	10.260

82.00	-17.78	-17.78	18.680	10.310	
82.08	-17.78	-17.78	18.660	10.290	
82.17	-17.78	-17.78	18.710	10.340	
82.25	-17.78	-17.78	18.710	10.290	
82.33	-17.78	-17.78	18.730	10.310	
82.42	-17.78	-17.78	18.710	10.310	
82.50	-17.78	-17.78	18.750	10.290	
82.58	-17.78	-17.78	18.710	10.260	2.80
82.67	-17.78	-17.78	18.730	10.260	

APPENDIX E

Raw data from laboratory tests utilized in energy loss analyses

September 28,1993
Head Loss Tests With Packer

Time (min)	Temperature Ambient (Celsius)	Temperature at Well Head (Celsius)	Pressure at Well Head (Pascals)	Pressure at Well Head (PSI)	Velocity at Well Head (cm/s)	Density of Air (g/cm^3)	Head Loss (Pascals)	Mass Flow Rate (g/cm^3)
0.02	21.94	21.78	-2433.86	-0.353	504.75	0.001162	-2080.03	5.66
0.03	21.94	21.78	-7122.06	-1.033	974.45	0.001107	-6382.41	10.41
0.05	21.89	21.78	-11075.49	-1.606	1168.40	0.001060	-10372.83	11.96
0.07	21.89	21.78	-11556.18	-1.676	1168.40	0.001055	-10884.89	11.89
0.08	21.89	21.72	-11399.22	-1.653	1169.57	0.001057	-10714.89	11.93
0.10	21.89	21.72	-11448.27	-1.660	1160.22	0.001056	-10768.41	11.82
0.12	21.89	21.72	-11565.99	-1.678	1168.40	0.001055	-10893.32	11.89
0.13	21.89	21.72	-11673.90	-1.693	1168.40	0.001054	-11009.03	11.88
0.15	21.89	21.78	-11242.26	-1.631	1149.71	0.001058	-10552.16	11.74
0.17	21.89	21.78	-11556.18	-1.676	1160.22	0.001055	-10885.89	11.81
0.18	21.89	21.78	-11595.42	-1.682	1135.68	0.001054	-10930.90	11.55
0.20	21.89	21.78	-11516.94	-1.670	1150.87	0.001055	-10845.03	11.72
0.22	21.89	21.78	-11252.07	-1.632	1126.34	0.001058	-10565.40	11.50
0.23	21.89	21.78	-11438.46	-1.659	1149.71	0.001056	-10761.27	11.72
0.25	21.89	21.78	-11565.99	-1.678	1160.22	0.001055	-10896.40	11.81
0.27	21.89	21.78	-11438.46	-1.659	1126.34	0.001056	-10764.08	11.48
0.28	21.89	21.78	-11497.32	-1.668	1149.71	0.001055	-10824.18	11.71
0.30	21.89	21.78	-11301.12	-1.639	1113.49	0.001058	-10619.13	11.37
0.32	21.89	21.78	-11222.64	-1.628	1126.34	0.001059	-10534.11	11.51
0.33	21.89	21.78	-11526.75	-1.672	1126.34	0.001055	-10858.47	11.47
0.35	21.89	21.83	-11546.37	-1.675	1126.34	0.001055	-10881.55	11.46
0.37	21.94	21.83	-11252.07	-1.632	1135.68	0.001058	-10566.30	11.60
0.38	21.94	21.83	-11095.11	-1.609	1126.34	0.001060	-10400.72	11.52
0.40	21.94	21.83	-11291.31	-1.638	1126.34	0.001058	-10609.18	11.50
0.42	21.94	21.78	-11605.23	-1.683	1149.71	0.001054	-10939.73	11.70
0.43	21.94	21.83	-11359.98	-1.648	1126.34	0.001057	-10682.36	11.49
0.45	21.94	21.83	-11418.84	-1.656	1113.49	0.001056	-10746.69	11.35
0.47	21.94	21.83	-11173.59	-1.621	1126.34	0.001059	-10484.00	11.51
0.48	21.94	21.83	-11193.21	-1.623	1128.67	0.001059	-10504.56	11.53
0.50	21.94	21.83	-11624.85	-1.686	1135.68	0.001054	-10964.55	11.55

0.52	22.00	21.83	-11526.75	-1.672	1135.68	0.001055	-10859.43	11.56
0.53	22.00	21.83	-11252.07	-1.632	1113.49	0.001058	-10568.94	11.37
0.55	22.00	21.89	-11359.98	-1.648	1126.34	0.001057	-10684.40	11.48
0.57	22.00	21.89	-11487.51	-1.666	1133.35	0.001055	-10819.79	11.54
0.58	22.00	21.83	-11232.45	-1.629	1135.68	0.001058	-10545.43	11.60
0.60	22.00	21.83	-11252.07	-1.632	1126.34	0.001058	-10567.42	11.50
0.62	22.00	21.83	-11232.45	-1.629	1126.34	0.001058	-10546.55	11.50
0.63	22.00	21.89	-11232.45	-1.629	1090.12	0.001058	-10552.81	11.13
0.65	22.00	21.83	-11134.35	-1.615	1113.49	0.001059	-10443.87	11.38
0.67	22.00	21.89	-11222.64	-1.628	1126.34	0.001058	-10538.13	11.50
0.68	22.00	21.89	-11252.07	-1.632	1135.68	0.001058	-10568.32	11.59
0.70	22.00	21.89	-10830.24	-1.571	1126.34	0.001063	-10122.66	11.55
0.72	22.00	21.89	-11193.21	-1.623	1127.51	0.001059	-10506.70	11.52
0.73	22.00	21.89	-11340.36	-1.645	1126.34	0.001057	-10663.48	11.49
0.75	22.00	21.89	-10967.58	-1.591	1135.68	0.001061	-10266.54	11.63
0.77	22.00	21.89	-11085.30	-1.608	1113.49	0.001060	-10393.83	11.39
0.78	22.00	21.89	-11065.68	-1.605	1104.14	0.001060	-10374.13	11.29
0.80	22.00	21.89	-11065.68	-1.605	1104.14	0.001060	-10374.13	11.29
0.82	22.00	21.89	-11006.82	-1.596	1113.49	0.001061	-10310.70	11.40
0.83	22.00	21.89	-11173.59	-1.621	1126.34	0.001059	-10486.00	11.51
0.85	22.00	21.89	-11153.97	-1.618	1126.34	0.001059	-10465.16	11.51
0.87	22.00	21.89	-10741.95	-1.558	1113.49	0.001064	-10031.21	11.43
0.88	22.00	21.89	-10594.80	-1.537	1104.14	0.001066	-9877.74	11.35
0.90	22.00	21.89	-10545.75	-1.530	1090.12	0.001066	-9827.97	11.22
0.92	22.00	21.89	-10428.03	-1.512	1090.12	0.001068	-9704.81	11.23
0.93	22.00	21.89	-10477.08	-1.520	1090.12	0.001067	-9756.08	11.22
0.95	22.00	21.89	-10624.23	-1.541	1104.14	0.001065	-9908.61	11.35
0.97	22.00	21.94	-10516.32	-1.525	1090.12	0.001066	-9799.02	11.22
0.98	22.00	21.89	-10653.66	-1.545	1104.14	0.001065	-9939.51	11.35
1.00	22.00	21.89	-10526.13	-1.527	1104.14	0.001066	-9805.78	11.36
1.02	22.00	21.89	-10535.94	-1.528	1090.12	0.001066	-9817.69	11.22
1.03	22.00	21.94	-9731.52	-1.411	1057.40	0.001076	-8988.07	10.97
1.05	22.06	21.89	-6011.57	-0.872	831.90	0.001119	-5331.62	8.99
1.07	22.00	21.89	-3279.48	-0.476	625.56	0.001151	-2825.54	6.95
1.08	22.00	21.94	-459.60	-0.067	261.02	0.001184	-384.02	2.98
1.10	22.06	21.94	-604.59	-0.088	229.01	0.001183	-508.11	2.61

1.12	22.06	22.00	-611.85	-0.089	275.04	0.001182	-513.01	3.14
1.13	22.06	22.00	-621.46	-0.090	284.27	0.001182	-520.89	3.24
1.15	22.06	22.00	-623.92	-0.090	288.71	0.001182	-522.83	3.29
1.17	22.06	21.94	-614.20	-0.089	279.36	0.001183	-514.78	3.19
1.18	22.06	22.00	-611.85	-0.089	288.71	0.001182	-512.56	3.29
1.20	22.06	21.94	-619.01	-0.090	279.36	0.001182	-518.87	3.19
1.22	22.06	22.00	-609.40	-0.088	279.36	0.001182	-510.79	3.19
1.23	22.06	22.00	-604.59	-0.088	279.36	0.001182	-506.70	3.19
1.25	22.06	21.94	-621.46	-0.090	284.39	0.001182	-520.79	3.25
1.27	22.06	21.94	-626.27	-0.091	284.04	0.001182	-524.89	3.24
1.28	22.06	21.94	-614.20	-0.089	285.44	0.001183	-514.57	3.26
1.30	22.06	22.00	-3750.36	-0.544	689.24	0.001146	-3246.74	7.62
1.32	22.06	21.94	-4429.22	-0.642	749.06	0.001138	-3861.00	8.22
1.33	22.06	21.94	-4439.03	-0.644	758.41	0.001138	-3869.22	8.33
1.35	22.06	21.94	-4493.96	-0.652	767.17	0.001137	-3919.01	8.42
1.37	22.06	21.94	-4477.28	-0.649	758.29	0.001137	-3904.42	8.32
1.38	22.06	21.94	-4460.61	-0.647	758.41	0.001137	-3889.07	8.32
1.40	22.06	21.94	-4470.42	-0.648	758.41	0.001137	-3898.10	8.32
1.42	22.06	21.94	-4475.32	-0.649	740.30	0.001137	-3904.15	8.12
1.43	22.06	21.94	-4472.38	-0.649	758.41	0.001137	-3899.90	8.32
1.45	22.06	21.94	-4429.22	-0.642	758.41	0.001138	-3860.20	8.33
1.47	22.06	21.94	-7897.05	-1.145	1007.16	0.001097	-7142.77	10.66
1.48	22.06	21.94	-8730.90	-1.266	1016.51	0.001087	-7973.97	10.67
1.50	22.06	21.94	-9084.06	-1.318	1031.70	0.001083	-8329.29	10.78
1.52	22.06	21.94	-9819.81	-1.424	1080.77	0.001074	-9076.35	11.21
1.53	22.06	21.89	-9878.67	-1.433	1080.77	0.001074	-9135.34	11.20
1.55	22.06	21.94	-10094.49	-1.464	1090.12	0.001071	-9359.36	11.27
1.57	22.06	21.89	-10369.17	-1.504	1090.12	0.001068	-9643.35	11.24
1.58	22.06	21.94	-10565.37	-1.532	1090.12	0.001066	-9850.40	11.21
1.60	22.06	21.89	-10604.61	-1.538	1090.12	0.001065	-9889.67	11.21
1.62	22.00	21.89	-11036.25	-1.601	1104.14	0.001060	-10342.96	11.30
1.63	22.00	21.89	-10908.72	-1.582	1104.14	0.001062	-10208.09	11.31
1.65	22.00	21.89	-10800.81	-1.567	1104.14	0.001063	-10094.28	11.33
1.67	22.00	21.89	-10791.00	-1.565	1113.49	0.001063	-10082.84	11.43
1.68	22.00	21.89	-11026.44	-1.599	1113.49	0.001061	-10331.47	11.40
1.70	22.00	21.89	-10751.76	-1.559	1104.14	0.001064	-10042.63	11.33

1.72	22.00	21.89	-10997.01	-1.595	1104.14	0.001061	-10301.42	11.30
1.73	22.00	21.89	-10908.72	-1.582	1090.12	0.001062	-10209.73	11.17
1.75	22.00	21.89	-10781.19	-1.564	1113.49	0.001063	-10072.51	11.43
1.77	22.00	21.89	-10791.00	-1.565	1104.14	0.001063	-10083.94	11.33
1.78	21.94	21.89	-11026.44	-1.599	1126.34	0.001061	-10329.94	11.53
1.80	22.00	21.89	-11330.55	-1.643	1108.81	0.001057	-10655.09	11.31
1.82	21.94	21.89	-11310.93	-1.641	1113.49	0.001057	-10633.63	11.36
1.83	21.94	21.89	-10938.15	-1.586	1104.14	0.001062	-10239.18	11.31
1.85	22.00	21.89	-10918.53	-1.584	1120.50	0.001062	-10216.52	11.48
1.87	22.00	21.94	-11173.59	-1.621	1104.14	0.001059	-10490.62	11.28
1.88	21.94	21.89	-11006.82	-1.596	1135.68	0.001061	-10308.05	11.63
1.90	22.00	21.89	-10800.81	-1.567	1104.14	0.001063	-10094.28	11.33
1.92	22.00	21.89	-11104.92	-1.611	1108.81	0.001060	-10415.18	11.34
1.93	22.00	21.94	-10820.43	-1.569	1108.81	0.001063	-10116.33	11.37
1.95	22.00	21.89	-10938.15	-1.586	1090.12	0.001062	-10240.82	11.17
1.97	22.00	21.89	-10761.57	-1.561	1090.12	0.001064	-10054.59	11.19
1.98	22.00	21.89	-10938.15	-1.586	1111.15	0.001062	-10238.36	11.38
2.00	22.00	21.89	-10653.66	-1.545	1071.42	0.001065	-9943.30	11.01
2.02	22.00	21.94	-10663.47	-1.547	1090.12	0.001065	-9953.34	11.20
2.03	22.00	21.89	-10477.08	-1.520	1104.14	0.001067	-9754.44	11.37
2.05	22.00	21.94	-10643.85	-1.544	1080.77	0.001065	-9933.82	11.11
2.07	22.00	21.89	-10428.03	-1.512	1090.12	0.001068	-9704.81	11.23
2.08	22.00	21.94	-10310.31	-1.495	1080.77	0.001069	-9584.88	11.15
2.10	22.00	21.94	-9859.05	-1.430	1087.78	0.001074	-9116.01	11.27
2.12	22.00	21.94	-9653.04	-1.400	1057.40	0.001076	-8907.37	10.98
2.13	22.00	21.94	-9633.42	-1.397	1057.40	0.001077	-8887.22	10.99
2.15	22.00	21.94	-9545.13	-1.384	1057.40	0.001078	-8796.63	11.00
2.17	22.00	21.89	-8858.43	-1.285	1007.16	0.001086	-8102.06	10.55
2.18	22.00	21.94	-7995.15	-1.160	983.79	0.001096	-7242.46	10.40
2.20	22.00	21.94	-7975.53	-1.157	983.79	0.001096	-7223.02	10.41
2.22	22.00	21.94	-6095.93	-0.884	859.94	0.001118	-5410.23	9.28
2.23	22.00	21.94	-4242.83	-0.615	730.83	0.001140	-3691.50	8.04
2.25	22.00	21.94	-4013.27	-0.582	717.16	0.001143	-3482.88	7.91
2.27	22.00	21.94	-2384.81	-0.346	551.25	0.001162	-2035.10	6.18
2.28	22.00	21.94	-2353.42	-0.341	536.88	0.001162	-2008.34	6.02
2.30	22.00	21.94	-2351.46	-0.341	536.88	0.001162	-2006.61	6.02

2.32	22.06	21.94	-2344.59	-0.340	551.25	0.001162	-1999.66	6.18
2.33	22.00	21.94	-2351.46	-0.341	541.79	0.001162	-2006.31	6.08
2.35	22.00	21.94	-2358.32	-0.342	551.48	0.001162	-2011.74	6.18
2.37	22.06	21.94	-2341.65	-0.340	541.79	0.001162	-1997.66	6.08
2.38	22.06	21.94	-2353.42	-0.341	551.25	0.001162	-2007.43	6.18
2.40	22.06	21.94	-2341.65	-0.340	541.79	0.001162	-1997.66	6.08
2.42	22.06	21.94	-2348.51	-0.341	541.55	0.001162	-2003.73	6.07
2.43	22.06	21.94	-2331.84	-0.338	541.79	0.001162	-1989.02	6.08
2.45	22.06	21.94	-2331.84	-0.338	541.79	0.001162	-1989.02	6.08
2.47	22.06	21.94	-2331.84	-0.338	551.48	0.001162	-1988.41	6.19
2.48	22.06	21.94	-2336.74	-0.339	544.24	0.001162	-1993.19	6.10
2.50	22.06	21.94	-2336.74	-0.339	551.25	0.001162	-1992.74	6.18
2.52	22.06	21.94	-2329.88	-0.338	541.79	0.001162	-1987.30	6.08
2.53	22.06	21.94	-2331.84	-0.338	551.25	0.001162	-1988.42	6.18
2.55	22.06	21.94	-6487.35	-0.941	914.86	0.001114	-5778.95	9.83
2.57	22.06	21.94	-7553.70	-1.096	956.92	0.001101	-6809.82	10.17
2.58	22.06	21.94	-7524.27	-1.091	956.92	0.001101	-6780.94	10.17
2.60	22.06	21.89	-7504.65	-1.088	947.57	0.001102	-6761.38	10.08
2.62	22.06	21.94	-7740.09	-1.123	956.92	0.001099	-6993.20	10.15
2.63	22.06	21.94	-7504.65	-1.088	966.27	0.001102	-6760.70	10.27
2.65	22.06	21.94	-7553.70	-1.096	956.92	0.001101	-6809.82	10.17
2.67	22.06	21.89	-7651.80	-1.110	956.92	0.001100	-6904.93	10.16
2.68	22.06	21.94	-7720.47	-1.120	956.92	0.001099	-6973.86	10.15
2.70	22.06	21.94	-7641.99	-1.108	966.27	0.001100	-6895.60	10.26
2.72	22.06	21.89	-7524.27	-1.091	956.92	0.001102	-6779.64	10.17
2.73	22.06	21.89	-5651.54	-0.820	841.25	0.001124	-4989.98	9.12
2.75	22.06	21.94	-3917.13	-0.568	707.82	0.001144	-3396.09	7.81
2.77	22.06	21.94	-3854.35	-0.559	707.82	0.001145	-3339.01	7.82
2.78	22.06	21.94	-3844.54	-0.558	707.82	0.001145	-3330.10	7.82
2.80	22.06	21.89	-3849.44	-0.558	707.82	0.001145	-3333.92	7.82
2.82	22.06	21.94	-3844.54	-0.558	707.82	0.001145	-3330.10	7.82
2.83	22.06	21.94	-3849.44	-0.558	699.05	0.001145	-3335.26	7.72
2.85	22.06	21.94	-1580.39	-0.229	431.49	0.001171	-1338.47	4.88
2.87	22.06	21.94	-1372.42	-0.199	367.46	0.001174	-1161.44	4.16
2.88	22.06	21.94	-1740.29	-0.252	468.06	0.001169	-1475.48	5.28
2.90	22.06	21.94	-2848.82	-0.413	589.46	0.001156	-2443.62	6.58

2.92	22.06	21.94	-2848.82	-0.413	602.43	0.001156	-2442.73	6.72
2.93	22.06	21.94	-2896.89	-0.420	611.42	0.001156	-2484.90	6.82
2.95	22.06	21.94	-2880.22	-0.418	602.43	0.001156	-2470.68	6.72
2.97	22.06	21.94	-2868.44	-0.416	611.42	0.001156	-2459.56	6.82
2.98	22.06	21.94	-2848.82	-0.413	611.42	0.001156	-2442.10	6.82
3.00	22.06	21.94	-2856.67	-0.414	611.42	0.001156	-2449.08	6.82
3.02	22.06	21.94	-2890.03	-0.419	611.42	0.001156	-2478.78	6.82
3.03	22.06	21.94	-2883.16	-0.418	611.42	0.001156	-2472.67	6.82
3.05	22.06	21.94	-2853.73	-0.414	602.43	0.001156	-2447.09	6.72
3.07	22.06	21.94	-2851.77	-0.414	611.42	0.001156	-2444.72	6.82
3.08	22.06	21.94	-652.86	-0.095	275.04	0.001182	-547.82	3.14
3.10	22.06	21.94	-606.94	-0.088	242.44	0.001183	-509.74	2.77
3.12	22.06	21.94	-761.26	-0.110	307.41	0.001181	-639.11	3.50
3.13	22.11	21.94	-774.01	-0.112	307.41	0.001181	-649.99	3.50
3.15	22.11	21.94	-769.10	-0.112	303.08	0.001181	-645.96	3.45
3.17	22.11	21.94	-764.20	-0.111	303.08	0.001181	-641.77	3.45
3.18	22.06	21.94	-761.26	-0.110	312.08	0.001181	-638.93	3.56
3.20	22.11	21.94	-761.26	-0.110	312.08	0.001181	-638.93	3.56
3.22	22.11	21.94	-761.26	-0.110	307.41	0.001181	-639.11	3.50
3.23	22.11	21.94	-1467.58	-0.213	417.24	0.001173	-1241.43	4.72
3.25	22.11	21.94	-2703.64	-0.392	575.20	0.001158	-2315.55	6.43
3.27	22.11	21.94	-2706.58	-0.393	598.10	0.001158	-2316.61	6.68
3.28	22.11	21.94	-2686.96	-0.390	589.46	0.001158	-2299.79	6.59
3.30	22.11	21.89	-2703.64	-0.392	589.22	0.001158	-2314.16	6.59
3.32	22.11	21.94	-2696.77	-0.391	597.99	0.001158	-2307.91	6.68
3.33	22.11	21.94	-2682.05	-0.389	589.46	0.001158	-2295.44	6.59
3.35	22.11	21.94	-2696.77	-0.391	589.22	0.001158	-2308.51	6.58
3.37	22.11	21.94	-2711.48	-0.393	589.22	0.001158	-2321.57	6.58
3.38	22.11	21.94	-628.72	-0.091	303.08	0.001182	-526.32	3.46
3.40	22.11	21.94	-558.68	-0.081	265.69	0.001183	-468.00	3.03
3.42	22.11	21.94	-532.09	-0.077	261.02	0.001184	-445.56	2.98
3.43	22.11	21.94	-541.71	-0.079	261.02	0.001183	-453.73	2.98
3.45	22.11	21.94	-534.55	-0.078	251.56	0.001183	-447.93	2.87
3.47	22.11	21.94	-536.90	-0.078	256.81	0.001183	-449.77	2.93
3.48	22.11	21.94	-517.58	-0.075	261.02	0.001184	-433.23	2.98
3.50	22.11	21.94	-544.16	-0.079	256.81	0.001183	-455.94	2.93

3.52	22.11	21.94	-742.62	-0.108	288.71	0.001181	-623.86	3.29
3.53	22.17	21.94	-1244.89	-0.181	394.45	0.001175	-1050.21	4.47
3.55	22.11	21.94	-1251.76	-0.182	389.66	0.001175	-1056.35	4.42
3.57	22.17	21.94	-1249.79	-0.181	389.43	0.001175	-1054.67	4.42
3.58	22.17	21.94	-1244.89	-0.181	403.80	0.001175	-1049.77	4.58
3.60	22.17	21.94	-1251.76	-0.182	404.03	0.001175	-1055.68	4.58
3.62	22.17	21.94	-1251.76	-0.182	404.03	0.001175	-1055.68	4.58
3.63	22.17	21.94	-1246.85	-0.181	408.12	0.001175	-1051.26	4.63
3.65	22.11	21.94	-1246.85	-0.181	389.43	0.001175	-1052.13	4.42
3.67	22.11	21.94	-1244.89	-0.181	408.12	0.001175	-1049.57	4.63
3.68	22.11	21.94	-2510.38	-0.364	564.69	0.001160	-2145.09	6.32
3.70	22.11	21.94	-2541.77	-0.369	574.97	0.001160	-2172.16	6.44
3.72	22.11	21.89	-2549.62	-0.370	574.03	0.001160	-2178.75	6.43
3.73	22.11	21.94	-2539.81	-0.368	574.03	0.001160	-2170.49	6.43
3.75	22.17	21.89	-2539.81	-0.368	575.20	0.001160	-2170.00	6.44
3.77	22.17	21.89	-2537.85	-0.368	578.94	0.001160	-2168.01	6.48
3.78	22.17	21.94	-2537.85	-0.368	574.03	0.001160	-2168.75	6.43
3.80	22.17	21.89	-2541.77	-0.369	574.03	0.001160	-2171.81	6.43
3.82	22.17	21.89	-2899.84	-0.421	657.34	0.001156	-2483.68	7.33
3.83	22.17	21.94	-6318.62	-0.916	878.64	0.001116	-5620.90	9.46
3.85	22.17	21.89	-6323.53	-0.917	887.98	0.001116	-5623.60	9.56
3.87	22.17	21.94	-6342.17	-0.920	894.99	0.001115	-5641.81	9.63
3.88	22.17	21.89	-6338.24	-0.919	887.98	0.001116	-5637.67	9.56
3.90	22.17	21.89	-6347.07	-0.921	887.98	0.001115	-5646.12	9.56
3.92	22.17	21.89	-6041.00	-0.876	887.98	0.001119	-5354.20	9.59
3.93	22.17	21.89	-6351.98	-0.921	887.98	0.001115	-5650.81	9.56
3.95	22.17	21.89	-2798.79	-0.406	597.99	0.001157	-2398.07	6.68
3.97	22.17	21.89	-1860.96	-0.270	486.52	0.001168	-1579.28	5.48
3.98	22.17	21.89	-1844.28	-0.267	486.52	0.001168	-1564.74	5.49
4.00	22.17	21.89	-1097.74	-0.159	371.55	0.001177	-924.46	4.22
4.02	22.17	21.89	-1092.83	-0.159	371.55	0.001177	-920.25	4.22
4.03	22.17	21.89	-1083.02	-0.157	371.55	0.001177	-911.82	4.22
4.05	22.17	21.94	-1089.89	-0.158	367.23	0.001177	-918.08	4.17
4.07	22.17	21.89	-1084.99	-0.157	371.55	0.001177	-913.51	4.22
4.08	22.17	21.89	-1087.93	-0.158	367.46	0.001177	-916.21	4.17
4.10	22.17	21.89	-1092.83	-0.159	371.55	0.001177	-920.25	4.22

4.12	22.17	21.94	-1058.50	-0.154	360.10	0.001177	-891.43	4.09
4.13	22.17	21.89	-430.66	-0.062	196.29	0.001185	-361.17	2.24
4.15	22.17	21.94	-416.14	-0.060	229.01	0.001185	-348.10	2.62
4.17	22.17	21.89	-756.35	-0.110	307.41	0.001181	-634.80	3.50
4.18	22.17	21.94	-1291.00	-0.187	386.97	0.001175	-1090.30	4.39
4.20	22.17	21.94	-1341.03	-0.194	412.80	0.001174	-1132.26	4.68
4.22	22.17	21.89	-2015.96	-0.292	509.42	0.001166	-1713.36	5.73
4.23	22.17	21.89	-2868.44	-0.416	602.43	0.001156	-2459.72	6.72
4.25	22.11	21.89	-2894.93	-0.420	611.42	0.001156	-2482.68	6.82
4.27	22.17	21.89	-3540.43	-0.513	680.24	0.001148	-3056.32	7.54
4.28	22.17	21.89	-4668.58	-0.677	767.17	0.001135	-4079.28	8.40
4.30	22.17	21.89	-4733.33	-0.687	767.17	0.001134	-4139.13	8.40
4.32	22.17	21.89	-5564.23	-0.807	831.90	0.001125	-4908.61	9.03
4.33	22.17	21.89	-6652.16	-0.965	905.51	0.001112	-5937.24	9.72
4.35	22.17	21.89	-6835.61	-0.991	914.86	0.001110	-6113.30	9.80
4.37	22.17	21.89	-7720.47	-1.120	947.57	0.001099	-6973.51	10.05
4.38	22.17	21.89	-7710.66	-1.118	966.27	0.001099	-6961.88	10.25
4.40	22.17	21.89	-8004.96	-1.161	974.45	0.001096	-7251.80	10.31
4.42	22.17	21.89	-8485.65	-1.231	1000.15	0.001090	-7727.97	10.52
4.43	22.17	21.83	-8760.33	-1.271	1016.51	0.001087	-8000.56	10.67
4.45	22.17	21.89	-9054.63	-1.313	1025.86	0.001084	-8298.50	10.73
4.47	22.17	21.83	-9368.55	-1.359	1039.88	0.001080	-8614.68	10.84
4.48	22.17	21.83	-9819.81	-1.424	1071.42	0.001075	-9073.96	11.11
4.50	22.17	21.89	-9868.86	-1.431	1057.40	0.001074	-9127.90	10.96
4.52	22.17	21.89	-10182.78	-1.477	1071.42	0.001070	-9451.41	11.07
4.53	22.17	21.89	-10172.97	-1.475	1074.93	0.001071	-9440.81	11.10
4.55	22.17	21.89	-10241.64	-1.485	1077.26	0.001070	-9511.94	11.12
4.57	22.17	21.83	-10467.27	-1.518	1090.12	0.001067	-9743.97	11.23
4.58	22.17	21.89	-10467.27	-1.518	1080.77	0.001067	-9746.91	11.13
4.60	22.17	21.89	-10153.35	-1.473	1057.40	0.001071	-9422.43	10.93
4.62	22.17	21.89	-10339.74	-1.500	1071.42	0.001069	-9614.80	11.05
4.63	22.17	21.83	-10300.50	-1.494	1104.14	0.001069	-9568.27	11.39
4.65	22.17	21.89	-10428.03	-1.512	1083.11	0.001068	-9705.62	11.16
4.67	22.17	21.83	-10555.56	-1.531	1090.12	0.001066	-9836.37	11.22
4.68	22.17	21.83	-10555.56	-1.531	1073.76	0.001066	-9838.26	11.05
4.70	22.17	21.89	-10545.75	-1.530	1104.14	0.001066	-9826.33	11.36

4.72	22.17	21.83	-10594.80	-1.537	1113.49	0.001066	-9874.75	11.45
4.73	22.17	21.89	-10428.03	-1.512	1116.99	0.001068	-9701.64	11.51
4.75	22.17	21.89	-10712.52	-1.554	1080.77	0.001064	-10004.07	11.10
4.77	22.17	21.83	-10575.18	-1.534	1080.77	0.001066	-9858.01	11.12
4.78	22.17	21.89	-10771.38	-1.562	1126.34	0.001064	-10060.65	11.56
4.80	22.17	21.83	-11046.06	-1.602	1104.14	0.001060	-10351.37	11.30
4.82	22.17	21.83	-10741.95	-1.558	1104.14	0.001064	-10030.39	11.34
4.83	22.17	21.89	-10830.24	-1.571	1104.14	0.001063	-10125.29	11.32
4.85	22.17	21.89	-10987.20	-1.594	1104.14	0.001061	-10291.04	11.30
4.87	22.17	21.89	-10957.77	-1.589	1071.42	0.001061	-10263.70	10.97
4.88	22.17	21.83	-10781.19	-1.564	1090.12	0.001064	-10073.33	11.19
4.90	22.17	21.83	-10506.51	-1.524	1104.14	0.001067	-9783.37	11.37
4.92	22.17	21.89	-10781.19	-1.564	1104.14	0.001063	-10073.61	11.33
4.93	22.17	21.83	-9172.35	-1.330	983.79	0.001082	-8420.99	10.28
4.95	22.17	21.83	-5600.53	-0.812	795.21	0.001124	-4945.19	8.63
4.97	22.17	21.83	-3511.00	-0.509	666.57	0.001149	-3030.24	7.39
4.98	22.17	21.89	-2457.41	-0.356	561.42	0.001161	-2098.10	6.29
5.00	22.11	21.89	-981.00	-0.142	362.20	0.001178	-824.71	4.12
5.02	22.17	21.89	-483.73	-0.070	247.12	0.001184	-404.84	2.82
5.03	22.17	21.89	-331.58	-0.048	214.99	0.001186	-276.82	2.46

VITA

Orrick Rowland Haney was born on November 25, 1969 in Anderson, South Carolina. He graduated from Tamassee-Salem High School as valedictorian in Salem, South Carolina in 1988. In the fall of 1988 he began studies at The Citadel, The Military College of South Carolina. At The Citadel he lead The Citadel Pipes and Drums while also excelling in Civil Engineering. He graduated cum laude with a Bachelor of Science Degree in Civil Engineering from The Citadel in May of 1992, and entered graduate school in the fall. Orrick completed his Master of Science Degree requirements in February of 1994 at Virginia Tech. He is currently working as an Environmental Engineer for Goldie & Associates in Seneca, South Carolina.